



Universitat Autònoma de Barcelona

Stereoselective Synthesis of Cyclobutane Nucleoside Analogues

PhD Thesis

Antoni Figueras Sorinas

2012

Supervised by:

Dr. Ramon Alibés Arqués

Dr. Félix Busqué Sánchez

Programa de doctorat en Química

Departament de Química

Facultat de Ciències

Memòria presentada per aspirar al grau
de Doctor per Antoni Figueras Sorinas

Antoni Figueras Sorinas

Vist-i-plau

Dr. Ramon Alibés Arqués

Dr. Félix Busqué Sánchez

Bellaterra, setembre de 2012

Part of the results of this thesis are described in the following scientific publications:

- “Synthesis, Anti-HIV Activity Studies, and in silico Rationalization of Cyclobutane-Fused Nucleosides” Figueras, A.; Miralles-Llumà, R.; Flores, R.; Rustullet, A.; Busqué, F.; Figueredo, M.; Font, J.; Alibés, R.; Maréchal, J.-D. *ChemMedChem* **2012**, 7, 1044-1056.
- “Synthesis and Antiviral Evaluation of Cyclobutane and Cyclobutene L-Nucleoside Analogues” Miralles-Llumà, R.; Figueras, A.; Álvarez-Larena, A.; Balzarini, J.; Figueredo, M.; Font, J.; Maréchal, J.-D.; Alibés, R.; Busqué, F. In preparation.

Table of Contents

Table of Contents

I. Introduction and Objectives

1. Introduction	3
2. Precedents	12
3. Objectives	20

II. [2+2] Photocycloaddition of Chiral Furanones to Ketene Diethyl Acetal

1. Introduction	25
1.1 Precedents	27
1.1.1 [2+2] Photocycloaddition of enones to asymmetric alkenes	27
1.1.2 [2+2] Photocycloaddition of enones to ketene acetals	33
1.1.3 [2+2] Photocycloaddition of 2(5 <i>H</i>)-furanones to ketene acetals	35
2. [2+2] Photocycloaddition of 2(5 <i>H</i>)-furanones to ketene diethyl acetal	38
2.1 Synthesis of 2(5 <i>H</i>)-furanones	38
2.2 [2+2] Photocycloaddition of 86 and 78 to ketene diethyl acetal.....	39
2.2.1 Structural determination of the photocycloadducts	41
3. Chapter II outline	45

III. Cyclobutane-Fused Nucleosides. Synthesis of Novel Nucleosides Bearing a Functionalized Cyclobutane Ring

1. Introduction	49
1.1 Basics of nucleoside structure	49
1.2 Furanose ring conformation. The pseudorotational cycle.....	50
1.3 Torsion angle χ	53
1.4 Torsion angle γ	53
2. Precedents	54
3. Synthesis of conformationally restricted nucleosides bearing a functionalized cyclobutane ring.....	65
3.1 Synthetic strategy overview	65
3.2 Synthesis of the conformationally restricted nucleosides 90-92	65
3.2.1 Preparation of acetate 88	65
3.2.2 Vorbrüggen <i>N</i> -glycosylation reaction	66
3.2.2.1 Reaction mechanism	66
3.2.2.2 <i>N</i> -glycosylation reaction. Introduction of thymine	67
3.2.3 Synthesis of the keto α - and β -nucleosides 237 and 90	70
3.2.4 Synthesis of the hydroxyl and methylene nucleosides 91 and 92	71

3.2.4.1 Synthesis of the hydroxyl nucleoside 91	71
3.2.4.2 Synthesis of the methylene nucleoside 92	73
4. Evaluation of the anti-HIV activity	76
5. Computational studies of cyclobutane-fused nucleosides	80
5.1 Docking study.....	80
5.2 Conformational study	83
6. Chapter III outline	87

IV. Cyclobutane L-Nucleosides. Enantiopure Synthesis of Novel Cyclobutane L-Nucleosides

1. Introduction	91
1.1 L-Nucleosides as antiviral agents	91
1.2 Carbocyclic nucleosides as antiviral agents	92
1.3 Carbocyclic L-nucleosides.....	101
2. Synthesis of cyclobutane L-nucleoside analogues.....	102
2.1 Synthetic strategy overview.....	102
2.2 Synthesis of the cyclobutane L-nucleosides 95-97	103
2.2.1 Synthesis of the common intermediate 81	103
2.2.2 Introduction of the nucleobase	105
2.2.2.1 The Mitsunobu reaction	105
2.2.2.1.1 Introduction of thymine	106
2.2.2.1.2 Introduction of 5-fluorouracil.....	109
2.2.2.1.3 Introduction of 2-amino-6-chloropurine	111
2.2.2.2 Mesylate displacement.....	113
2.2.3 Synthesis of the thymine nucleoside 95	115
2.2.4 Synthesis of the 5-fluorouracil nucleoside 96	117
2.2.5 Synthesis of the O^6 -methylguanine nucleoside 97	118
2.3 Synthesis of the thymine nucleoside 98	120
2.3.1 Oxidative cleavage of nucleoside 95	120
2.3.2 Approximation A. <i>p</i> -Methoxybenzyl as the 3' protecting group	122
2.3.2.1 Synthesis of the <i>p</i> -methoxybenzyl intermediate 333	123
2.3.2.2 Attempt of diol deprotection.....	125
2.3.3 Approximation B. Benzyl as the 3' protecting group	125
2.3.3.1 Synthesis of the benzyl intermediate 338	125
2.3.3.2 Synthesis of nucleoside 98	126
3. Evaluation of the antiviral activity	129
4. Chapter IV outline	132

V. Synthesis of Double-Headed Nucleosides and Their Incorporation Into Oligonucleotides

1. Introduction	135
1.1 Introduction to nucleic acid structure	135
1.1.1 Secondary structure	136
1.2 Oligonucleotide synthesis	138
1.2.1 Thermal denaturation	139
1.3 Nucleic acids as therapeutic agents	140
2. Synthesis of double-headed nucleosides	141
2.1 Precedents	141
2.2 Synthetic strategy overview	142
2.3 Synthesis of the building blocks	142
2.3.1 Propargylation of thymine and adenine	142
2.3.2 Tritylation of 5-iodo-2'-deoxyuridine	146
2.3.3 Synthesis and tritylation of 5-iodo- <i>N</i> ⁴ -acetyl-2'-deoxycytidine	147
2.4 Synthesis of the double-headed nucleosides 341-344	148
2.4.1 The Sonogashira reaction	148
2.4.2 Synthesis of 341-344	149
2.5 Oligonucleotide synthesis	153
2.5.1 Phosphoramidite synthesis	153
2.5.2 Oligonucleotide synthesis and thermal denaturation studies	155
3. Chapter V outline	156
VI. Summary	159
VII. Experimental Section	
1. General methods	165
2. Chapter II	167
2.1 Synthesis of (<i>S</i>)-5-hydroxymethyl-2(5 <i>H</i>)-furanone, 53	167
2.2 Synthesis of (<i>S</i>)-5- <i>tert</i> -butyldimethylsilyloxymethyl-2(5 <i>H</i>)-furanone, 86	168
2.3 Synthesis of (<i>S</i>)-5-pivaloyloxymethyl-2(5 <i>H</i>)-furanone, 78	169
2.4 Synthesis of 1,1-diethoxyethylene, 138	169
2.5 [2+2] Photocycloaddition of 86 to 1,1-diethoxyethylene	170
2.6 [2+2] Photocycloaddition of 78 to 1,1-diethoxyethylene	172
3. Chapter III	173
3.1 Synthesis of the keto α - and β -nucleosides 237 and 90	173
3.2 Synthesis of the hydroxyl nucleoside 91	177
3.3 Synthesis of the methylene nucleoside 92	178

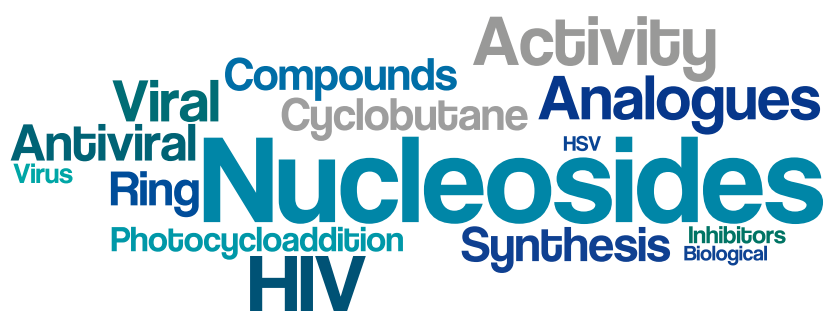
Table of Contents

4. Chapter IV	180
4.1 Synthesis of the common intermediate 81	180
4.2 Nucleobase introduction. Preparation of 318 , 320 and 323	184
4.3 Synthesis of the thymine nucleoside 95	189
4.4 Synthesis of the 5-fluorouracil nucleoside 96	190
4.5 Synthesis of the <i>O</i> ⁶ -methylguanine nucleoside 97	192
4.6 Synthesis of the thymine nucleoside 98	193
5. Chapter V	199
5.1 Synthesis of the building blocks.....	199
5.2 Synthesis of the double-headed nucleosides 341-344	204
5.3 Synthesis of phosphoramidites 364 and 365	207
VIII. References	211
IX. ¹H- and ¹³C-NMR spectra of selected compounds	223
X. Formula Index	257

Spectra appendices – Supplemented flash drive

I. Introduction and Objectives

Nucleoside Analogues as Antiviral Agents





1. INTRODUCTION

Every year millions of people are infected by different types of viruses, such as the human immunodeficiency virus (HIV), the herpes simplex virus (HSV), the varicella zoster virus (VZV), the human cytomegalovirus, or the hepatitis B and C viruses (HBV and HCV). Although vaccines have helped to control some of these viral diseases (e.g. smallpox, polio, HBV), for most of them no vaccines are available (e.g. HIV, HCV), or are either under development or in different stages of clinical trials (e.g. human papillomavirus, influenza, VZV).¹ The treatment for both latter cases relies entirely on the administration of drugs that inhibit viral development.

Of the mentioned viral diseases, particularly dramatic is the case of HIV, the agent causing acquired immunodeficiency syndrome (AIDS), which according to the United Nations programme on HIV/AIDS, it is estimated to affect more than 34 million people.²

HIV, as all viruses, requires the biological machinery of the host cell to replicate. It belongs to the *retroviridae* family, which are RNA-based viruses that take advantage of the enzyme called reverse transcriptase (RT) to transcribe their genetic information into DNA.

¹ (a) Arvin, A. M.; Greenberg, H. B. *Virology* **2006**, *344*, 240-249. (b) Weigand, K.; Stremmel, W.; Encke, J. *World J. Gastroenterol.* **2007**, *13*, 1897-1905. (c) Quan, D.; Cohrs, R. J.; Mahalingam, R.; Gilden, D. H. *Ther. Clin. Risk. Manag.* **2007**, *3*, 633-639. (d) Richardson, J. S.; Dekker, J. D.; Croyle, M. A.; Kobinger, G. P. *Hum. Vaccines* **2010**, *6*, 439-449. (e) Swaminathan, S.; Batra, G.; Khanna, N. *Expert Opin. Ther. Patents* **2010**, *20*, 819-835. (f) Luring, A. S.; Jones, J. O.; Andino, R. *Nat. Biotechnol.* **2010**, *28*, 573-579.

² UNAIDS. Together we will end AIDS. www.unaids.org. Accessed 14/08/2012.

The life cycle of HIV starts when a virion, a virus particle, binds to specific receptors of the host cell and fuses with it (Figure 1). After that, the viral RNA and various enzymes, including reverse transcriptase, integrase, ribonuclease and protease are injected into the cell cytoplasm. Then, reverse transcriptase starts transcribing the viral RNA into DNA, which enters the nucleus and is added to the cell genome by the enzyme integrase. This integrated viral DNA remains inactive until certain transcription factors are expressed. When it becomes active, the viral DNA is transcribed into mRNA by RNA polymerase. This mRNA is processed and used to make viral proteins and new viral RNA chains. The new viral genetic material is then assembled into new virions, which leave the host cell by a process called budding. Finally, these new viral particles can infect new healthy cells and start the cycle all over again.

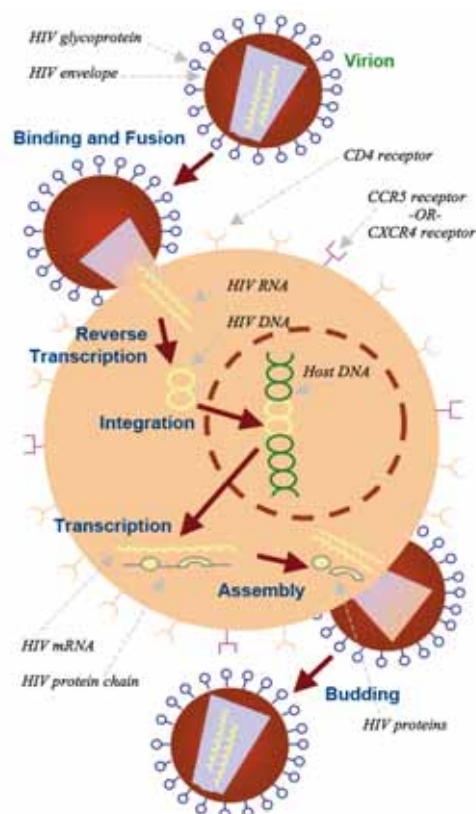


Figure 1. HIV life cycle.³

The discovery of Idoxuridine (5-iodo-2'-deoxyuridine, Figure 2), *ca.* 50 years ago,⁴ as a drug to treat HSV, established the dawning of antiretroviral therapy. Another nucleoside analogue, Zidovudine⁵ (AZT) was the first drug that could successfully interfere with HIV life cycle, preventing its replication. In 1987, it became the first compound to be specifically approved as an anti-HIV drug by the U.S. Food and Drug Administration (FDA).

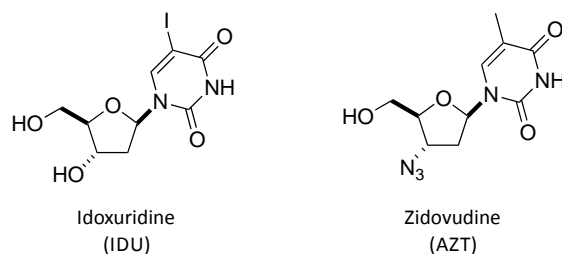


Figure 2. Structures of Idoxuridine and Zidovudine.

³ AIDSinfo. www.aidsinfo.nih.gov/ContentFiles/HIVLifeCycle_FS_en.pdf. Accessed 14/08/2012.

⁴ Prusoff, W. H. *Biochim. Biophys. Acta* **1959**, *32*, 295-296.

⁵ Mitsuya, H.; Weinhold, K. J.; Furman, P. A.; St. Clair, M. H.; Lehrman, S. N.; Gallo, R. C.; Bolognesi, D.; Barry, D. W.; Broder, S. *Proc. Natl. Acad. Sci. USA* **1985**, *82*, 7096-7100.

Since the discovery of AZT, nucleoside analogues emerged as the cornerstone of antiretroviral therapy, and a myriad of structurally modified nucleosides have been synthesized and screened for anti-HIV activity.⁶

The plethora of anti-HIV drugs can be classified upon which stage of the virus life cycle is targeted: nucleoside reverse transcriptase inhibitors (NRTIs), non-nucleoside reverse transcriptase inhibitors (NNRTIs), protease inhibitors (PIs), integrase inhibitors (INIs), fusion inhibitors and co-receptor inhibitors. Due to the high mutation rate of HIV, the only way to prevent the development of resistance is to completely block viral replication.⁷ This can be achieved by the administration of a combination of drugs, usually three (e.g. two NRTIs and one PI), a treatment known as highly active antiretroviral therapy (HAART). To date, besides AZT, the FDA has approved six more NRTIs for the treatment of HIV (Figure 3). The resemblance of these compounds to natural nucleosides grants good interaction with the viral RT, while the lack of the 3'-hydroxyl group interrupts chain elongation when they are incorporated into the growing strand of DNA. To accomplish this objective, this hydroxyl group has been replaced by other functionalities such as an azido group (AZT), a hydrogen atom (Zalcitabine (ddC) and Didanosine (ddI)) or by a double bond between the 2' and 3' positions (Stavudine (d4T)).

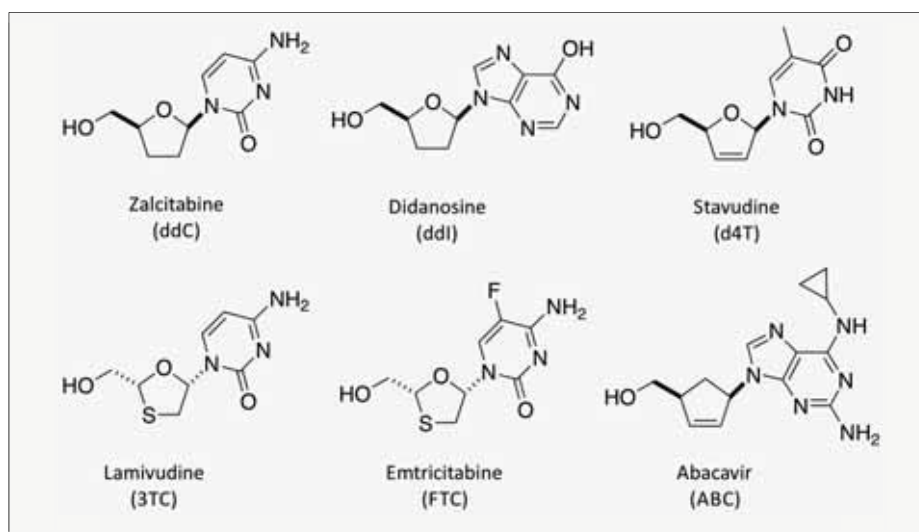


Figure 3. Structures of the FDA-approved NRTIs.

⁶ (a) De Clercq, E. *Future Med. Chem.* **2010**, *2*, 1049-1053 and references cited therein. (b) De Clercq, E. *J. Med. Chem.* **2010**, *53*, 1438-1450. (c) De Clercq, E. *Annu. Rev. Pharmacol. Toxicol.* **2011**, *51*, 1-24.

⁷ Sarafianos, S. G.; Marchand, B.; Das, K.; Himmel, D. M.; Parniak, M. A.; Hughes, S. H.; Arnold, E. *J. Mol. Biol.* **2009**, *385*, 693-713.

Further structural modifications led to the discovery of the antiviral activity of carbocyclic and L-nucleosides. The use of L-enantiomers of natural and modified nucleosides as antiviral agents has increased dramatically in recent years.⁸ Several L-nucleoside analogues such as Lamivudine (3TC) and Emtricitabine (FTC), have shown promising activities against a wide range of viral infections. On the other hand, carbocyclic nucleosides such as Abacavir (ABC), compounds in which the furanose oxygen has been replaced by a methylene unit, have also attracted remarkable synthetic attention due to their improved resistance to hydrolytic processes and enhanced lipophilicity.^{9,10}

The mechanism of action of nucleoside analogues starts with three steps of kinase-catalyzed phosphorylation to convert the 2',3'-dideoxynucleosides to their 5'-triphosphate forms. Then, the 5'-triphosphates can interact with virus-specific polymerases, acting as a competitive inhibitor or an alternate substrate for these target enzymes, usually preventing further viral nucleic acid chain elongation. As an example, Figure 4 shows the phosphorylation of ddC to their 5'-triphosphate form, which may eventually interact with the viral RT.

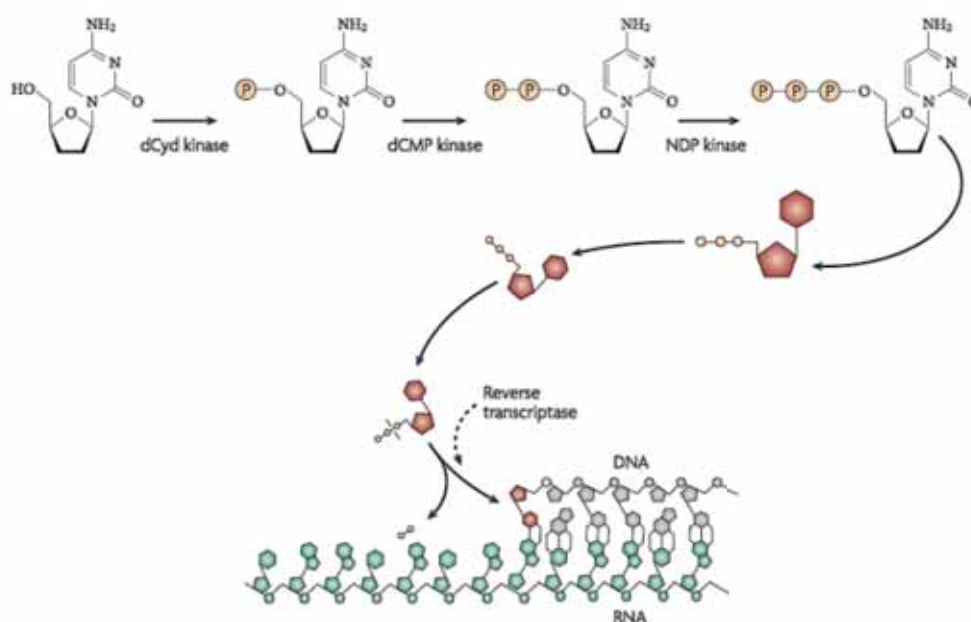


Figure 4. Mechanism of action of the nucleoside analogue ddC.¹¹

⁸ Mathé, C.; Gosselin, G. *Antiviral Res.* **2006**, *71*, 276-281 and references cited therein.

⁹ (a) Jeong, L. S.; Lee, J. A. *Antivir. Chem. Chemother.* **2004**, *15*, 235-250. (b) Amblard, F.; Nolan, S. P.; Agrofoglio, L. A. *Tetrahedron* **2005**, *61*, 7067-7080.

¹⁰ For recent examples see: (a) Liu, L. J.; Hong, J. H. *Nucleosides, Nucleotides & Nucleic Acids* **2010**, *29*, 216-227. (b) Douadi, A.; Brémond, P.; Lanez, T.; Pannecouque, C.; Audran, G. *Synlett* **2011**, *1*, 111-115. (c) Gadthula, S.; Rawal, R. K.; Sharon, A.; Wu, D.; Korba, B.; Chu, C. K. *Bioorg. Med. Chem. Lett.* **2011**, *21*, 3982-3985.

¹¹ De Clercq, E. *Nat. Rev. Drug. Discov.* **2007**, *6*, 1001-1018.

Apart from the aforementioned compounds, seven more NRTIs are undergoing clinical trials as anti-HIV candidates (Figure 5).¹² Apricitabine (ATC) and Amdoxovir (DAPD) present additional heteroatoms on the ribose ring, with ATC having a sulphur atom instead of the natural oxygen and DAPD exhibiting a dioxolane-type structure. Racivir (RCV) is a racemic mixture of FTC (both enantiomers display anti-HIV activity) and Elvucitabine (L-d4FC) is another L-nucleoside, which has shown to be as effective as 3TC while displaying higher intracellular half-life.¹³ Festinavir (4'-Ed4T) and Alovudine (FLT) are analogues of d4T and thymidine, respectively. The former presents an additional ethynyl group at the 4'-position while the latter has a fluorine atom instead of the hydroxyl group. Finally, KP-1212 is the only compound that is non-chain terminating. Its antiviral activity comes from the ability of the modified nucleobase to induce mutations on the viral genome.¹⁴

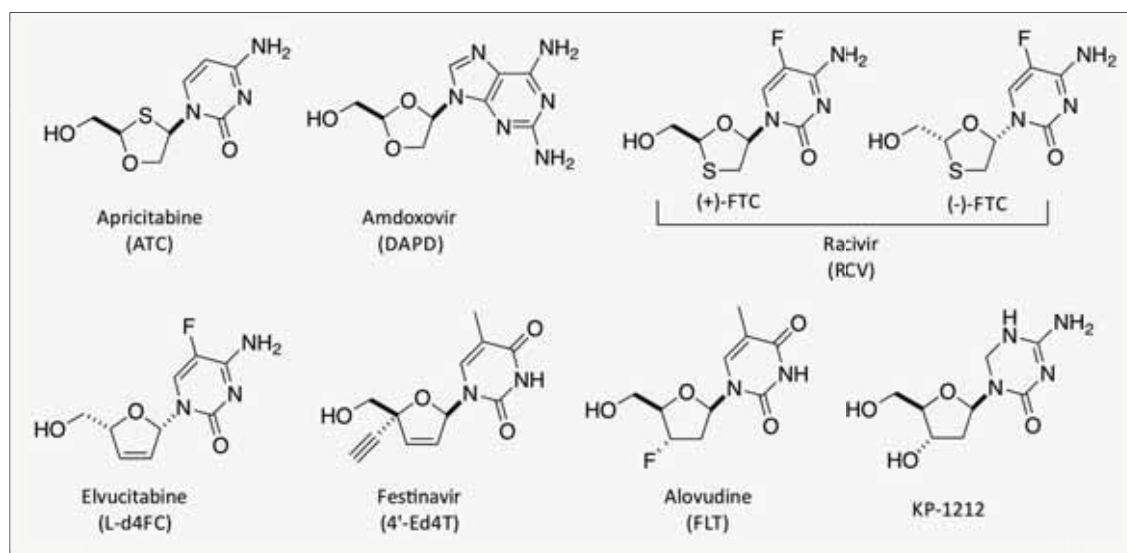


Figure 5. NRTIs currently undergoing clinical trials.

It is well known that the conformation and puckering of the glycon moiety of nucleosides play a critical role in modulating their biological activity. In recent years, the search for more active and selective antiviral agents has been directed towards the synthesis of nucleoside derivatives with fixed sugar-ring puckering.¹⁵ These compounds can be classified in three main families (Figure 6): bicyclonucleosides, obtained by bonding two atoms of the sugar ring via an alkylene unit or analogues; cyclonucleosides, obtained when the furanose ring is connected to the

¹² Cihlar, T.; Ray, A. S. *Antiviral Res.* **2010**, *85*, 39-58.

¹³ Dutschman, G. E.; Bridges, E. G.; Liu, S.-H.; Gullen, E.; Guo, X.; Kukhanova, M.; Cheng, Y.-C. *Antimicrob. Agents Chemother.* **1998**, *42*, 1799-1804.

¹⁴ Harris, K. S.; Brabant, W.; Styrchak, S.; Gall, A.; Daifuku, R. *Antiviral Res.* **2005**, *67*, 1-9.

¹⁵ For recent reviews see: (a) Mathé, C.; Périgaud, C. *Eur. J. Org. Chem.* **2008**, 1489-1505. (b) Lebreton, J.; Escudier, J.-M.; Arzel, L.; Len, C. *Chem. Rev.* **2010**, *110*, 3371-3418.

nucleobase; and cyclic phosphoesters, obtained by linking the nucleobase or the furanose ring to the phosphorus atom.

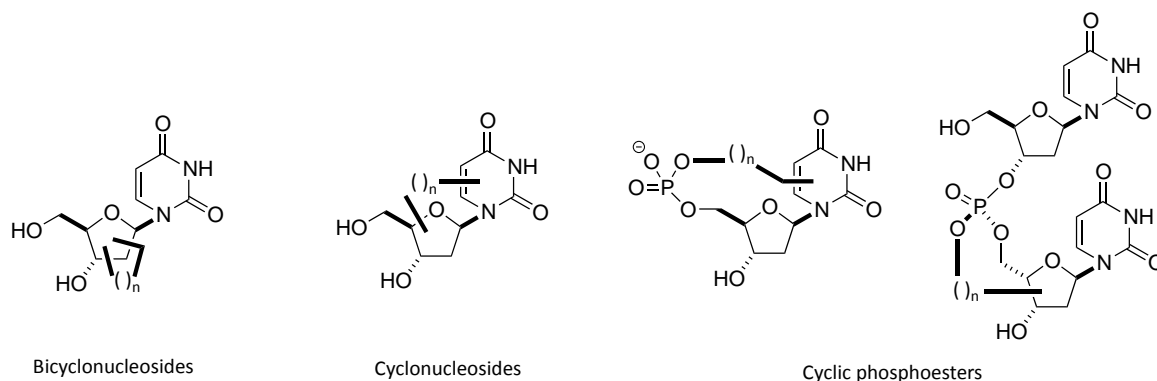


Figure 6. Types of nucleosides with restricted conformations.

The bicyclonucleosides have been so far the most studied family. Thus, bicyclonucleosides bearing a 2',3'-, 2',4'-, or 3',4'-bicyclic core have been synthesized (Figure 7).^{15,§}

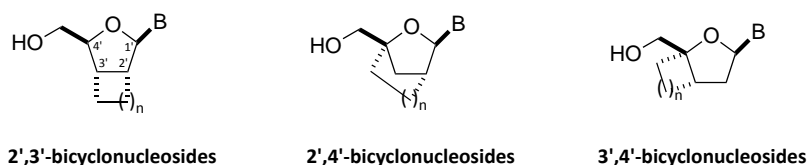


Figure 7. Examples of 2',3'-, 2',4'- and 3',4'-bicyclonucleosides.

Among them, this work will focus on those conformationally locked by the presence of an alkyl chain or analogues fused to the 2',3'-positions. The synthetic efforts towards these targets have led to the preparation of several nucleosides with restricted binding conformations. Nevertheless, only a few of these compounds have been evaluated as antiviral agents, and basically, their biological evaluation has been limited to HIV (Figure 8). Thus, of the series of *endo*-oriented cyclopropane nucleosides **1** described by Chu and co-workers,¹⁶ none of them showed significant activity against HIV in human PBM cells. Within their *exo*-counterparts, only the cytosine and thymine derivatives **2** and **3** have been evaluated. While the former showed weak activity,¹⁷ the latter was found inactive.¹⁸ Finally, Gotor and Theodorakis described the

[§] In this work, the usual non-systematic numbering of the nucleosides has been used. The systematic numbering of these compounds can be found in the experimental section.

¹⁶ Chun, B. K.; Olgen, S.; Hong, J. H.; Newton, M. G.; Chu, C. K. *J. Org. Chem.* **2000**, *65*, 685-693.

¹⁷ Beard, R. A.; Butler, P. I.; Mann, J.; Parlett, N. K. *Carbohydr. Res.* **1990**, *205*, 87-91.

¹⁸ Sard, H. *Nucleosides Nucleotides* **1994**, *13*, 2321-2328.

synthesis of the family of cyclohexene nucleosides **4**.¹⁹ In this case, moderate activity was found for the inosine derivative ($EC_{50}=12.3 \mu\text{M}$).

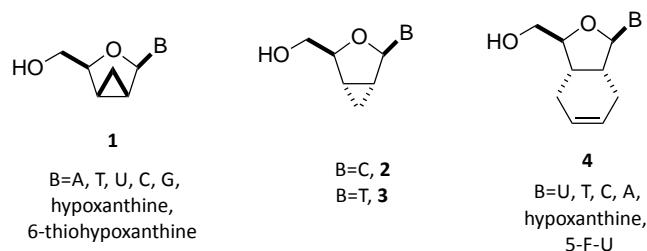


Figure 8. Some examples of constrained nucleosides evaluated as antiviral agents.

These conformational constraints are not only limited to simple carbon chains; compounds containing 2',3'-fused heterocycles (i.e. oxirane and oxetane rings) have also been prepared (Figure 9). Thus, in 1988, Webb and co-workers described the synthesis and antiviral evaluation of the *endo*-oxiranes **5**.²⁰ In this case, the cytosine derivative showed significant anti-HIV activity, however, its cytotoxicity was also important. The adenine nucleosides **6** and **7** synthesized by De Clercq and co-workers²¹ were also tested against HIV without success. On the other hand, the oxetane series include structures such as **8** and **9**. The oxetane derivative **8**, synthesized by Mikhailopulo et al. was tested against several viruses including HSV-1 and HSV-2 but it was found inactive.²² Lastly, Nielsen and co-workers synthesized the AZT analogue **9**, although it neither showed activity against HIV.²³

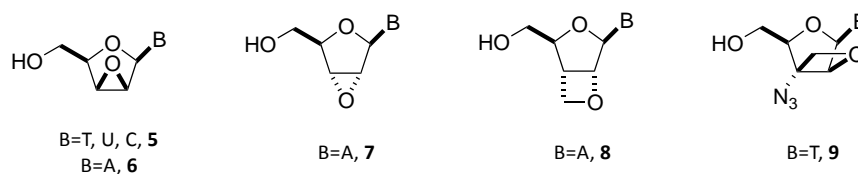


Figure 9. Nucleosides constrained by the presence of a 2',3'-fused heterocycle.

Unfortunately, the scarce number of analogues that have been hitherto evaluated is hampering a broader conformational-activity study that could help to determine the conformational preferences of the targeted enzymes. In this regard, our group is developing a

¹⁹ Díaz-Rodríguez, A.; Sanghvi, Y. S.; Fernández, S.; Schinazi, R. F.; Theodorakis, E. A.; Ferrero, M.; Gotor, V. *Org. Biomol. Chem.* **2009**, *7*, 1415-1423.

²⁰ Webb, T. R.; Mitsuya, H.; Broder, S. *J. Med. Chem.* **1988**, *31*, 1475-1479.

²¹ Herdewijn, P.; Balzarini, J.; Baba, M.; Pauwels, R.; Van Aerschot, A.; Janssen, G.; De Clercq, E. *J. Med. Chem.* **1988**, *31*, 2040-2048.

²² Mikhailopulo, I. A.; Poopeiko, N. E.; Tsvetkova, T. M.; Marochkin, A. P.; Balzarini, J.; De Clercq, E. *Carbohydr. Res.* **1996**, *285*, 17-28.

²³ Sørensen, M. H.; Nielsen, C.; Nielsen, P. *J. Org. Chem.* **2001**, *66*, 4878-4886.

research program directed to the synthesis and conformational analysis of a novel class of nucleoside analogues with the glycone moiety conformationally restricted by a two-carbon chain fused to the 2' and 3' positions of the sugar ring (Figure 10).²⁴ Introduction of the carbon chain flattens the sugar ring and, at the same time, confers a certain degree of rigidity comparable to that of d4T and d4A. Moreover, the higher lipophilicity of the C₂ fragment over the double bond should improve cell penetration and increase resistance to hydrolytic processes.²⁵ In an attempt to expand the scope of this study, the cyclobutene analogues **12** and **13**, the 2'-halonucleosides **14-19** and the aza-derivatives **20** and **21** have been recently synthesized.²⁶

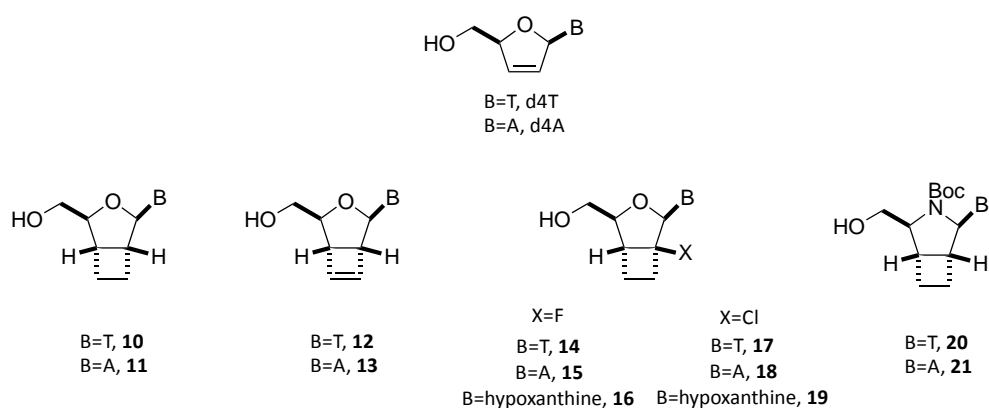


Figure 10. Structures of **d4T**, **d4A** and nucleosides built on a bicyclo[3.2.0]heptane scaffold.

As it has been mentioned earlier, carbocyclic nucleosides constitute another interesting family of nucleoside analogues. These nucleosides have been a subject of great interest in synthetic medicinal chemistry for the past decades.²⁷ Particularly, the discovery of Abacavir²⁸ and Entecavir (ETV)²⁹ as effective antiviral agents prompted the study of various carbocyclic nucleosides (Figure 11). This search for new active nucleoside analogues has been primarily focused on the cyclopentane derivatives. Examples of their three, four and six-member counterparts are much more limited, even though they have shown interesting biological properties. For example, compound **22**, described by Tsuji and co-workers, was found to be highly active against HSV-1,

²⁴ (a) Alibés, R.; Álvarez-Larena, A.; de March, P.; Figueredo, M.; Font, J.; Parella, T.; Rustullet, A. *Org. Lett.* **2006**, *8*, 491-494.

²⁵ York, J. L. *J. Org. Chem.* **1981**, *46*, 2171-2173.

²⁶ (a) Flores, R.; Alibés, R.; Figueredo, M.; Font, J. *Tetrahedron* **2009**, *65*, 6912-6917. (b) Flores, R.; Rustullet, A.; Alibés, R.; Álvarez-Larena, A.; de March, P.; Figueredo, M.; Font, J. *J. Org. Chem.* **2011**, *76*, 5369-5383.

²⁷ For a recent review see: Wang, J.; Rawal, R. K.; Chu, C. K. In *Medicinal Chemistry of Nucleic Acids*, John Wiley & Sons: Hoboken, NJ, USA, 2011, Chapter 1, 1-100.

²⁸ Crimmins, M. T.; King, B. W. *J. Org. Chem.* **1996**, *61*, 4192-4193.

²⁹ Bisacchi, G. S.; Chao, S. T.; Bachard, C.; Daris, J. P.; Innaïmo, S.; Jacobs, G. A.; Kocy, O.; Lapointe, P.; Martel, A.; Merchant, Z.; Slusarchyk, W. A.; Sundeen, J. E.; Young, M. G.; Colonno, R.; Zahler, R. *Bioorg. Med. Chem. Lett.* **1997**, *7*, 127-132.

HSV-2 and VZV.³⁰ In a similar manner, the cyclobutane nucleosides Cyclobut-A, **23**, and Cyclobut-G (Lobucavir), **24**, exhibited a broad-spectrum of antiviral activity against HBV and herpes viruses.³¹ Finally, the cyclohexene nucleoside Cyclohexenyl-G, **25**, displayed powerful activity against herpes virus.³² The interesting antiviral profile of this compound prompted our research group to design an enantiodivergent approach towards the cyclohexenyl nucleoside analogues **26** and **27**.³³

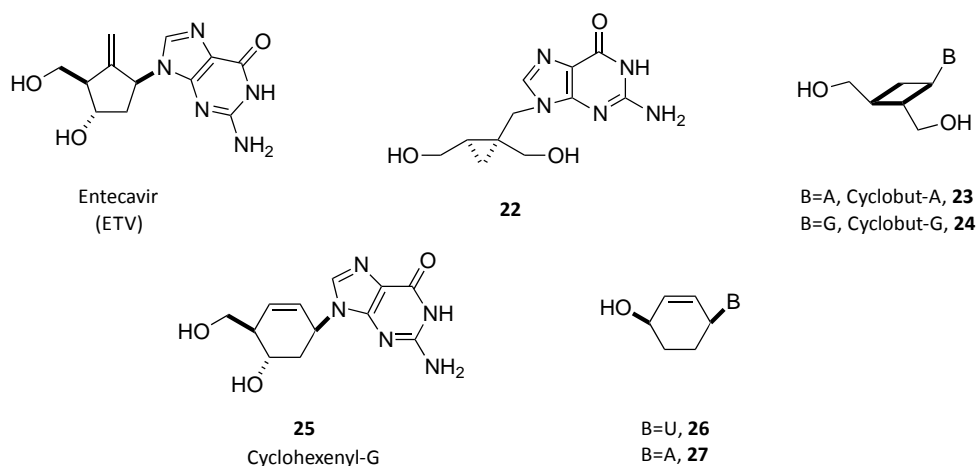


Figure 11. Biologically active carbocyclic nucleosides.

Although the synthesis of nucleoside analogues has advanced considerably, more efficient and practical methods are still in demand for the preparation of chiral key intermediates leading to biologically active compounds.

³⁰ (a) Sekiyama, T.; Hatsuya, S.; Tanaka, Y.; Uchiyama, M.; Ono, N.; Iwayama, S.; Oikawa, M.; Suzuki, K.; Okunishi, M.; Tsuji, T. *J. Med. Chem.* **1998**, *41*, 1284-1298. (b) Iwayama, S.; Ono, N.; Ohmura, Y.; Suzuki, K.; Aoki, M.; Nakazawa, H.; Oikawa, M.; Kato, T.; Okunishi, M.; Nishiyama, Y. *Antimicrob. Agents Chemother.* **1998**, *42*, 1666-1670.

³¹ (a) Honjo, M.; Maruyama, T.; Sato, Y.; Horii, T. *Chem. Pharm. Bull.* **1989**, *37*, 1413-1415. (b) Ichikawa, Y.-I.; Narita, A.; Shiozawa, A.; Hayashi, Y.; Narasaka, K. *J. Chem. Soc., Chem. Commun.* **1989**, 1919-1921.

³² Wang, J.; Froeyen, M.; Hendrix, C.; Andrei, G.; Snoeck, R.; De Clercq, E.; Herdewijn, P. *J. Med. Chem.* **2000**, *43*, 736-745.

³³ Ferrer, E.; Alibés, R.; Busqué, F.; Figueredo, M.; Font, J.; de March, P. *J. Org. Chem.* **2009**, *74*, 2425-2432.

2. PRECEDENTS

In the last couple of decades, our research group has synthesized several natural cyclobutane compounds using as a key step a [2+2] photochemical reaction of a chiral 2(5*H*)-furanone with different alkenes. Thus, pheromones such as (+)-Grandisol,³⁴ **28** (Figure 12), secreted by male boll weevil (*Anthonomus grandis*) and (+)-Lineatin,³⁵ **29**, secreted by female ambrosia beetles (*Trypodendron lineatum*) have been successfully synthesized. The same strategy has also allowed the preparation of the advanced intermediate **30** (Figure 13), which could lead to sesquiterpenes Dunniane,³⁶ **31**, and Cumacrene,³⁷ **32**, (isolated from the chinese plant *Illicium dunnianum* and from the californian cypress *Cupressus macrocarpa*, respectively).

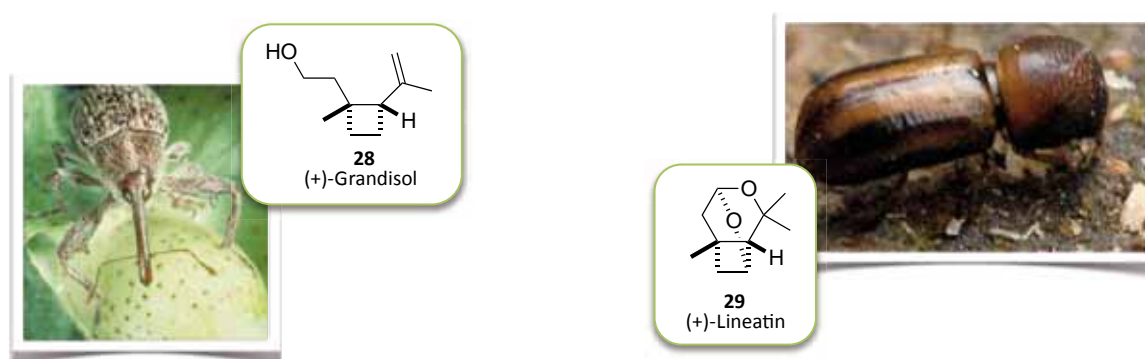


Figure 12. Structure of the pheromones (+)-Grandisol and (+)-Lineatin.

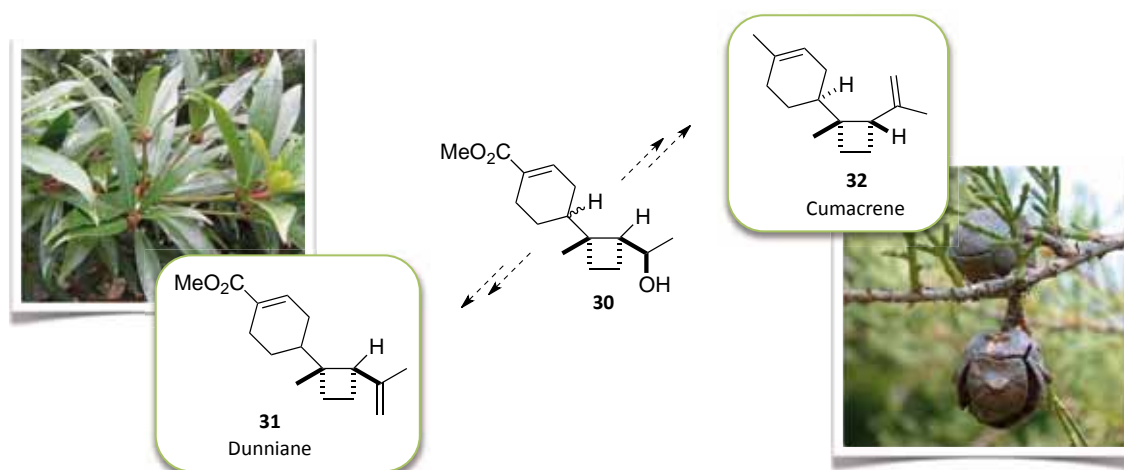


Figure 13. Structure of the sesquiterpenes Dunniane and Cumacrene.

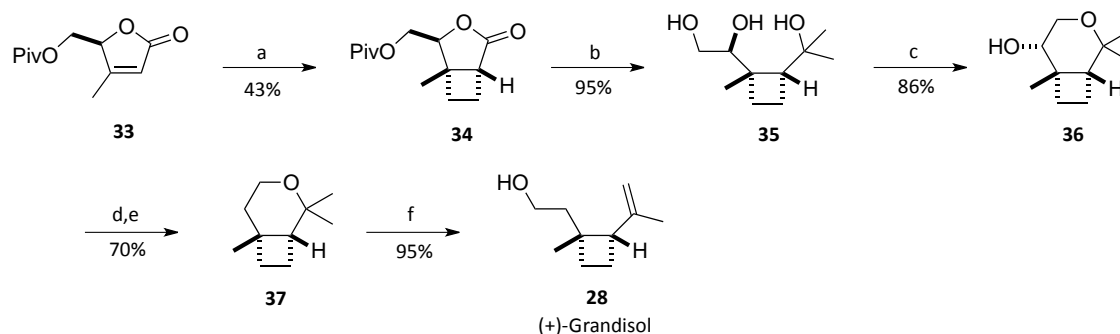
³⁴ Tumilson, J. H.; Hardee, D. D.; Gueldner, R. C.; Thompson, A. C.; Hedin, P. A.; Minyard, J. P. *Science* **1969**, *166*, 1010-1012.

³⁵ MacConnell, J. G.; Borden, J. H.; Silverstein, R. M.; Stokink, E. *J. Chem. Ecol.* **1977**, *3*, 549-561.

³⁶ Sy, L.-K.; Brown, G. D. *Phytochemistry* **1998**, *47*, 301-302.

³⁷ Cool, L. G. *Phytochemistry* **2005**, *66*, 249-260.

The synthesis of (+)-Grandisol started from the chiral 2(5*H*)-furanone **33** (Scheme 1).³⁸ Construction of the cyclobutane ring was stereoselectively accomplished by the [2+2] photocycloaddition of **33** to ethylene. Then, treatment with an excess of MeLi resulted in the addition of two methyl groups to the lactone carbonyl carbon and simultaneous removal of the pivaloyl protecting group. From this point, cyclization and removal of the secondary hydroxyl group using the Barton-McCombie methodology led to the bicyclo compound **37**, which upon treatment with LDA afforded (+)-Grandisol in 24% global yield.



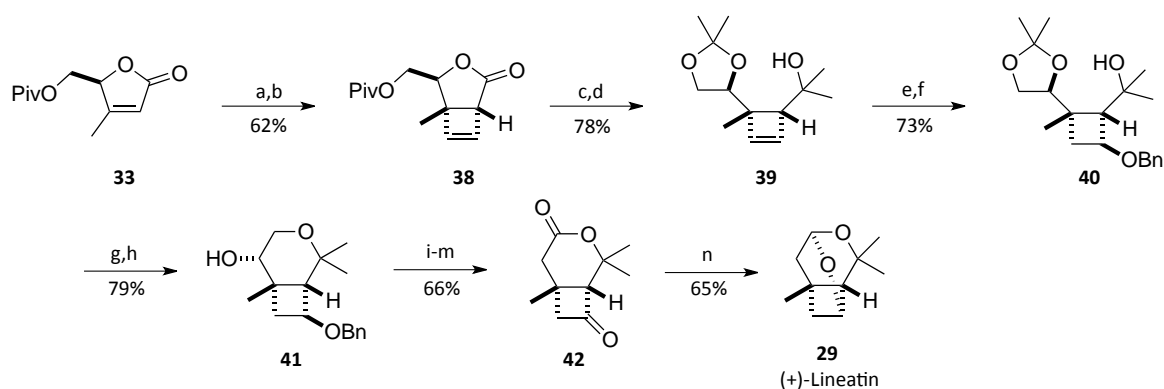
Scheme 1. Synthesis of (+)-Grandisol.

Pheromone (+)-Lineatin was synthesized using the same chiral precursor **33** (Scheme 2).³⁹ Photocycloaddition of **33** to (*Z*)-1,2-dichloroethylene and subsequent reductive dehalogenation of the photochemical mixture using Zn under MW irradiation provided adduct **38** as a major compound.

After functionalization of the cyclobutene ring by means of an oxymercuration-demercuration process, the pyran ring was installed and oxidized to the keto lactone **42**, which was converted into the target compound by double carbonyl reduction and acid-catalyzed acetalization. The natural compound was obtained in 15% global yield.

³⁸ Alibés, R.; Bourdelande, J. L.; Font, J.; Parella, T. *Tetrahedron* **1996**, *52*, 1279-1292.

³⁹ (a) Alibés, R.; de March, P.; Figueredo, M.; Font, J.; Racamonde, M.; Parella, T. *Org. Lett.* **2004**, *6*, 1449-1452. (b) Racamonde, M.; Alibés, R.; Figueredo, M.; Font, J.; de March, P. *J. Org. Chem.* **2008**, *73*, 5944-5952.

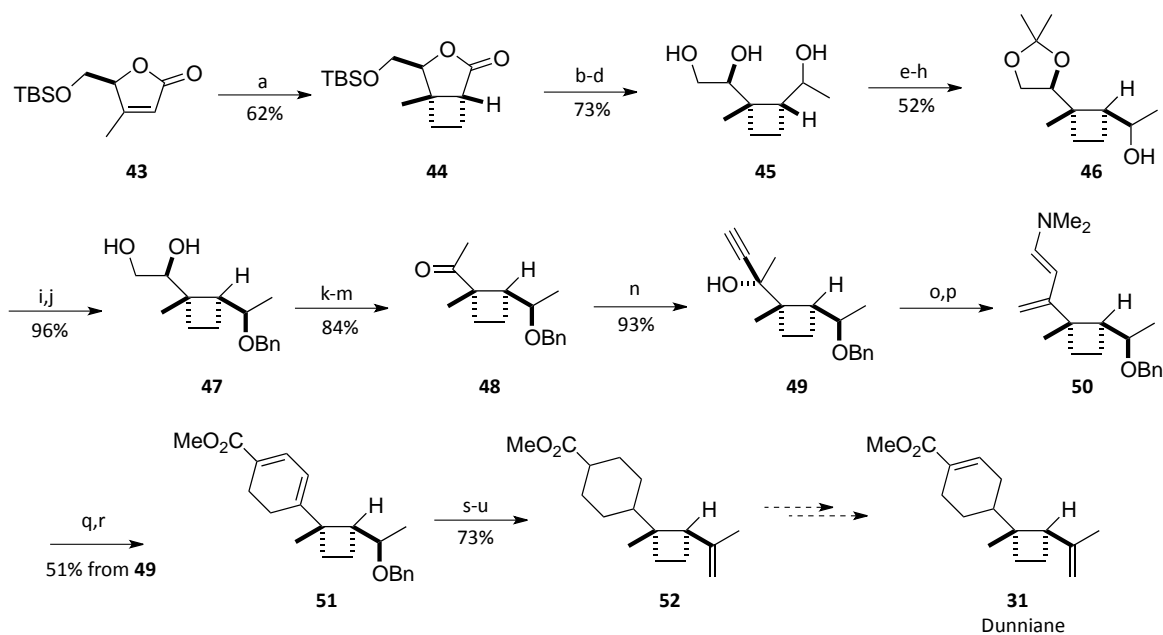


a) $h\nu$, (Z)-1,2-dichloroethylene, CH_3CN ; b) Zn, EtOH (80%), MW; c) MeLi, THF; d) *p*-TsOH, acetone; e) $\text{Hg}(\text{OAc})_2$, THF- H_2O , NaBH_4 , NaOH; f) NaH, BnBr, THF; g) TFA, MeOH- H_2O ; h) TsCl, DMAP, py; i) TCDI, THF; j) Bu_3SnH , AIBN, toluene; k) H_2 , Pd/C, EtOAc/AcOH; l) DMP, CH_2Cl_2 ; m) RuCl_3 , NaIO_4 , CCl_4 - H_2O ; n) DIBAL-H, Et_2O , tartaric acid.

Scheme 2. Synthesis of (+)-Lineatin.

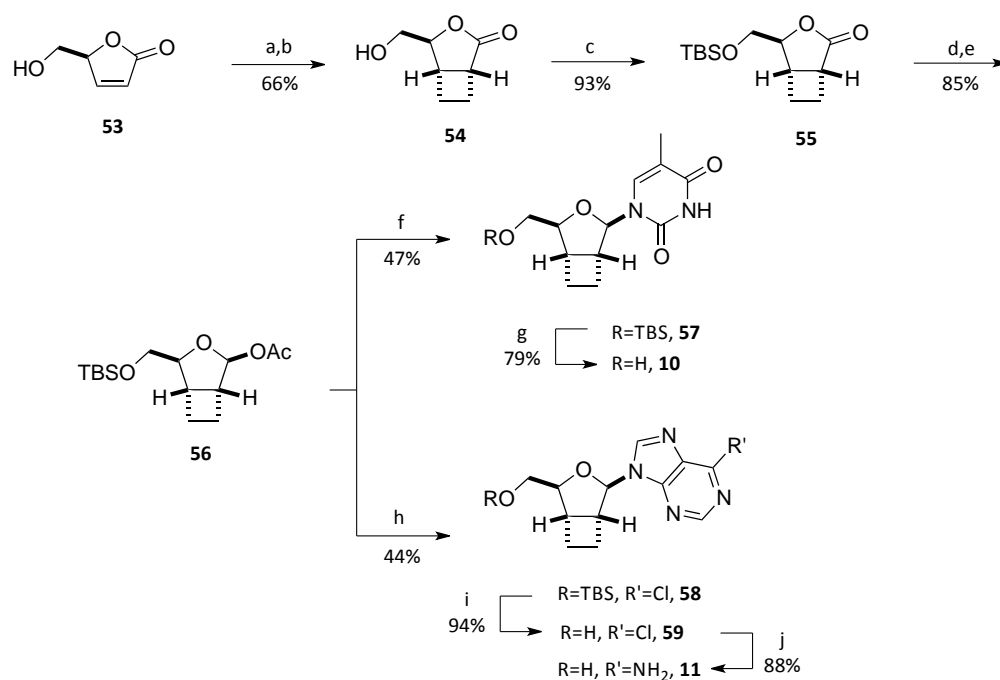
Recently, intermediate **52**, which presents the entire carbon skeleton of sesquiterpenes Dunniane and Cumacrene, has been synthesized.⁴⁰ Its preparation started with the [2+2] photocycloaddition of furanone **43** to ethylene to establish the cyclobutane ring (Scheme 3). Successive transformations allowed access to the methylketone **48**, which was alkylated affording propargyl alcohol **49**. Then, this alcohol was converted by a Meyers-Schuster type rearrangement into a diene, which served as substrate for a Diels-Alder reaction with methyl acrylate to construct the six-membered ring. Finally, hydrogenation and Dess-Martin oxidation followed by a methylenation reaction delivered **52** in 7% global yield.

⁴⁰ Parés, S.; Alibés, R.; Figueredo, M.; Font, J.; Parella, T. *Eur. J. Org. Chem.* **2012**, 1404-1417.



Scheme 3. Synthesis of key intermediate **52**.

The [2+2] photocycloaddition of chiral 2(5*H*)-furanones to alkenes has also been successfully applied to the synthesis of cyclobutane nucleosides. In 2006,²⁴ we reported the synthesis of the conformationally restricted nucleosides **10** and **11** (Scheme 4). The preparation of both compounds started from the ready available 2(5*H*)-furanone **53**, which was subjected to a photochemical reaction with (*Z*)-1,2-dichloroethylene in acetonitrile followed by a dihydrodehalogenation reaction with tri-*n*-butyltin hydride and AIBN in refluxing toluene to deliver the cycloadduct **54** as the major isomer. Successive modifications and introduction of the nucleobase under Vorbrüggen glycosylation conditions afforded the targeted 3-oxabicyclo[3.2.0]heptane nucleosides in seven steps and 19% yield for the thymine analogue **10**, and eight steps and 18% yield for the adenine analogue **11**.



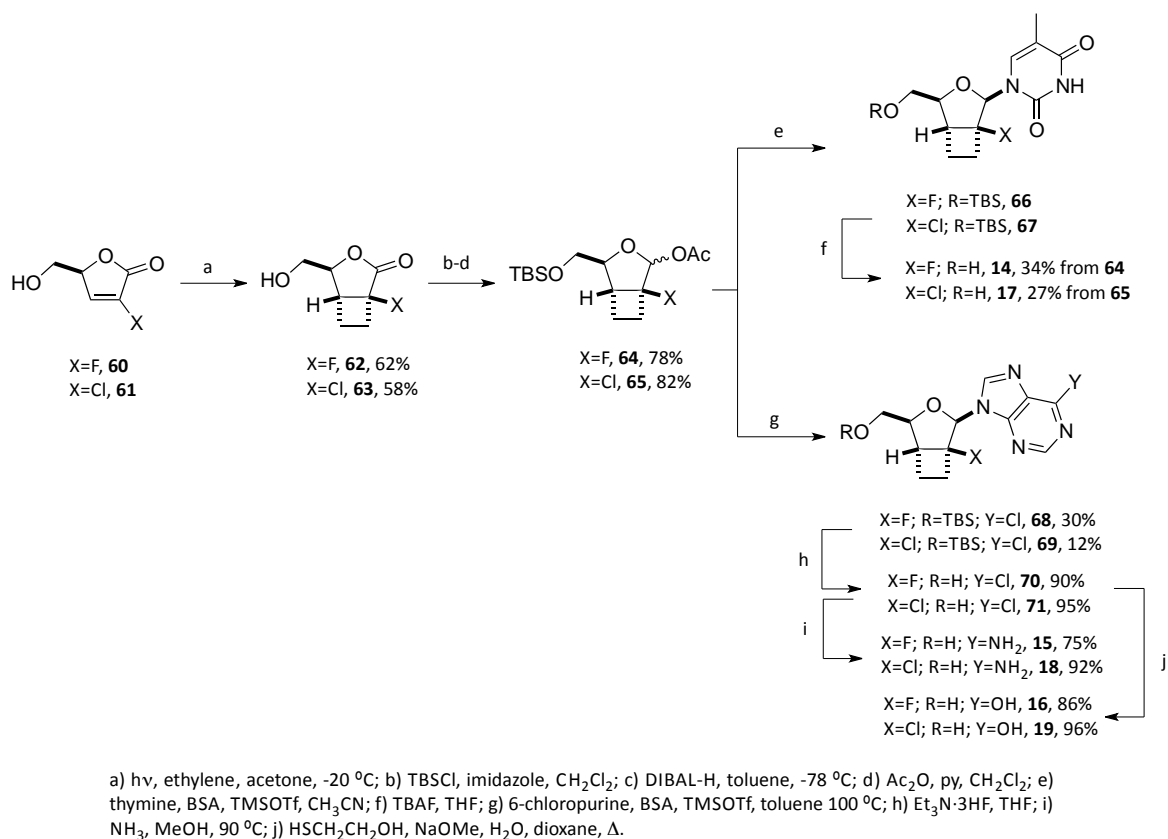
Scheme 4. Synthesis of the 3-oxabicyclo[3.2.0]heptane nucleoside analogues **10** and **11**.

This last derivative was found to exhibit moderate activity against HIV-1 ($EC_{50}=17.8 \mu\text{g/mL}$)^{26b} and stimulated the study of related compounds. Thus, in an attempt to enhance their antiviral activity, the cyclobutene analogues of **10** and **11**, and nucleosides bearing heteroatoms on their structure were envisaged. Hence, following similar approximations, cyclobutene nucleosides **12** and **13**, the 2'-halonucleosides **14-19** (Scheme 5), and the azanucleosides **20** and **21** (Scheme 6), were synthesized.

Since the presence of a fluorine atom at the 2'-position of a nucleoside is known to stabilize the glycosyl bond and provides interesting biological properties,^{41,42} our research group has developed a sequence to prepare restricted nucleoside analogues bearing a halogen atom (either fluorine or chlorine) at the 2' position (Scheme 5).^{26b} The synthesis followed a similar photocycloaddition-acetylation-glycosylation pattern described above and provided the six novel nucleosides **14-19** with yields comprised between 5-16%. Interestingly, the chlorine derivative **18** showed moderate activity against HIV-1 ($EC_{50}=22.9 \mu\text{g/mL}$).

⁴¹ (a) Smart, B. E. *J. Fluorine Chem.* **2001**, *109*, 3-11. (b) Shimizu, M.; Hiyama, T. *Angew. Chem. Int. Ed.* **2005**, *44*, 214-231.

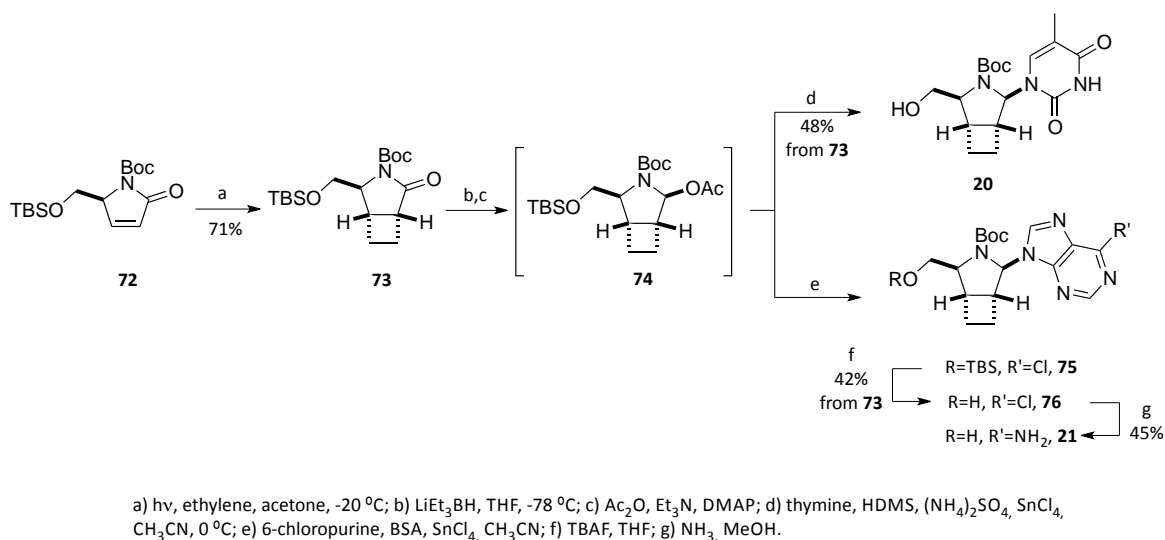
⁴² (a) Ruxrungtham, K.; Boone, E.; Ford, H. Jr.; Driscoll, J. S.; Davey, R. T.; Lane, H. C. *Antimicrob. Agents Chemother.* **1996**, *40*, 2369-2374. (b) Ma, T.; Pai, S. B.; Zhu, Y. L.; Lin, J. S.; Shanmuganathan, K.; Du, J.; Wang, C.; Kim, H.; Newton, M. G.; Cheng, Y.-C.; Chu, C. K. *J. Med. Chem.* **1996**, *39*, 2835-2843.



Scheme 5. Synthesis of the 2'-halonucleosides **14-19**.

To date, several examples of azanucleosides, compounds in which the furanose ring has been replaced by a pyrrolidine ring, have been described.⁴³ However, 2',3'-cyclobutane-fused azanucleosides had remained unexplored. For this reason, a synthetic route to nucleosides **20** and **21** was designed (Scheme 6).^{26a} In this approach, the bicyclic core was established by the [2+2] photocycloaddition of ethylene to the γ -lactam **72**. Reduction and acetylation of the resulting hemiaminal and nucleobase introduction delivered nucleosides **20** and **21** in 34% and 13% yield, respectively. These two novel azanucleosides were evaluated for anti-HIV-1 activity, however, none of them showed activity below the 25 μ g/mL threshold.

⁴³ (a) Yokoyama, M.; Momotake, A. *Synthesis* **1999**, 9, 1541-1554. (b) Romeo, G.; Chiacchio, U.; Corsaro, A.; Merino, P. *Chem. Rev.* **2010**, 110, 3337-3370.



Scheme 6. Synthesis of azanucleosides **20** and **21**.

The interesting biological properties of carbocyclic nucleosides have already been pointed out on the previous section, and two of the few cyclobutane nucleosides synthesized to date, Cyclobut-A and G, have been highlighted. These two compounds are analogues of Oxetanocin-A (Figure 14), a naturally occurring oxetane nucleoside isolated from the fermentation broth of *Bacillus megaterium*,⁴⁴ which was found to exhibit antiviral and antibacterial properties.⁴⁵ On top of that, subsequent studies of this distinctive nucleoside unveiled strong HIV expression inhibition.⁴⁶

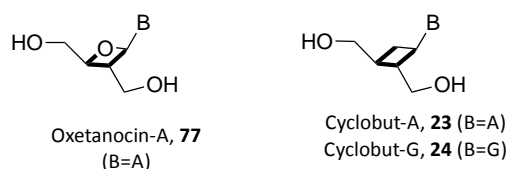


Figure 14. Oxetanocin-A and their carbocyclic analogues.

Despite the number of syntheses leading to Cyclobut-A, the majority of them involve large number of steps resulting in low overall yields. Taking into account these results, our research group undertook the task of trying to improve those synthetic approaches.

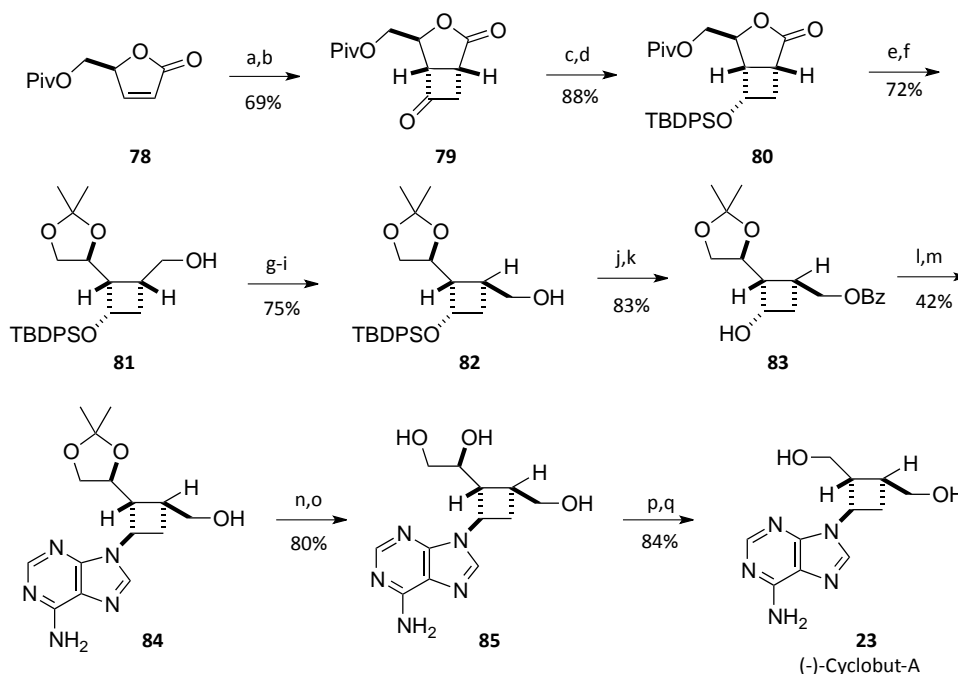
Our synthesis began with the [2+2] photocycloaddition of ketene diethyl acetal to the pivaloyl-protected 2(5*H*)-furanone **78** (Scheme 7). Subsequent hydrolysis of the acetal on the obtained adduct rendered the bicyclic cyclobutanone **79**. Further modifications led to lactone **80**, which was reduced, protected as an acetonide and epimerized to give **82**. Then, protection of the

⁴⁴ Shimada, N.; Hasegawa, S.; Harada, T.; Tomisawa, T.; Fujii, A.; Takita, T. *J. Antibiot.* **1986**, *39*, 1623-1625.

⁴⁵ Nakamura, H.; Hasegawa, S.; Shimada, N.; Fujii, A.; Takita, T.; Takita, Y. *J. Antibiot.* **1986**, *39*, 1626-1629.

⁴⁶ Hoshino, H.; Shimizu, N.; Shimada, N.; Takita, T.; Takeuchi, T. *J. Antibiot.* **1987**, *40*, 1077-1078.

primary hydroxyl group, introduction of the adenine moiety by a classical S_N2 methodology and hydrolysis of the acetonide, delivered the cyclobutane **85**. Finally, oxidative cleavage of the 1,2-diol and reduction of the resulting aldehyde afforded (-)-Cyclobut-A, **23**, in 17 steps and 4% global yield.⁴⁷



a) $h\nu$, ketene diethyl acetal, diethyl ether, $-20\text{ }^\circ\text{C}$; b) *p*-TsOH, acetone, $56\text{ }^\circ\text{C}$; c) L-Selectride, THF, $-78\text{ }^\circ\text{C}$; d) TBDPSCI, imidazole, THF; e) LiAlH_4 , THF, $0\text{ }^\circ\text{C}$; f) acetone, CuSO_4 , HCl (cat.); g) DMP, CH_2Cl_2 ; h) Na_2CO_3 , MeOH; i) NaBH_4 , MeOH; j) BzCl, py, CH_2Cl_2 ; k) TBAF, THF; l) MsCl, Et_3N , CH_2Cl_2 ; m) adenine, K_2CO_3 , 18-C-6, DMF, $120\text{ }^\circ\text{C}$; n) Na_2CO_3 , MeOH; o) TFA- H_2O ; p) NaIO_4 , THF- H_2O ; q) NaBH_4 , MeOH, $0\text{ }^\circ\text{C}$.

Scheme 7. Synthesis of (-)-Cyclobut-A.

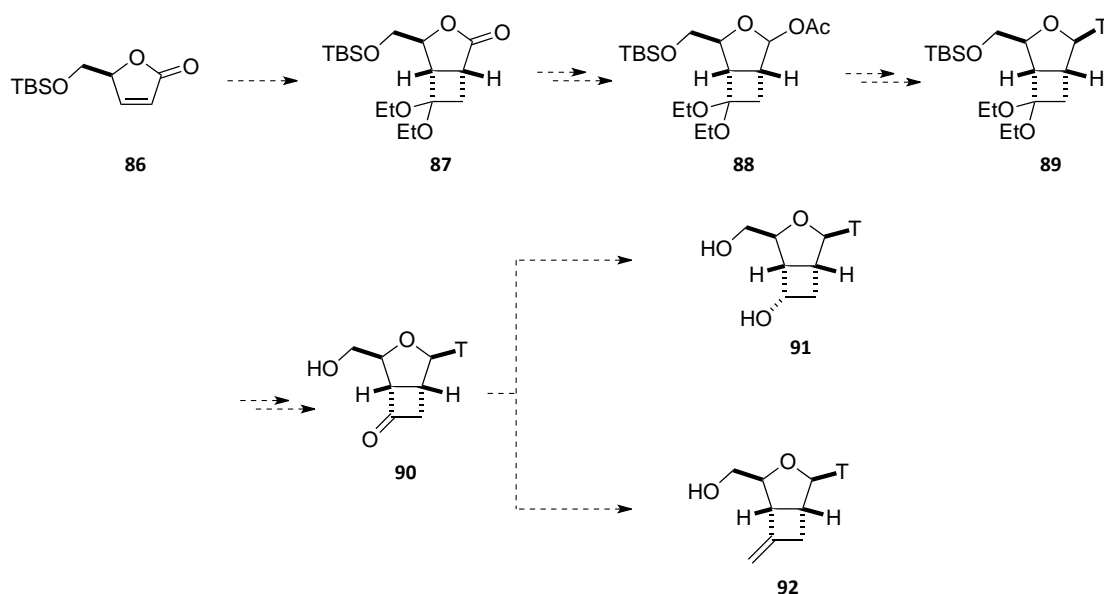
⁴⁷ Rustullet, A.; Alibés, R.; de March, P.; Figueredo, M.; Font, J. *Org. Lett.* **2007**, *9*, 2827-2830.

3. OBJECTIVES

Considering this background, the present work is aimed towards the enantioselective synthesis of novel cyclobutane nucleosides and their evaluation as potential antiviral agents. Consequently, we have focused on two main objectives which share the utilization of a [2+2] photocycloaddition reaction as a key step to create the cyclobutane core.

□ **Objective 1. Synthesis of cyclobutane-fused nucleosides bearing an additional functionalization on the cyclobutane ring.**

In order to complement our studies on conformationally restricted nucleosides, we plan to synthesize the enantiopure thymine nucleosides **90-92** (Scheme 8) which are analogues of d4T. Their synthesis will start with a [2+2] photocycloaddition of **86** to 1,1-diethoxyethylene to install the functionalized cyclobutane present in the bicyclic lactone **87**. Reduction and acetylation of this intermediate will provide acetate **88**, a suitable substrate to introduce the nucleobase using the Vorbrüggen *N*-glycosylation methodology and achieve the keto-nucleoside **90**. The carbonyl moiety in **90** would provide a site for further modifications to obtain other analogues featuring for example a hydroxyl group, **91**, or a methylene unit, **92**.

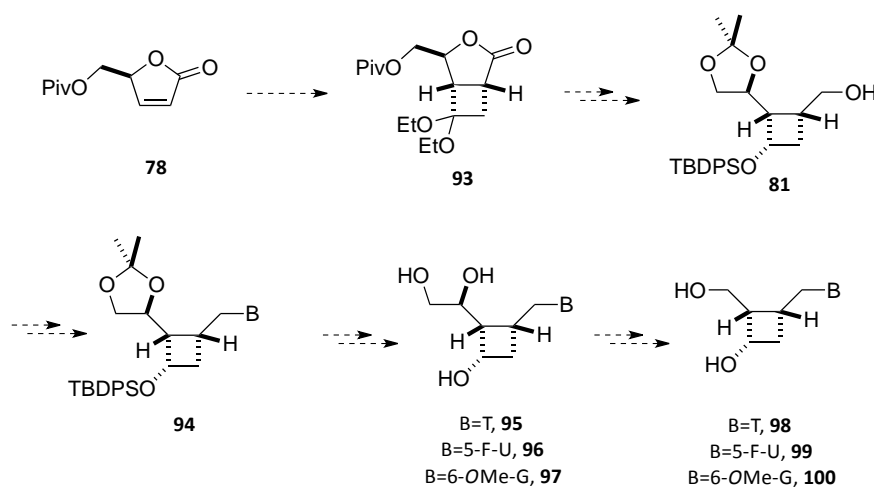


Scheme 8. Planned synthetic strategy towards the conformationally restricted nucleosides **90-92**.

Finally, these novel bicyclo[3.2.0]heptane nucleosides would be screened for antiviral activity and a molecular modelling study would be performed in order to shed light on their interaction with the enzymes involved in the three phosphorylation steps as well as HIV-RT.

□ **Objective 2. Synthesis of cyclobutane L-nucleoside analogues.**

The second objective is devoted to the enantiopure synthesis and antiviral activity evaluation of the novel cyclobutane L-nucleosides **95-100** (Scheme 9). In this case, we plan to exploit an analogous synthetic sequence to reach the known intermediate **81**, a key substrate that should allow introduction of different nucleobases employing Mitsunobu's methodology. Then, these intermediates will be transformed into the family of trihydroxylated nucleosides, **95-97**. Lastly, we will attempt an oxidative cleavage of these substrates that would lead to the new group of nucleoside analogues **98-100**.



Scheme 9. Planned synthetic strategy towards the synthesis of cyclobutane L-nucleosides **95-100**.

Finally, these newly synthesized cyclobutane L-nucleosides would be screened for antiviral activity against different viruses such as HSV, vaccinia virus and influenza.

II. [2+2] Photocycloaddition

of Chiral Furanones to Ketene Diethyl Acetal

A word cloud of chemistry-related terms. The most prominent words are 'Reaction' and 'Photocycloaddition'. Other visible terms include 'Ketene', 'Synthesis', 'Solvent', 'Anti 2+2', 'Unsaturated', 'Regioselectivity', 'Alkene', 'Cyclobutane', 'Enone', 'Furanones', 'Acetal', 'HT', and 'Cycloadducts'.

Ketene
Synthesis Solvent
Reaction Anti 2+2 Unsaturated
Regioselectivity
Alkene
Cyclobutane Enone
Furanones Acetal HT
Cycloadducts
Photocycloaddition



1. INTRODUCTION

In our planned approach towards nucleosides **90-92** and **95-100** (Figure 15), the [2+2] photocycloaddition reaction plays a pivotal role to construct the cyclobutane core.

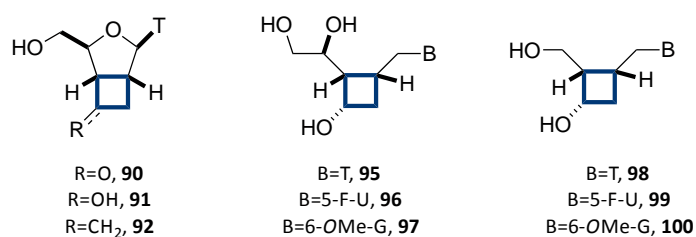


Figure 15. Synthetic targets of this work.

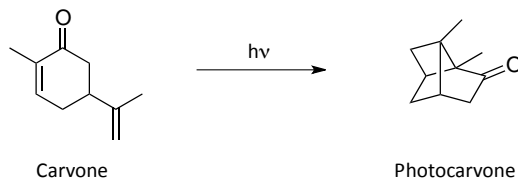
Photochemical reactions have been used to produce highly functionalized structures from simple substrates.⁴⁸ In particular, a number of challenging natural products bearing complex skeletons have been synthesized using photochemical processes.

The most widely used is the [2+2] photocycloaddition of α,β -unsaturated ketones or esters to unsaturated substrates, a convenient methodology when it comes to the synthesis of products with a cyclobutane moiety. The discovery of this reaction is granted to Ciamician and Silber one hundred years ago, who using sunlight as energy source transformed some organic compounds such as Carvone.⁴⁹ Although they could not elucidate unequivocally the photoproducts, these examples are considered the first [2+2] photocycloaddition reactions.

⁴⁸ For recent reviews see: (a) Iriondo-Alberdi, J.; Greaney, M. F. *Eur. J. Org. Chem.* **2007**, 4801-4815. (b) Hoffmann, N. *Chem. Rev.* **2008**, *108*, 1052-1103. (c) Bach, T.; Hehn, J. P. *Angew. Chem. Int. Ed.* **2011**, *50*, 1000-1045.

⁴⁹ Ciamician, G.; Silber, P. *Chem. Ber.* **1908**, *41*, 1928-1935.

Fifty years later, Büchi & Goldman reproduced the experiment and were able to characterize the product formed, naming it photocarvone (Scheme 10).⁵⁰ This work instigated other publications by Corey,⁵¹ Eaton⁵² and de Mayo,⁵³ who pioneered the interest on this reaction and recognized its synthetic potential.



Scheme 10. Intramolecular [2+2] photocycloaddition of Carvone.

Since then, the [2+2] photocycloaddition of enones to olefins has been widely used in natural product synthesis as a key step to create cyclobutane rings, allowing the synthesis of very complex and hindered molecules (Scheme 11). For instance, inter- or intramolecular versions of this reaction have been used in the total synthesis of Biyouyanagin A, **101**,⁵⁴ α -Bourbonene, **102**,⁵⁵ Kelsoene, **103**,⁵⁶ and Italicene, **104**.⁵⁷ It has also been applied to the synthesis of highly functionalized cyclobutane intermediates such as **105**,⁵⁸ used in Crimmins' synthesis of Ginkgolide B, or **107**,⁵⁹ an advanced intermediate in the still uncompleted synthesis of the diterpene Bielschowskysin.

⁵⁰ Büchi, G.; Goldman, I. M. *J. Am. Chem. Soc.* **1957**, *79*, 4741-4748.

⁵¹ Corey, E. J.; Bass, J. D.; LeMahieu, R.; Mitra, R. B. *J. Am. Chem. Soc.* **1964**, *86*, 5570-5583.

⁵² (a) Eaton, P. E. *J. Am. Chem. Soc.* **1962**, *84*, 2344-2348. (b) Eaton, P. E. *Tetrahedron Lett.* **1964**, *5*, 3695-3698. (c) Eaton, P. E. *Acc. Chem. Res.* **1968**, *1*, 50-57.

⁵³ de Mayo, P.; Reid, S. T.; Yip, R. W. *Can. J. Chem.* **1964**, *42*, 2828-2835.

⁵⁴ Nicolaou, K. C.; Sarlah, D.; Shaw, D. M. *Angew. Chem. Int. Ed.* **2007**, *46*, 4708-4711.

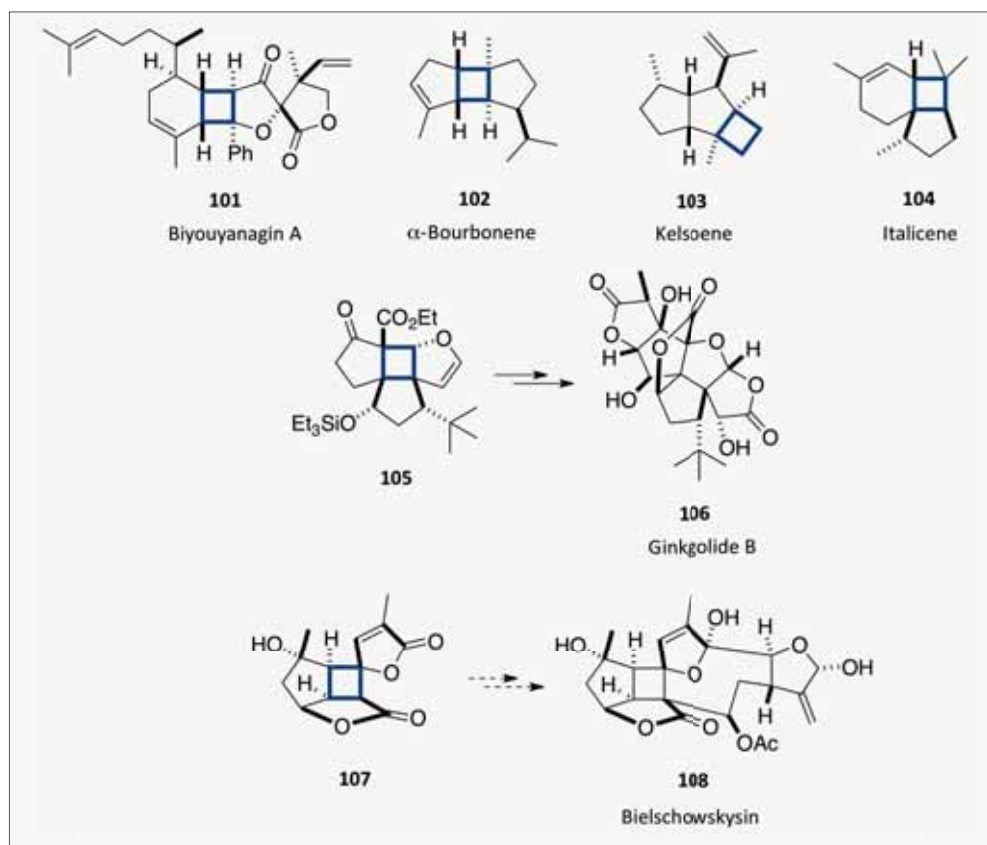
⁵⁵ White, J. D.; Gupta, D. N. *J. Am. Chem. Soc.* **1968**, *90*, 6171-6177.

⁵⁶ Piers, E.; Orellana, A. *Synthesis* **2001**, 2138-2142.

⁵⁷ Faure, S.; Piva, O. *Tetrahedron Lett.* **2001**, *42*, 255-259.

⁵⁸ Crimmins, M. T.; Pace, J. M.; Nantermet, P. G.; Kim-Meade, A. S.; Thomas, J. B.; Watterson, S. H.; Wagman, A. S. *J. Am. Chem. Soc.* **2000**, *122*, 8453-8463.

⁵⁹ Doroh, B.; Sulikowski, G. A. *Org. Lett.* **2006**, *8*, 903-906.



Scheme 11. Examples of cyclobutane-containing natural products.

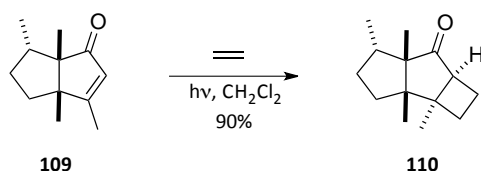
1.1 Precedents

1.1.1 [2+2] Photocycloaddition of enones to asymmetric alkenes

Many studies about induction of stereoselectivity in the photochemical reaction of cyclic α,β -unsaturated ketones with unsaturated substrates have been performed and applied to stereoselective synthesis.⁶⁰ A stereogenic center within the cyclic enone has been described to act as an effective control device producing good facial diastereoselectivity in many cases.

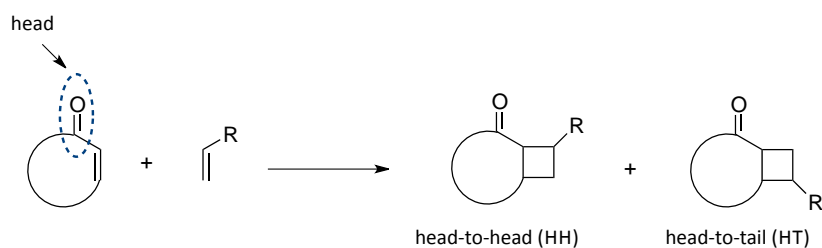
As an example, in the aforementioned synthesis of Kelsoene, **103**, Piers and Orellana described that the photochemical reaction of **109** with ethylene proceeded with total stereoselectivity, affording the tricyclic ketone **110** derived from an exclusive approach of the ethylene from the less hindered face of the enone **109** (Scheme 12).

⁶⁰ See for example: (a) Lange, G. L.; Decicco, C.; Tan, S. L.; Chamberlain, G. *Tetrahedron Lett.* **1985**, *26*, 4707-4710. (b) Demuth, M.; Palomer, A.; Sluma, H.-D.; Dey, A. K.; Krüger, C.; Tsay, Y.-H. *Angew. Chem. Int. Ed. Engl.* **1986**, *25*, 1117-1119. (c) Tsutsumi, K.; Nakano, H.; Furutani, A.; Endou, K.; Merpuge, A.; Shintani, T.; Morimoto, T.; Kakiuchi, K. *J. Org. Chem.* **2004**, *69*, 785-789. (d) García-Expósito, E.; Álvarez-Larena, A.; Branchadell, V.; Ortuño, R. M. *J. Org. Chem.* **2004**, *69*, 1120-1125. (e) Kemmler, M.; Herdtweck, E.; Bach, T. *Eur. J. Org. Chem.* **2004**, 4582-4595.



Scheme 12. [2+2] Photocycloaddition of **109** to ethylene.

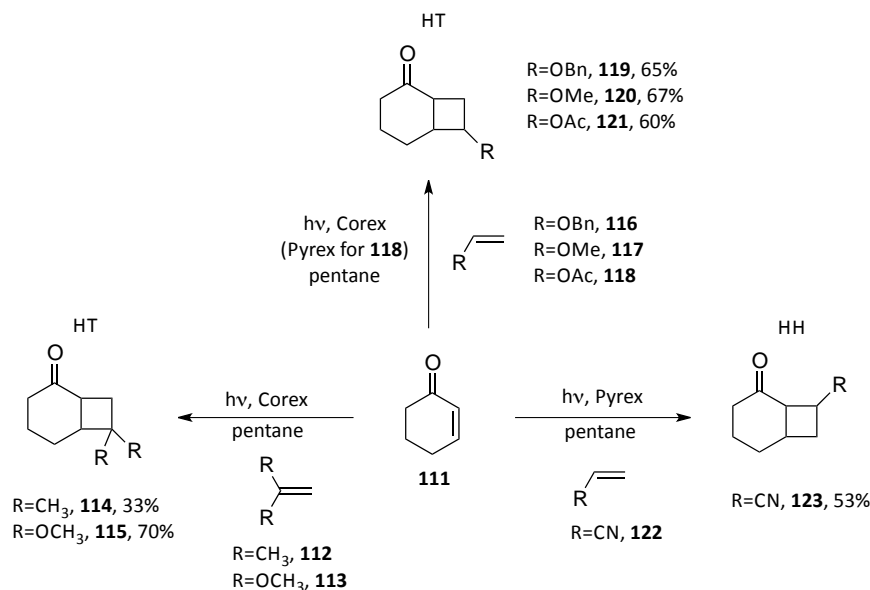
The use of asymmetric alkenes can limit the synthetic applicability of the [2+2] photocycloaddition due to the formation of regioisomers. Thus, in the [2+2] photocycloaddition of a cyclic enone to an asymmetric alkene, mixtures of head-to-head (HH) and head-to-tail (HT) compounds can be obtained (Scheme 13). In this nomenclature the carbonyl group from the enone is taken as reference (head). If the alkene substituent lies at the same side of the carbonyl group, the regioisomer is called head-to-head (HH), whereas if it lies in the opposite side it is termed head-to-tail (HT).



Scheme 13. Possible regioisomers obtained in the [2+2] photocycloaddition of a cyclic enone to an asymmetric alkene.

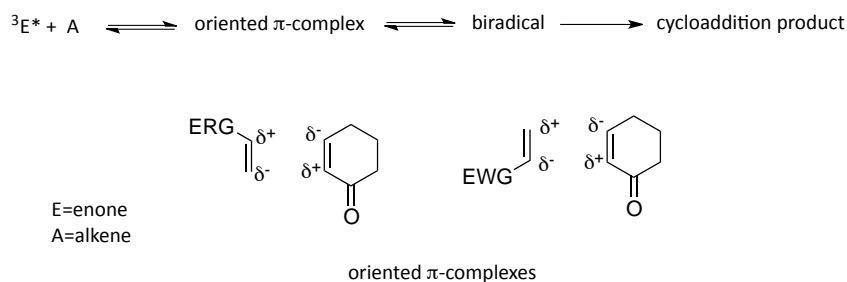
The first example of the use of an asymmetric alkene in a [2+2] photocycloaddition with a cyclic enone was reported by Corey and co-workers in the year 1964, and described the reaction between 2-cyclohexenone and isobutene.⁶¹ Later, the same authors expanded the scope of the study with different mono and disubstituted alkenes.⁵¹ The major products obtained in these reactions are shown in Scheme 14.

⁶¹ Corey, E. J.; Mitra, R. B.; Uda, H. *J. Am. Chem. Soc.* **1964**, *86*, 485-492.



Scheme 14. [2+2] Photocycloaddition of cyclohexenone to substituted alkenes.

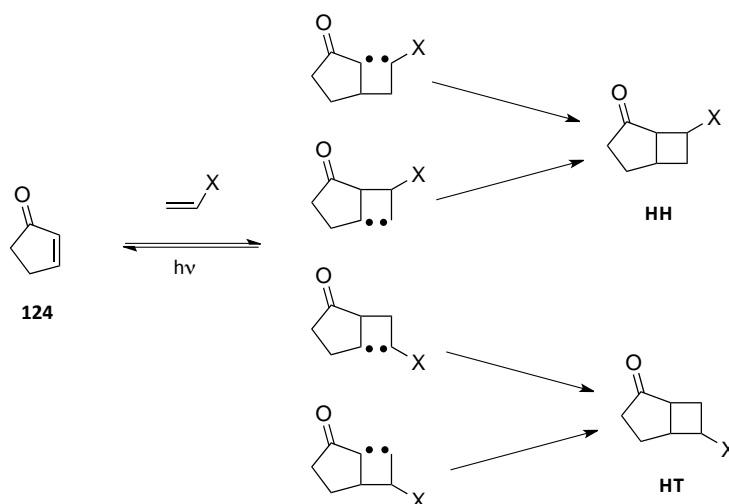
These studies disclosed that the reactions of enones with electronically rich olefins rendered mainly HT regioisomers, while the reactions that involved electronically poor olefins afforded mainly HH regioisomers. Considering these observations, Corey proposed that the first step of the reaction should involve the interaction of the enone triplet state with the ground state of the alkene to give an oriented π -complex (Scheme 15).⁵¹ This π -complex (which was later renamed as *exciplex*) could then progress to the formation of 1,4-biradicals (*vide infra*) and the final cycloadducts, which would retain the same regiochemistry of the π -complex. The formation of the exciplex would be governed by electrostatic interactions between partial charges of the polarized excited enone (with a polarization opposite to that of its ground state) and the alkene in its ground state polarization.



Scheme 15. Corey's mechanistic proposal.

This mechanistic proposal allowed to predict the regioselectivity of the reaction on the basis of the polarization of the olefin (Corey's rule). However, although this rule allowed to rationalize most experimental results, it failed to justify some cases, particularly those with alkenes bearing electron withdrawing groups (EWG). Moreover, no experimental evidence has been found that

supports the formation of the exciplex. For this reason, Bauslaugh proposed an alternative mechanism in which the 1,4-biradicals were directly formed without requiring exciplex formation (Scheme 16).⁶² In this mechanism, the regioselectivity of the process would be governed by the ratio of biradical intermediates formed and their tendency to revert to the initial substrates or progress to the final products. Further studies by Schuster⁶³ as well as radical trapping experiments carried out by Weedon and co-workers,⁶⁴ confirmed Bauslaugh's hypothesis.



Scheme 16. Biradical intermediates postulated by Bauslaugh for the [2+2] photocycloaddition of enones to asymmetric alkenes.

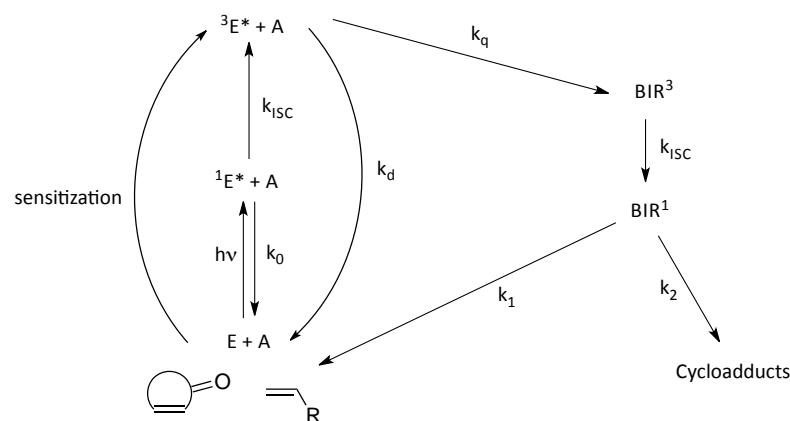
The currently accepted mechanism for the reaction is shown in Scheme 17.⁶⁵ According to this proposal, the carbonyl α,β -unsaturated compound is excited to the singlet state 1E through an $n\pi^*$ or $\pi\pi^*$ type excitation, which can experience an intersystem crossing leading to the excited triplet state 3E (it is also possible to promote an enone to the triplet state by the use of a sensitizer). This triplet state can evolve directly to the formation of triplet biradicals, BIR^3 . Then, the biradicals BIR^3 , would experience a spin inversion to the singlet state BIR^1 . At this stage, competition between reverting to initial substrates (k_1) and formation of the final cycloadducts (k_2) would establish the regioselectivity of the process.

⁶² Bauslaugh, P. G. *Synthesis* **1970**, 287-300.

⁶³ (a) Schuster, D. I.; Heibel, G. E.; Caldwell, R. A.; Tang, W. *Photochem. Photobiol.* **1990**, *52*, 645-648. (b) Schuster, D. I.; Dunn, D. A.; Heibel, G. E.; Brown, P. B.; Rao, J. M.; Woning, J.; Bonneau, R. *J. Am. Chem. Soc.* **1991**, *113*, 6245-6255. (c) Kaprinidis, N. A.; Lem, G.; Courtney, S. H.; Schuster, D. I. *J. Am. Chem. Soc.* **1993**, *115*, 3324-3325.

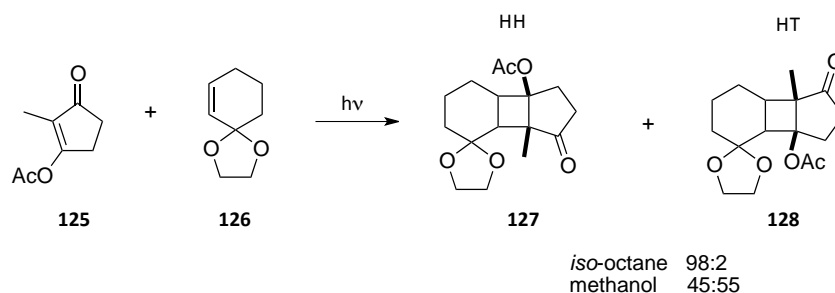
⁶⁴ (a) Hastings, D. J.; Weedon, A. C. *J. Am. Chem. Soc.* **1991**, *113*, 8525-8527. (b) Andrew, D.; Hastings, D. J.; Oldroyd, D. L.; Rudolph, A.; Weedon, A. C.; Wong, D. F.; Zhang, B. *Pure & Appl. Chem.* **1992**, *64*, 1327-1334. (c) Andrew, D.; Weedon, A. C. *J. Am. Chem. Soc.* **1995**, *117*, 5647-5663.

⁶⁵ For a review see: Schuster, D. I.; Lem, G.; Kaprinidis, N. A. *Chem. Rev.* **1993**, *93*, 3-22 and references cited therein.



Scheme 17. The currently accepted Bauslaugh-Schuster-Weedon mechanism.

Several examples can be found in the literature showing a significant influence of the solvent polarity on the regioselectivity of the reaction. For instance, in 1968, Challand and de Mayo reported the study of the photocycloaddition between cyclopentenone **125** and alkene **126** (Scheme 18),⁶⁶ showing a notable variation on the regioisomer distribution with the solvent's polarity.

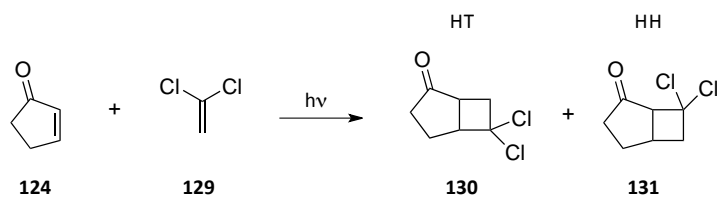


Scheme 18. Effect of solvent polarity on the [2+2] photocycloaddition of **125** to **126**.

A few years later, Loufty and de Mayo reported the photocycloaddition of cyclopentenone to 1,1-dichloroethylene to afford the HT product as the major regioisomer.⁶⁷ As shown in Scheme 19, the ratio of the HH regioisomer over the HT increased with the polarity of the solvent.

⁶⁶ Challand, B. D.; de Mayo, P. *Chem. Comm.* **1968**, 982-983.

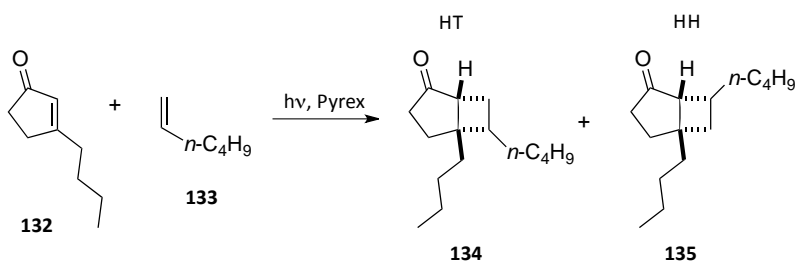
⁶⁷ Loufty, R. O.; de Mayo, P. *Can. J. Chem.* **1972**, *50*, 3465-3471.



Solvent	HT:HH (%)
cyclohexane	85:15
diethyl ether	84:16
acetonitrile	71:29

Scheme 19. Effect of solvent polarity on the [2+2] photocycloaddition of cyclopentenone to 1,1-dichloroethylene.

In general, the predictions made following the Corey's rule are more accurate in apolar solvents than in polar solvents. However, some deviations from this rule have been described. As an example, this situation was reported by de Mayo and co-workers in the photocycloaddition of **132** to 1-hexene (Scheme 20).⁶⁸ Contrarily to what it would be expected following Corey's model, the authors found that the formation of the HH isomer decreased when the polarity of the solvent was increased.



Solvent	ϵ^a	HT:HH (%)
cyclohexane	2.02	53:47
diethyl ether	4.34	57:43
ethyl acetate	6.02	59:41
methanol	32.63	62:38
acetonitrile	37.50	63:37

^a data taken from the cited article

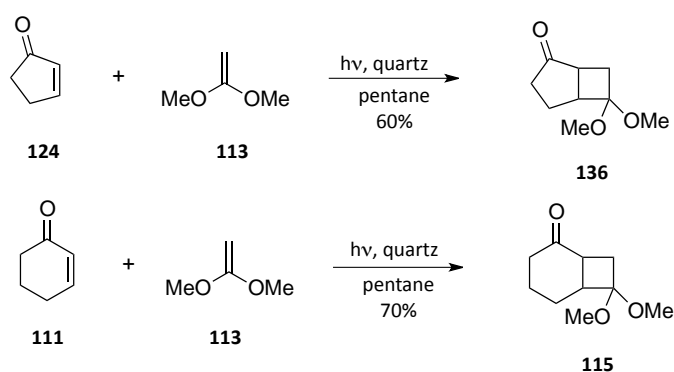
Scheme 20. Effect of solvent polarity on the reaction between **132** and 1-hexene.

Since the Bauslaugh-Schuster-Weedon mechanism does not allow to predict the effect of the polarity of the solvent on the regioselectivity of a [2+2] photocycloaddition reaction involving asymmetric alkenes, this effect has to be evaluated in every single case.

⁶⁸ Berenjjan, N.; de Mayo, P.; Sturgeon, M.-E.; Sydnes, L. K.; Weedon, A. C. *Can. J. Chem.* **1982**, *60*, 425-436.

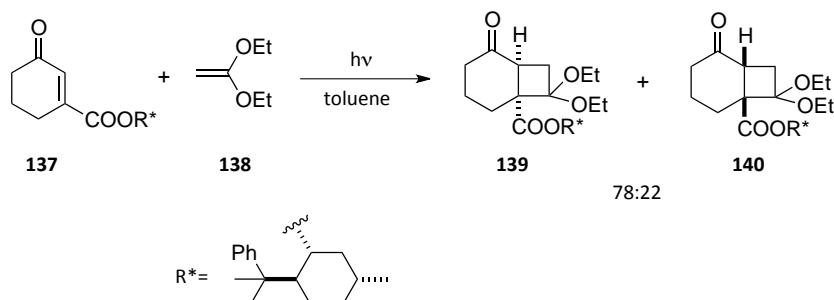
1.1.2 [2+2] Photocycloaddition of enones to ketene acetals

Ketene acetals are synthetically useful reagents because they bear a masked ketone functionalization. The first example of a [2+2] photocycloaddition of cyclic enones to a ketene acetal was described by Corey and co-workers in 1964.⁵¹ In particular, the authors found that under irradiation through a quartz filter in pentane, the [2+2] photocycloaddition of cyclopentenone and cyclohexenone to 1,1-dimethoxyethylene afforded only the HT regioisomers in moderate yields (Scheme 21).



Scheme 21. First examples of [2+2] photocycloadditions of enones to 1,1-dimethoxyethylene.

In this kind of reaction, chiral induction by attaching chiral auxiliaries to the enone or the alkene has also been studied.⁶⁹ Thus, in 1986, Scharf and co-workers achieved a moderate diastereomeric ratio in the reaction between the cyclohexenone **137** and 1,1-diethoxyethylene using 8-phenylmenthol as the chiral auxiliary (Scheme 22).⁷⁰



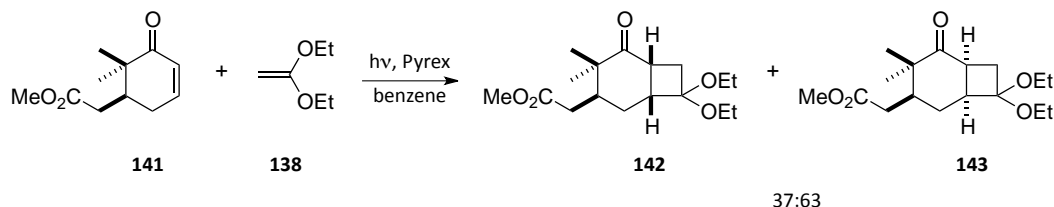
Scheme 22. Induction of asymmetry in the [2+2] photocycloaddition of ketene diethyl acetal using a chiral auxiliary.

In general, the stereochemistry of the photocycloadducts will be controlled by the steric hindrance at both faces of the enone. Nevertheless, other factors may influence the ratio of the

⁶⁹ Herzog, H.; Koch, H.; Scharf, H.-D.; Runsink, J. *Chem. Ber.* **1987**, *120*, 1737-1740.

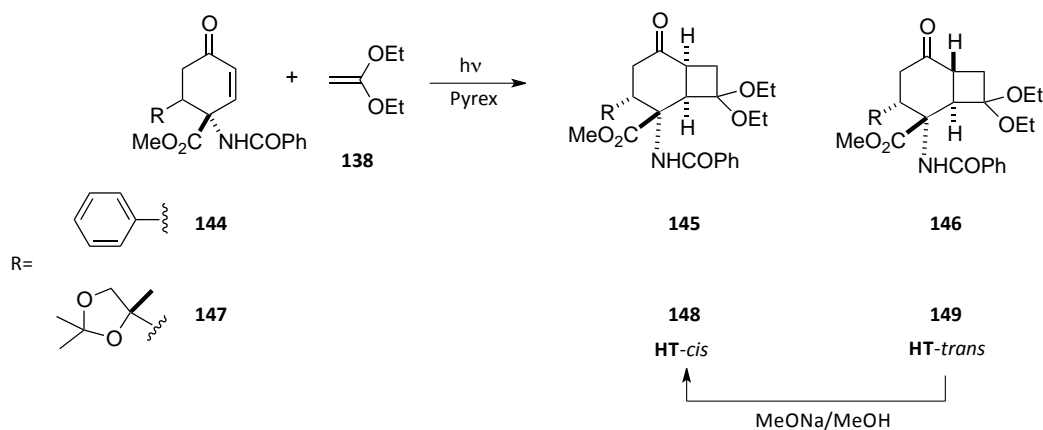
⁷⁰ Herzog, H.; Koch, H.; Scharf, H.-D.; Runsink, J. *Tetrahedron* **1986**, *42*, 3547-3558.

final products. This is the case of the reaction between the ester **141** and 1,1-diethoxyethylene to give a *ca.* 40:60 mixture of the two possible diastereomers, with **143** as the major product of the reaction, resulting from the approach of the alkene from the most hindered face of the enone, which was described by Liu and Chan in 1982 (Scheme 23).⁷¹



Scheme 23. Chiral induction in the [2+2] photocycloaddition of **141** to ketene diethyl acetal.

More recently, Ortuño and co-workers studied the [2+2] photocycloaddition of the enantiomerically pure cyclohexenones **144** and **147** to ketene diethyl acetal in acetone and acetonitrile (Scheme 24).^{60d} The authors described a completely regioselective process and a moderate *cis/trans* ratio. Moreover, they carried out theoretical calculations to rationalize the obtained results, which led them to conclude that the regiochemistry of the reaction was determined by the rate of formation of the 1,4-biradicals and not by the relative stability of these species.



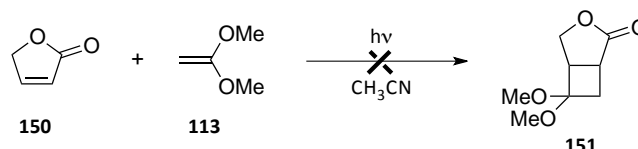
Enone	Solvent	Yield	<i>cis/trans</i> ratio
144	acetone	49	4.4
144	acetonitrile	77	2.2
147	acetone	42	1.2
147	acetonitrile	27	0.8

Scheme 24. Study of the [2+2] photocycloaddition of **144** and **147** to ketene diethyl acetal.

⁷¹ Liu, H.-J.; Chan, W. H. *Can. J. Chem.* **1982**, *60*, 1081-1091.

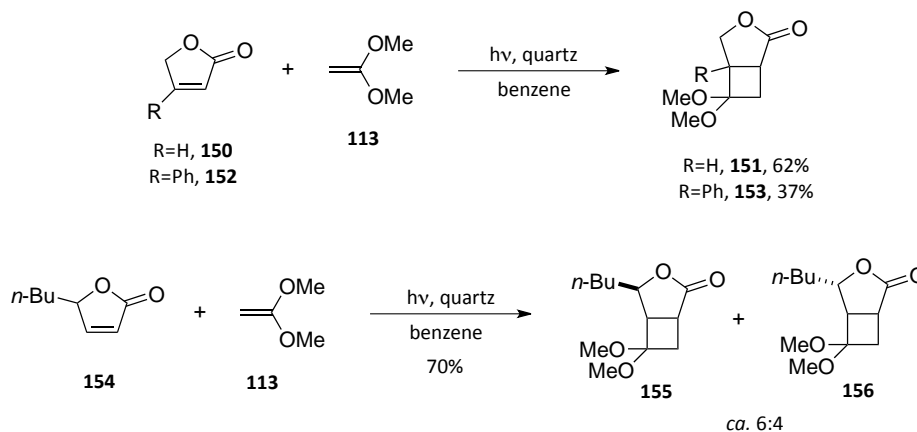
1.1.3 [2+2] Photocycloaddition of 2(5*H*)-furanones to ketene acetals

Despite its synthetic potential, the [2+2] photocycloaddition of 2(5*H*)-furanones to ketene acetals has been barely explored. In 1972, Tada and co-workers reported the first example of this photoreaction,⁷² which consisted in the reaction between γ -crotonolactone and ketene dimethyl acetal (Scheme 25). Nevertheless, when these two compounds were irradiated using a low pressure mercury lamp, no evolution was observed.



Scheme 25. Attempt of the [2+2] photochemical reaction between γ -crotonolactone and ketene dimethyl acetal.

Four years later, Kosugi and co-workers published an extensive study of the [2+2] photocycloaddition of 2(5*H*)-furanones to different unsaturated substrates, which included the reaction of lactones **150**, **152** and **154** with ketene dimethyl acetal (Scheme 26).⁷³ Contrarily to Tada's findings, the authors obtained the corresponding adducts when the irradiation was performed in benzene. In both reactions, only HT regioisomers were obtained, and in the case of lactone **154**, poor diastereoselectivity was achieved.



Scheme 26. Photochemical reaction of 2(5*H*)-furanones **150**, **152** and **154** with ketene dimethyl acetal.

At this point, it is necessary to define the *anti/syn* nomenclature that has been used to describe the cycloadducts derived from the different possible approximations of the unsaturated substrate to the diastereotopic faces of the 5-substituted 2(5*H*)-furanones. Thus, an *anti*

⁷² Tada, M.; Kokubo, T.; Sato, T. *Tetrahedron* **1972**, *28*, 2121-2125.

⁷³ Kosugi, H.; Sekiguchi, S.; Sekita, R.; Uda, H. *Bull. Chem. Soc. Jpn.* **1976**, 520-528.

cycloadduct is formed whenever the unsaturated substrate approaches the 2(5*H*)-furanone from the less hindered β face, whereas a *syn* adduct is produced when the unsaturated substrate approaches from the opposite α face (Figure 16).

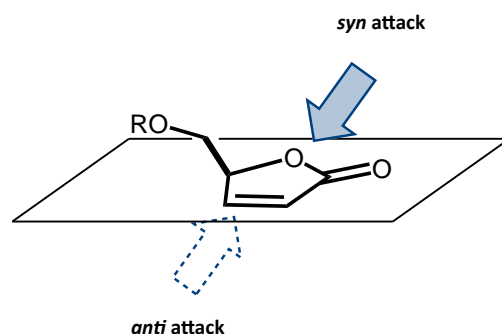


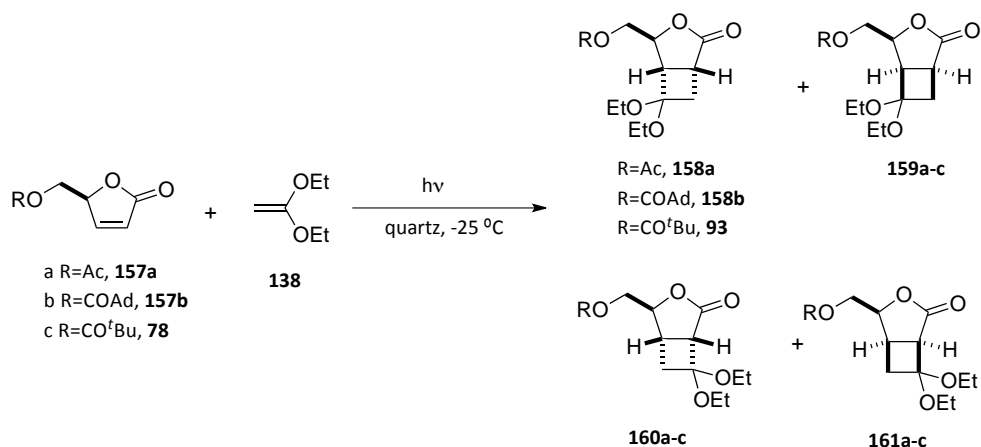
Figure 16. *Anti/syn* approximation of an unsaturated substrate to a 2(5*H*)-furanone.

Examples of the enantiopure version of the [2+2] photocycloaddition of furanones to ketene acetals are very limited. In fact, to the best of our knowledge, the only existing studies have been described by our research group.^{47,74}

In particular, we have investigated the regio- and diastereoselectivity of the reaction between 1,1-diethoxyethylene and the chiral 2(5*H*)-furanones **157a-b** and **78** among others (Scheme 27).⁷⁴ The photoreaction of these lactones in acetonitrile (entries 1-3) was accomplished in reasonably good yields (*ca.* 70%) and moderate regio- and stereoselectivities. A remarkable solvent effect was unveiled when these cycloadditions were performed in diethyl ether (entries 4-6) or hexane (entries 7-9). In the less polar solvents, the regioselectivity was notably enhanced up to 93:7, while the stereoselectivity decreased slightly.

On the other hand, while the size of the acyl substituent has little influence on the regioselectivity, a slight increase of the *anti* adducts was observed on going from the acetyl group to the bulkier adamantyl and pivaloyl residues.

⁷⁴ Rustullet, A.; Racamonde, M.; Alibés, R.; de March, P.; Figueredo, M.; Font, J. *Tetrahedron* **2008**, *64*, 9442-9447.

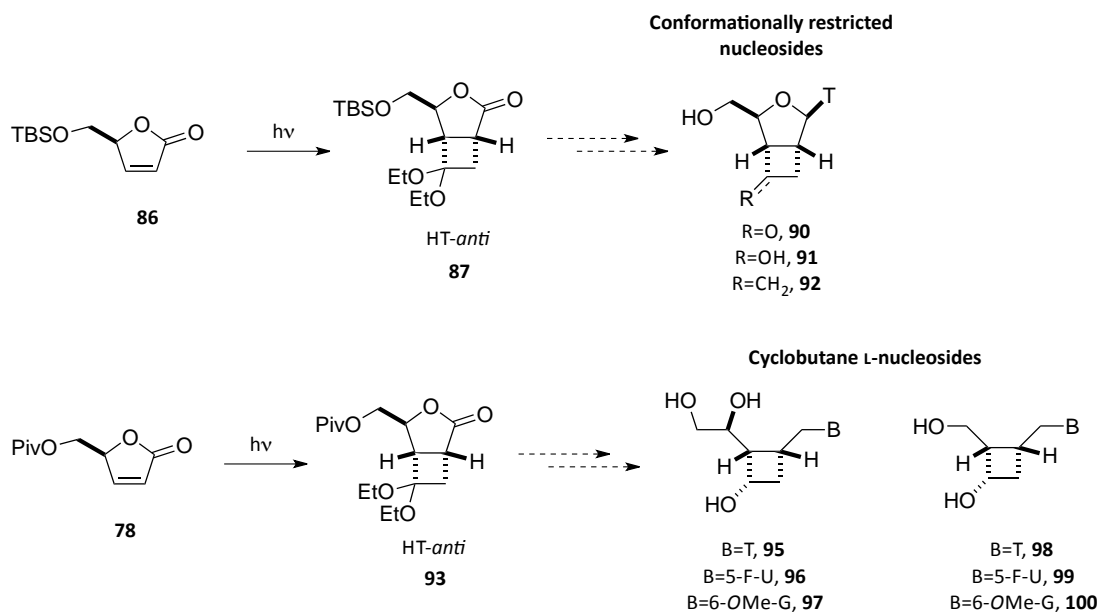


Entry	2(5H)-furanone	Solvent	t	Yield ^a (%)	158:159:160:161 ^b (%)	HT/HH (%)	<i>anti/syn</i> (%)
1	157a	acetonitrile	3.3 h	75	47:31:15:7	78:22	62:38
2	157b	acetonitrile	1.9 h	77	50:21:22:7 ^c	71:29	72:28
3	78	acetonitrile	2 h	61	50:22:21:7	72:28	71:29
4	157a	diethyl ether	2.25 h	78	51:41:5:3	92:8	56:44
5	157b	diethyl ether	2.25 h	50	52:39:6:3 ^c	91:9	58:42
6	78	diethyl ether	2.3 h	75	58:34:5:3	92:8	63:37
7	157a	hexane	11.2 h	37	48:42:6:4	90:10	54:46
8	157b	hexane	1.6 h	66	57:36:4:3 ^c	93:7	61:39
9	78	hexane	2.5 h	72	52:39:6:3	91:9	58:42

^a Isolated yield after column chromatography. ^b Isomer ratio from GC analysis of the crude reaction mixture. ^c Isomer ratio from ¹³C NMR of the crude reaction mixture.

Scheme 27. [2+2] Photocycloaddition of 2(5H)-furanones **157a-b** and **78** to 1,1-diethoxyethylene.

Taking these results into account, and considering that our strategy to synthesize the conformationally restricted nucleosides **90-92** and the cyclobutane L-nucleosides **95-100** involved the construction of the functionalized cyclobutane via the photochemical reaction of 2(5H)-furanones **86** and **78** with ketene diethyl acetal (Scheme 28), suitable reaction conditions should be found to obtain predominantly the HT-*anti* adducts **87** and **93**.



Scheme 28. 2(5*H*)-furanones chosen as starting materials towards the synthesis of cyclobutane nucleosides.

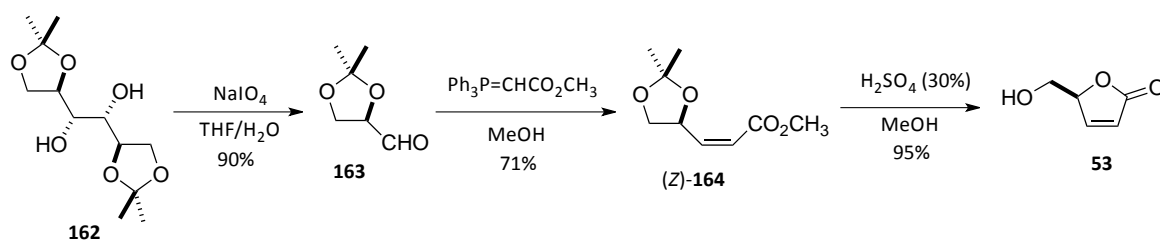
2. [2+2] PHOTOCYCLOADDITION OF 2(5*H*)-FURANONES TO KETENE DIETHYL ACETAL

2.1 Synthesis of 2(5*H*)-furanones

The (-)-(*S*)-5-hydroxymethyl-2(5*H*)-furanone, **53**, and their *O*-derivatives are widely used precursors for the synthesis of natural products.⁷⁵ This lactone is easily available in multigram scale following the synthetic procedure described by Mann and co-workers (Scheme 29).⁷⁶ The synthetic pathway starts with the oxidative cleavage of the *D*-mannitol diacetonide **162** with sodium periodate in a 9:1 mixture of THF and H₂O to afford aldehyde **163**. Reaction of this volatile aldehyde with methoxycarbonylmethylene(triphenyl)phosphorane in MeOH gives a *ca.* 4:1 mixture of the (*Z*)- and (*E*)-alkenes. The major *Z*-isomer **164** is treated with a catalytic amount of acid in MeOH to furnish 2(5*H*)-furanone **53** in 95% yield. Thus, the overall yield for the three steps is 61%.

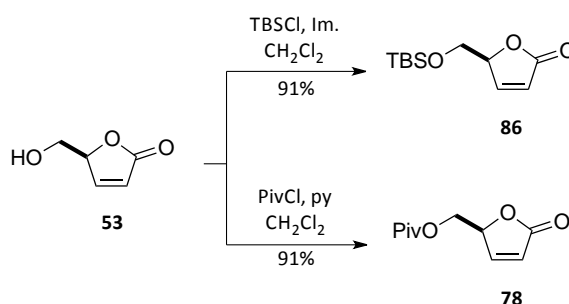
⁷⁵ De Souza, M. V. N. *Mini-Rev. Org. Chem.* **2005**, *2*, 139-145.

⁷⁶ Mann, J.; Parlett, N. K.; Thomas, A. J. *Chem. Res. Synop.* **1987**, 369.



Scheme 29. Synthesis of the 2(5*H*)-furanone **53**.

Then, the 2(5*H*)-furanone **53** was easily protected by treatment with TBSCl and imidazole in CH_2Cl_2 , providing **86** in 91% yield (Scheme 30). In an analogous manner, treatment of **53** with pivaloyl chloride and pyridine in CH_2Cl_2 afforded **78** in 91% yield.

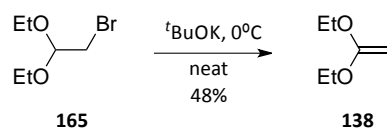


Scheme 30. Protection of **53** as the TBS and Piv derivatives.

2.2 [2+2] Photocycloaddition of **86** and **78** to ketene diethyl acetal

With 2(5*H*)-furanones **86** and **78** in hands, we turned our attention to investigate their photochemical reaction with 1,1-diethoxyethylene.

Unfortunately, during the course of this work, 1,1-diethoxyethylene was discontinued from our usual suppliers. Since then, the product has been synthesized following a procedure described by Venneri and Warketin (Scheme 31).⁷⁷ Accordingly, bromoacetaldehyde diethyl acetal, **165**, was reacted directly with $t\text{BuOK}$ to give 1,1-diethoxyethylene in 48% yield.



Scheme 31. Synthesis of 1,1-diethoxyethylene.

Next, we targeted its [2+2] photocycloaddition to the 2(5*H*)-furanone **86**. As it has already been mentioned, the solvent of the reaction plays a pivotal role in the regio- and diastereoselectivity of the process. Thus, we decided to study this reaction in two solvents of

⁷⁷ Venneri, P. C.; Warketin, J. *Can. J. Chem.* **2000**, *78*, 1194-1203.

different polarity such as acetonitrile and diethyl ether. The reaction was initially performed in a small scale (Scheme 32, entries 1 and 2) using a high-pressure 125W mercury lamp and small photochemical reactors (*ca.* 100-300 mL capacity). The evolution of the reaction was monitored by GC analyses of aliquots of the reaction mixture.

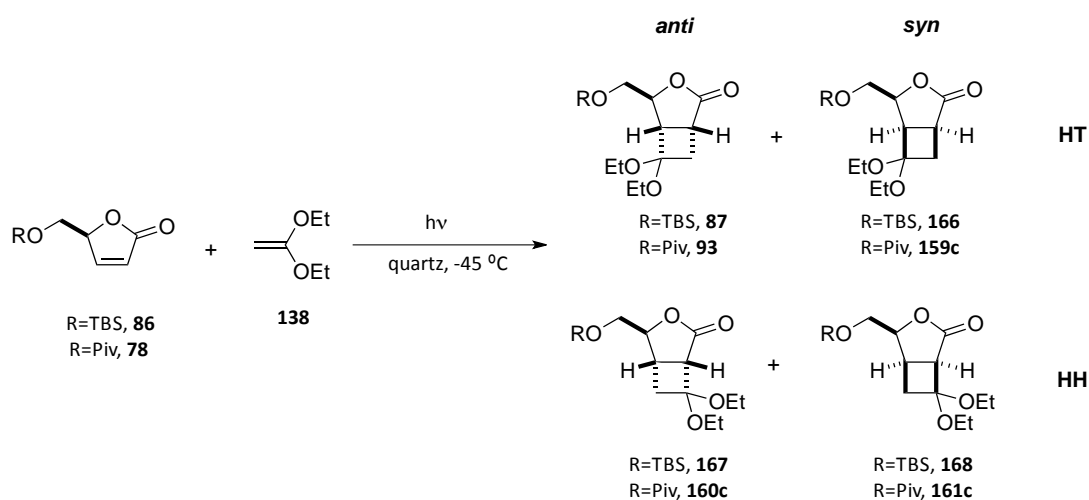
The first experiment was performed in acetonitrile, giving the four adducts **87** and **166-168** in a ratio of 61:18:16:5 and 62% yield (entry 1). The facial diastereoselectivity of the process clearly favoured the attack from the less hindered face of the furanone (77:23). The two main HT-photoadducts **87** and **166** could be separated by column chromatography, delivering the targeted HT-*anti* regioisomer **87** in 38% yield and the *syn* regioisomer **166** in 11% yield. All attempts to separate the minor HH regioisomers were unsuccessful.

Remarkably, when the reaction was carried out in diethyl ether (entry 2), the facial diastereoselectivity was slightly lower (72:28), but the regioselectivity of the process was highly enhanced, giving a 91:9 ratio of the HT:HH products and a slightly better yield (77%). Since this improved regioselectivity was synthetically more convenient, we used diethyl ether as the solvent to scale up the reaction to 2 g of 2(5*H*)-furanone **86** (entry 3). This reaction was carried out with a medium-pressure 400W mercury lamp in a 1 L reactor, achieving similar regio- and diastereoselectivities and delivering the mixture of the four photocycloadducts in 83% global yield. Further purification of this mixture rendered the targeted isomer **87** in 46% isolated yield.⁷⁸

The data gathered from these experiments is in accordance with that previously obtained for furanones **157** and **78** (Scheme 27); the regioselectivity of the reaction was notably higher when the less polar solvent was used, while the facial diastereoselectivity was somewhat lower.

Next, we focused on the preparation of the Piv-substituted photocycloadduct **93**. The reaction between the 2(5*H*)-furanone **78** and 1,1-diethoxyethylene had already been carried out in our research group although in small scale (entries 4 and 5).^{47,74} Therefore, we decided to scale up this reaction to 2 g of the starting 2(5*H*)-furanone. Thus, upon irradiation with a medium-pressure 400W mercury lamp, the reaction rendered a mixture of the four photocycloadducts in a ratio of 60:35:3:2 and 68% yield (entry 6). Purification of the crude by flash chromatography delivered the targeted HT-*anti* cycloadduct **93** in 37% yield and the *syn* regioisomer **159c** in 20% yield. Again, separation of the HH regioisomers was unsuccessful.

⁷⁸ Figueras, A.; Miralles-Llumà, R.; Flores, R.; Rustullet, A.; Busqué, F.; Figueredo, M.; Font, J.; Alibés, R.; Maréchal, J.-D. *ChemMedChem* **2012**, *7*, 1044-1056.



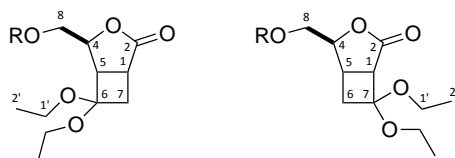
Entry	R	Solvent	Amount (g)	Yield ^a	t	HTa:HTs:HHa:HHs ^b (%)	HT:HH (%)	anti:syn (%)
1	TBS	CH ₃ CN	0.125	62	1h	61:18:16:5	79:21	77:23
2	TBS	Et ₂ O	0.125	77	1h	66:25:6:3	91:9	72:28
3	TBS	Et ₂ O	2.0	83	5h	64:29:5:2	93:7	69:31
4 ^c	Piv	CH ₃ CN	0.108	61	2h	50:22:21:7	72:28	71:29
5 ^c	Piv	Et ₂ O	0.100	75	2h	58:34:5:3	92:8	63:37
6	Piv	Et ₂ O	2.0	68	5h	60:35:3:2	95:5	63:37

^a Isolated yield after column chromatography. ^b Isomer ratio from GC analysis of the crude reaction mixture. ^c Data from refs. 47, 74.

Scheme 32. [2+2] Photocycloaddition of the 2(5*H*)-furanones **86** and **78** to ketene diethyl acetal.

2.2.1 Structural determination of the photocycloadducts

The structural elucidation of the photocycloadducts has been carried out by analysis of 1D and 2D NMR experiments. The stereochemistry of adducts **167-168** and **160c-161c** has been assigned by analysis of a mixture of both isomers since its separation was not possible. The most representative data is shown in Table 1.



Cycloadduct	H1	H4	H5	C5
 87	2.96 ddd $J_{1,7}=9.9$ Hz $J_{1,5}=8.2$ Hz $J_{1,7}=4.4$ Hz	4.81 ddd $J_{4,8}=3.7$ Hz $J_{4,8}=2.7$ Hz $J_{4,5}=2.0$ Hz	3.11 dddd $J_{5,1}=8.2$ Hz $J_{5,4}=2.0$ Hz $J_{5,7}=1.7$ Hz $J_{5,7}=0.9$ Hz	47.2
 166	3.03 ddd $J_{1,5}=8.2$ Hz $J_{1,7}=4.0$ Hz $J_{1,7}=1.2$ Hz	4.54 ddd $J_{4,8}=7.1$ Hz $J_{4,5}=5.8$ Hz $J_{4,8}=4.6$ Hz	3.12 dd $J_{5,1}=8.2$ Hz $J_{5,4}=5.8$ Hz	47.3
 167	3.40-3.30 m	4.45-4.30 m	2.88-2.70 m	29.5
 168	3.50-3.40 m	4.54 ddd $J_{4,8}=9.3$ Hz $J_{4,8}=6.4$ Hz $J_{4,5}=4.9$ Hz	3.03-2.90 m	29.3
 93	3.05-2.95 m	4.99 ddd $J_{4,5}=1.8$ Hz	3.05-2.95 m	46.8
 159c	3.01 ddd $J_{1,5}=8.2$ Hz $J_{1,7}=7.7$ Hz $J_{1,7}=5.0$ Hz	4.70-4.53 m	3.16 dd $J_{5,1}=8.2$ Hz $J_{5,4}=5.7$ Hz	47.3
 160c	3.60-3.30 m	4.55 m	2.69 m	28.9
 161c	3.70-3.20 m	4.64 ddd $J_{4,5}=5.7$ Hz	2.95 m	28.7

Table 1. Relevant spectroscopic data of the photocycloadducts.

The *anti/syn* stereochemistry of the products can be determined by the value of the coupling constant between H4 and H5. In the *anti* cycloadducts, the dihedral angle between these two protons is close to 90°, resulting in coupling constants with values around 0 Hz. Contrarily, for the *syn* cycloadducts, the dihedral angle is around 0°, hence the coupling constant should be higher. As an example, the assignment of the photocycloadducts derived from the 2(5*H*)-furanone **86** (R=TBS) is shown below.

Table 2 shows the values of $J_{4,5}$ for cycloadducts **87** and **166-168**. Although it has not been possible to determine the value of $J_{4,5}$ for compound **167**, its *anti* assignment could be determined considering the *anti/syn* assignment of the other three cycloadducts.

Cycloadduct	$J_{4,5}$ (Hz)
87	2.0
166	5.8
167	-
168	4.9

Table 2. Coupling constant between H4 and H5 for cycloadducts **87** and **166-168**.

The regiochemistry of the cycloadducts has been determined with the aid of HMBC experiments. The spectra of **87** and **166** show cross peaks between C2 and H7 and between C6 and H4, evidencing a HT constitution (Figures 17 and 18).

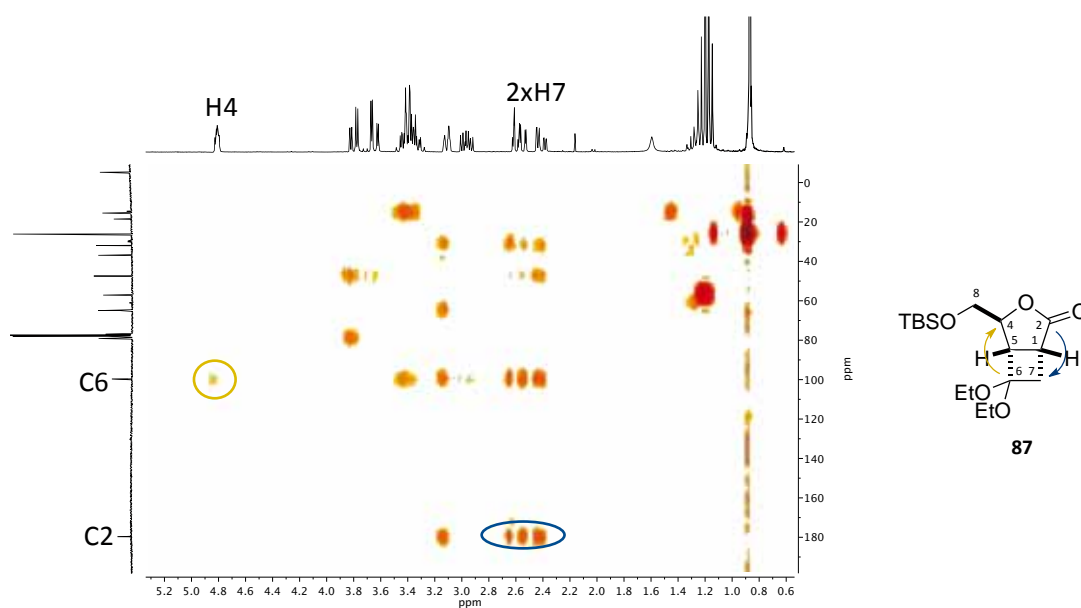


Figure 17. HMBC spectrum (250 MHz, CDCl₃) of **87**.

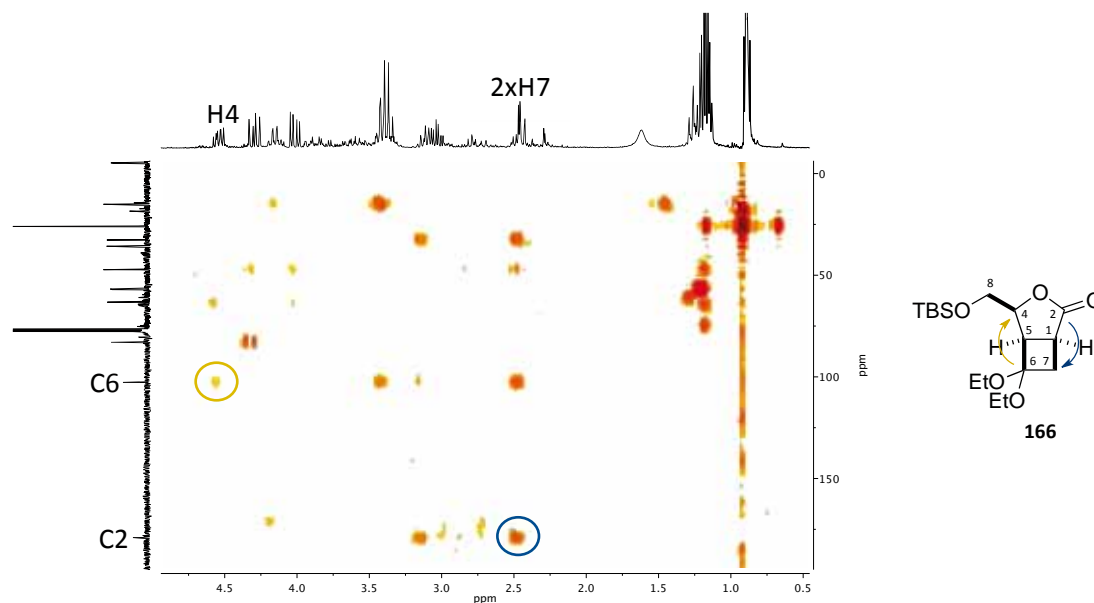


Figure 18. HMBC spectrum (250 MHz, CDCl_3) of **166**.

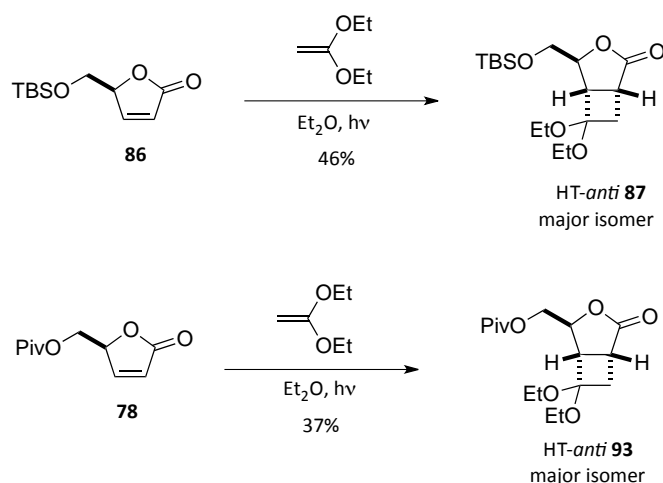
Additional evidence of the regiochemical assignment is given by the ^{13}C NMR spectra, where the signal of C5 of the HT isomers appears downfield shifted ($\delta \sim 47.3$) compared to the HH adducts ($\delta \sim 29.4$), due to the deshielding effect of the ketal oxygen atoms (Table 3).

Cycloadduct	δ
87	47.2
166	47.3
167	29.5
168	29.3

Table 3. Chemical shift of C5 for cycloadducts **87** and **166-168**.

3. CHAPTER II OUTLINE

In this chapter, the [2+2] photocycloaddition of 5-substituted 2(5*H*)-furanones **86** and **78** to ketene diethyl acetal has been studied. These reactions have been scaled up to 2 g of the starting enone and the solvent effect on the yield, regio- and diastereoselectivity of the process has been discussed. The best reaction conditions to obtain the HT-*anti* photocycloadducts as the major isomers involved the use of diethyl ether as the solvent, leading to compounds **87** and **93** in 46% and 37% yield, respectively.



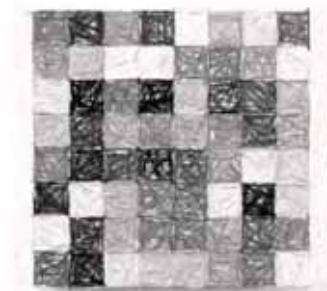
Scheme 33. Chapter II summary.

With the major HT-*anti* cycloadducts **87** and **93** in hand, we turned our attention to prepare the target nucleoside analogues as it is shown in the forthcoming chapters.

III. Cyclobutane-Fused Nucleosides

Synthesis of Novel Nucleosides Bearing a Functionalized
Cyclobutane Ring





1. INTRODUCTION

The antiviral activity of the 2',3'-dideoxynucleosides is often modulated by the nature and stereochemical arrangement of the functional groups present on the sugar moiety. In general, nucleosides require determined conformational features in order to bind successfully to the target enzyme. Thus, over the last years, the conformational behaviour of natural and modified nucleosides has arisen as a decisive factor of the final nucleoside-enzyme interaction.

One strategy for pre-organizing nucleoside conformation is to increase the rigidity of the normally flexible nucleoside by chemical modification. Thus, different structural modifications have been introduced into the glycon moiety to modulate the conformational behaviour of nucleosides in order to enhance their biological activity (Chapter I, section 1). In this section, the main parameters that are used to describe the conformational behaviour of nucleosides are presented.^{15,79}

1.1 Basics of nucleoside structure

The typical structure of nucleosides has two molecular fragments: D-ribo or D-2'-deoxyribofuranose as the sugar moiety and a purine or pyrimidine aglycone. Those two moieties are covalently bonded from N1 of pyrimidine [uracil (U), thymine (T) and cytosine (C)] or N9 of purine [adenine (A) and guanine (G)] to C1' of the glycone in a β -configuration (Figure 19).

⁷⁹ Neidle, S. *Principles of nucleic acid structure*, Academic Press: Amsterdam, 2008.

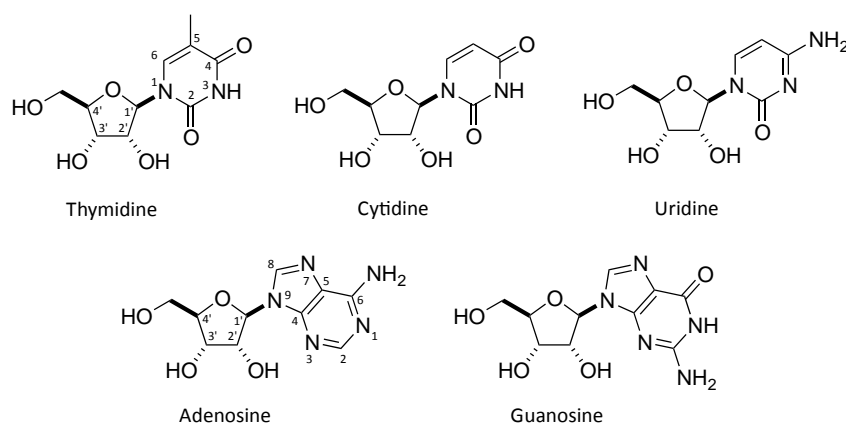


Figure 19. Natural nucleosides.

1.2 Furanose ring conformation. The pseudorotational cycle

The furanose ring of nucleosides is not flat, usually featuring one or two atoms out of the plane. This displacement from planarity is called *puckering*. If one atom is significantly displaced out of the plane, the conformation is denoted as *envelope* (E) whereas if two atoms are shifted from the plane of the others, the resulting conformation is referred as *twist* (T) (Figure 20).

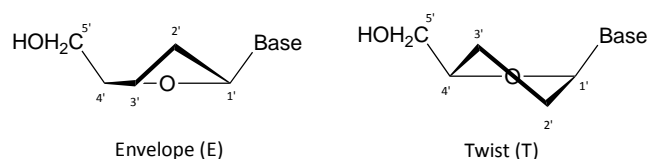


Figure 20. Conformations of the furanose ring.

In practice, these two limit conformations are rarely observed. Much more frequently, neither the four atoms forming a plane in an envelope conformation are coplanar, nor the deviation from the plane of the two atoms in a twist form is exactly the same. Therefore, the largest displacement from planarity is called major puckering whereas the minimum deviation is called minor puckering.

If the atom that is displaced from the plane is at the same side of C5', it is called *endo*. While if the atom is on the opposite face, it is termed *exo*. There is an abbreviated conformational nomenclature that describes these conformations.⁸⁰ In this nomenclature, the number of the carbon atom that is displaced from the plane is indicated as a super- or subscript depending if the atom is *endo* or *exo*, respectively. Preference is given to the atom that exhibits the major puckering, appearing before the letter (E or T), while the atom showing the minor puckering appears after the letter. Thus, a C3'-endo-C2'-exo twist asymmetric conformation, where C3' is

⁸⁰ Sundaralingam, M. J. *Am. Chem. Soc.* **1971**, *93*, 6644-6647 and references cited therein.

more deviated from the plane (major puckering) than C2' (minor puckering) is abbreviated as 3T_2 (Figure 21). In the case that both atoms show a twist symmetric deviation, the conformation should be labelled as 3_2T . Finally, C3'-exo and C2'-endo envelopes should be represented as ${}_3E$ and 2E , respectively.

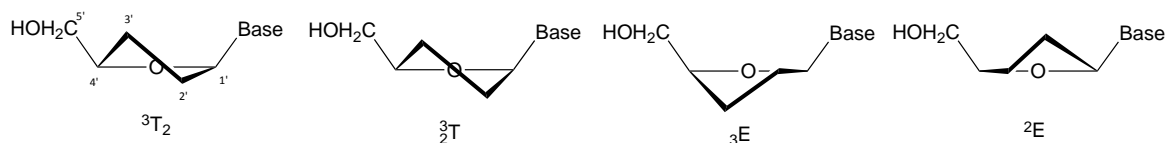


Figure 21. Examples of abbreviated representations of a nucleoside furanose ring.

This nomenclature is an approximation as it only considers certain puckers. In order to deal with the intermediate cases, the concept of pseudorotation, which was firstly introduced for cyclopentane rings,⁸¹ was developed.⁸²

The complete definition of the conformational behaviour of a nucleoside requires the determination of four principal structural parameters: the pseudorotational angle P , the maximum pucker amplitude v_{max} , and the torsion angles χ and γ .

The conformation of the furanoside ring and its deviation from planarity are characterized by the pseudorotational angle P and the maximum puckering amplitude, v_{max} (Figure 22). The value of P is calculated from the endocyclic torsion angles v_0 - v_4 . The maximum pucker amplitude v_{max} is a representation of the maximal deviation of the ring and it depends on the value of P and the torsion angle v_2 .

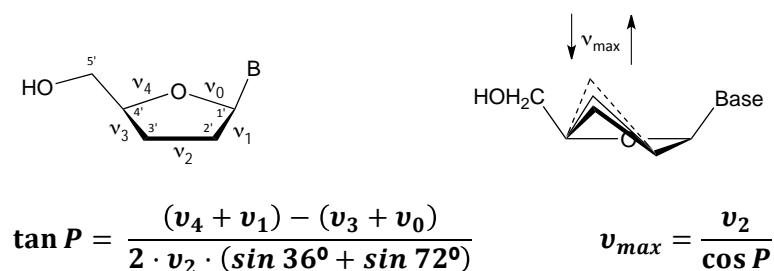


Figure 22. Pseudorotational angle P and maximum pucker amplitude v_{max} .

The graphic representation of these two parameters is named pseudorotational cycle and it is a handy tool to visually compare nucleoside conformations. In this cycle, twist and envelope conformations alternate every 18° and by convention, the pseudorotation angle $P=0^\circ$ is attributed to the north conformation 3_2T .

⁸¹ Kilpatrick, J. E.; Pitzer, K. S.; Spitzer, R. *J. Am. Chem. Soc.* **1947**, *69*, 2483-2488.

⁸² Altona, C.; Sundaralingam, M. *J. Am. Chem. Soc.* **1972**, *94*, 8205-8212.

For the great majority of natural nucleosides, the values of P are centered around two preferred conformations.⁸³ The first region of characteristic conformations is on the first quadrant of the pseudorotational cycle, and it comprises the nucleosides showing 3E conformation ($0^\circ \leq P \leq 36^\circ$). The second region is on the second quadrant and it comprises the nucleosides showing 2E conformation ($144^\circ \leq P \leq 180^\circ$) (Figure 23, shaded areas).

These two conformations, in solution, are in equilibrium, transitioning from one to another through an east-type conformation.⁸⁴ The typical v_{\max} values of both conformations range between 30 and 40° . For v_{\max} values below 20° , the furanose ring is considered to be almost planar.

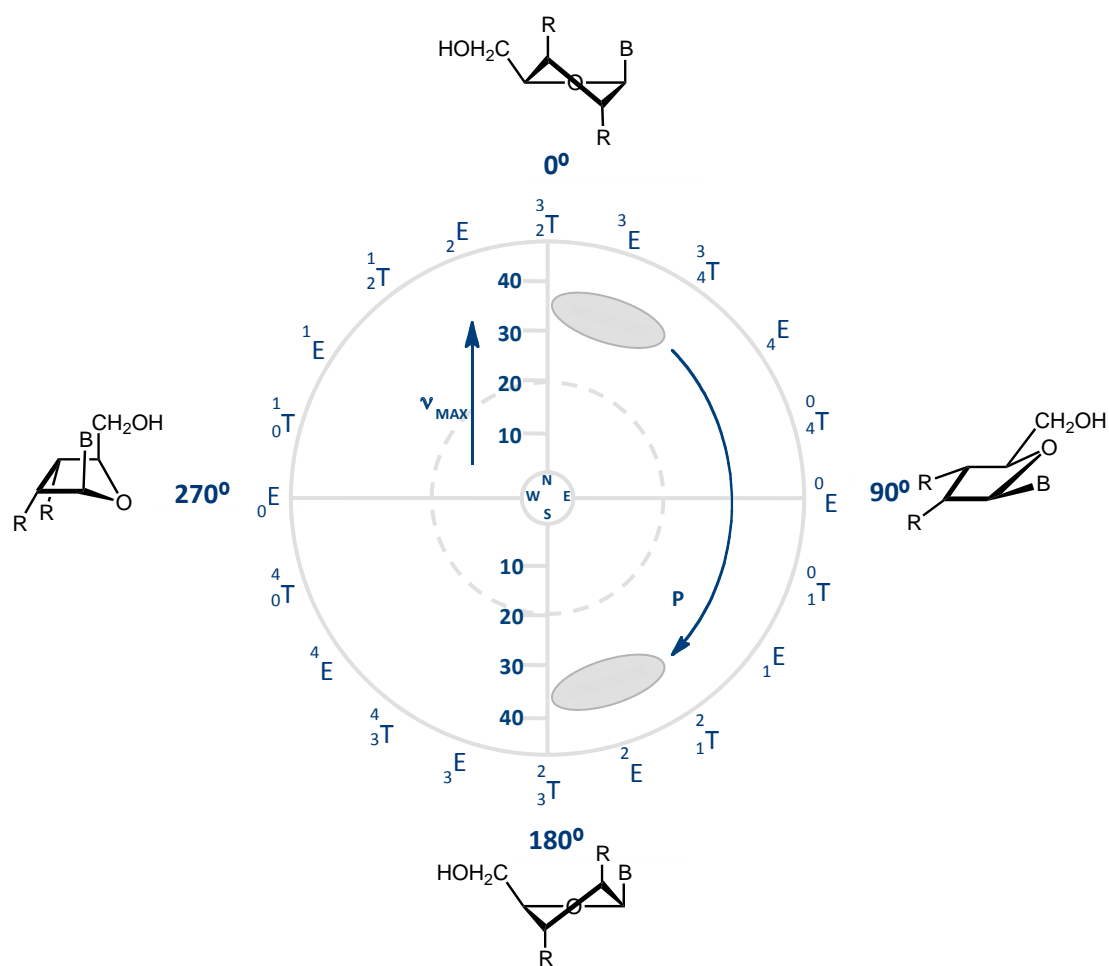


Figure 23. The pseudorotational cycle. Shaded areas indicate the most common conformations of natural nucleosides.

⁸³ De Leeuw, H. P. M.; Haasnoot, C. A. G.; Altona, C. *Isr. J. Chem.* **1980**, *20*, 108-126.

⁸⁴ Plavec, J.; Tong, W.; Chattopadhyaya, J. *J. Am. Chem. Soc.* **1993**, *115*, 9734-9746.

1.3 Torsion angle χ

The torsion angle χ determines the *syn* or *anti* disposition of the base relative to the sugar moiety. For purine bases this angle is defined by O4'-C1'-N9-C4, whereas for pyrimidines is the angle defined by O4'-C1'-N1-C2. Therefore, a *syn* disposition will be found whenever the C2 carbonyl of the pyrimidines or the N3 of purines lies over the sugar. Contrarily, an *anti* disposition will be found when the cited atoms lie on the opposite direction. Figure 24 shows the *anti* and *syn* definition for a pyrimidine nucleoside.

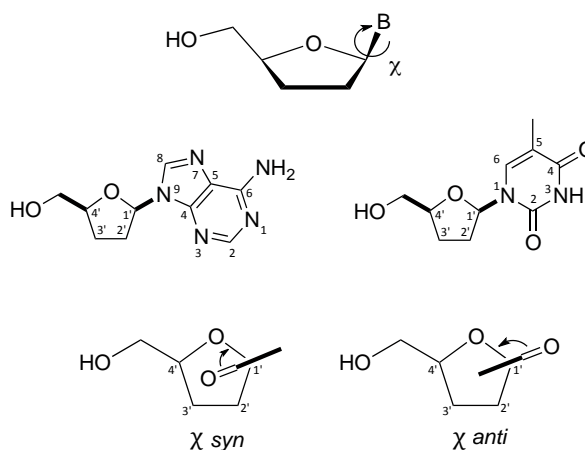


Figure 24. The torsion angle χ .

1.4 Torsion angle γ

The rotation angle γ is defined by O5'-C5'-C4'-C3', and is due to the rotation of the exocyclic C4'-C5' bond (Figure 25). Rotation around this bond allows different dispositions of O5'. Qualitatively, these multiple orientations are named +gauche (γ^+) and -gauche (γ^-) when O5' is found *ca.* 60° of C3' and trans (γ^t) when it is located antiperiplanar to it.

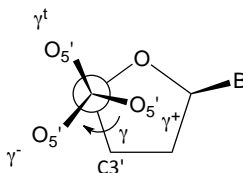


Figure 25. The torsion angle γ

2. PRECEDENTS

The concept of applying structural constraints to nucleosides in order to fix their conformation and modify their biological activity has been introduced in Chapter 1. Unfortunately, although the research on this field has led to a wide range of structurally diverse bicyclonucleosides, conformation-activity studies are limited. This section summarizes the synthesis, biologic evaluation and conformational studies of some diverse nucleosides restricted by the presence of three to six membered rings fused to the sugar moiety. In order to provide a clear relation with the following section, cyclobutane-fused nucleosides are discussed at the end.

Figure 26 shows different nucleoside analogues conformationally restricted by the presence of a 2',3'-fused cyclopropane ring (also named methano-nucleosides) that have been reported to date.

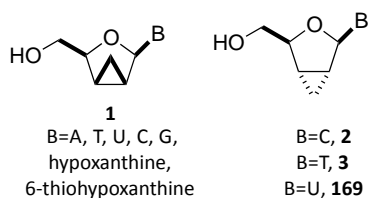
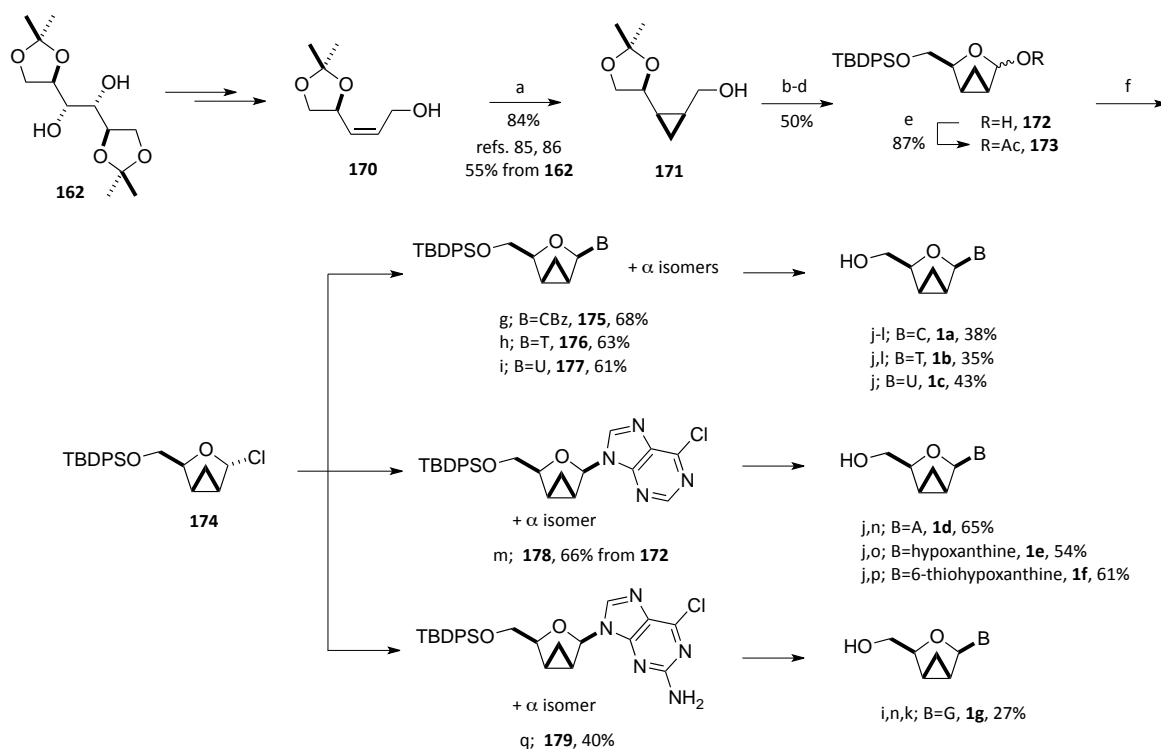


Figure 26. Examples of reported bicyclo[3.1.0]-fused nucleosides

Of these nucleosides, the synthesis of the family of analogues **1** by Chu and co-workers is one of the few works that features both biological and conformational studies.¹⁶ This group of nucleosides was synthesized starting from the D-mannitol diacetone **162** (Scheme 34). From this compound, the construction of the cyclopropane core was achieved via a Simmons-Smith reaction to give intermediate **171** in 6 steps and 55% yield.^{85,86} Then, envisioning a Vorbrüggen type glycosylation, cyclopropane **171** was transformed into acetate **173**. However, attempts of introducing different nucleobases using Vorbrüggen conditions led mainly to the undesired α -isomers. This issue could be circumvented by transforming the acetate into the chlorine intermediate **174**, allowing the introduction of the base via S_N2 reaction. This alternative strategy provided the β anomers of the seven methano-nucleosides **1a-g** as the major isomers.

⁸⁵ Morikawa, T.; Sasaki, H.; Hanai, R.; Shibuya, A.; Taguchi, T. *J. Org. Chem.* **1994**, *59*, 97-103.

⁸⁶ Zhao, Y.; Yang, T.-F.; Lee, M. G.; Chun, B. K.; Du, J.; Schinazi, R. F.; Lee, D.-W.; Newton, M. G.; Chu, C. K. *Tetrahedron Lett.* **1994**, *35*, 5405-5408.



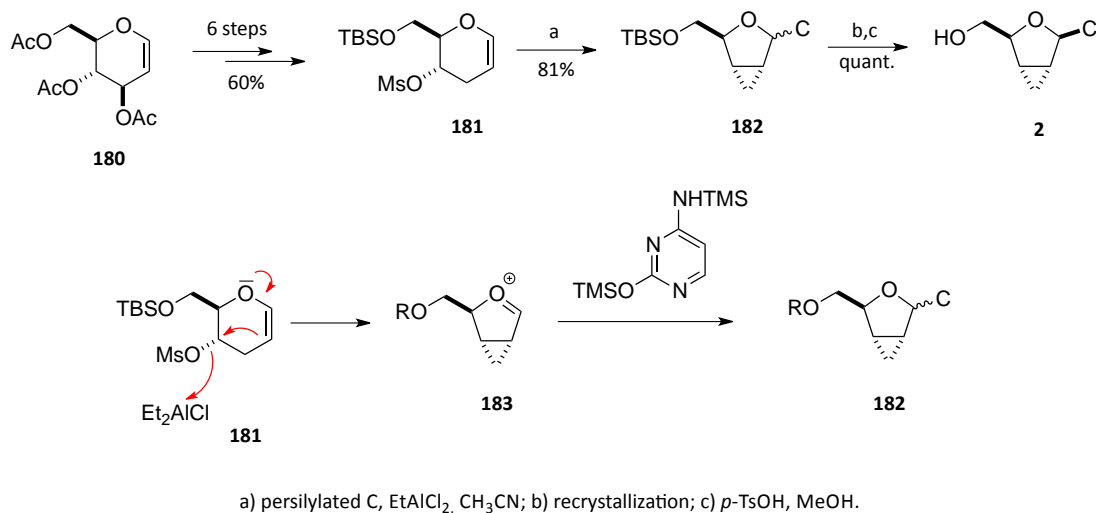
Scheme 34. Synthesis of the methano-nucleosides **1a-g**.

The adenine derivative **1d** provided adequate crystals for X-ray analysis, revealing a ${}^0\text{E}$ conformation of the furanose ring with a pseudorotational angle P of 91.7° and a puckering degree ν_{max} of 34.5° .[‡] Unfortunately, none of these cyclopropane-cored nucleosides showed significant activity against HIV.

Alternative ways to construct the cyclopropane core have been employed to synthesize the bicyclo[3.1.0] *exo*-nucleosides **2**, **3** and **169**. Thus, in 1989, Okabe and Sun were able to synthesize the cytidine nucleoside **2** by means of an intramolecular rearrangement (Scheme 35).⁸⁷ This methodology took advantage of the activation of the mesylate leaving group on the D-glucal **181** by a Lewis acid to produce the oxonium intermediate **183**. This intermediate was trapped with the silylated base to give the targeted nucleoside **2** after recrystallization and cleavage of the 5'-silyl group. By applying the same methodology, Sard was able to successfully synthesize the thymine derivative **3**.¹⁸

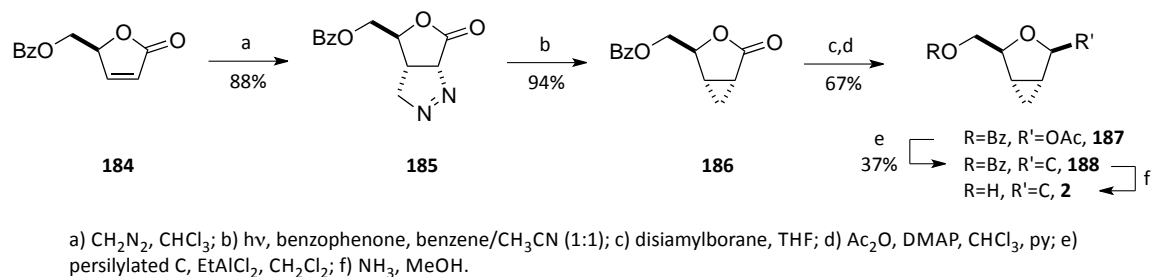
[‡] The nucleosides that appear in this section with reported conformational parameters are located in the pseudorotational cycle that can be found at the end of this section.

⁸⁷ Okabe, M.; Sun, R.-C. *Tetrahedron Lett.* **1989**, *30*, 2203-2206.



Scheme 35. Synthesis of the cyclopropane nucleoside **2**.

Alternatively, in 1990, Mann and co-workers reported another synthesis of the cytidine nucleoside **2** based on a 1,3-dipolar cycloaddition of diazomethane to the chiral 2(*5H*)-furanone **184** to create the cyclopropane core (Scheme 36).¹⁷ Then, nitrogen exclusion, reduction and acetylation of lactone **186** and subsequent glycosidation led to **188**, which upon benzoate cleavage afforded the desired cytidine analogue **2**. This nucleoside has been evaluated against HIV displaying weak activity.



Scheme 36. Synthesis of the cyclopropane nucleoside **2**.

The uridine member of this family, **169** (Figure 26), has also been synthesized.⁸⁸ However, in this case, Chattopadhyaya and co-workers described the formation of the cyclopropane ring using a Michael induced ring closure. Unlike the thymine and cytosine analogues, this uracil nucleoside has not been biologically tested. Nevertheless, this compound is the only one of this family with reported conformational information. Remarkably, its crystal structure revealed a practically planar furanose ring ($\nu_{\max}=8.8^\circ$) with a pseudorotational angle *P* of 86.7° , corresponding to a O4'-endo pucker.

⁸⁸ Wu, J.-C.; Chattopadhyaya, J. *Tetrahedron* **1990**, *46*, 2587-2592.

Apart from these cyclopropane-cored nucleosides, several oxirane derivatives have also been described (Figure 27). Among them, compounds **5-7** have been evaluated for anti-HIV activity, with the cytosine derivative exhibiting significant activity at concentrations as low as 1 μM .^{20,21} Unfortunately, the cytotoxicity of this analogue was also found to be substantial.

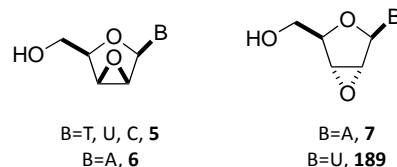


Figure 27. Examples of reported bicyclo[3.1.0]-fused nucleosides

To date, the thymine derivative **5** is the only of these oxirane nucleosides with reported conformational parameters.⁸⁹ The X-ray analysis of this compound revealed a unit cell containing two conformationally independent molecules differing only on the *N*-glycosidic bond. The torsion angle χ of one molecule was found to be -121.9° corresponding to a common *anti* conformation, while the value of this angle on the other molecule was 121.2° , corresponding to a rare high-*syn* conformation. The pseudorotational angle *P* of these molecules was found to be 98.9° and 97.6° , and the puckering degree ν_{max} was 29.2° and 33.1° . Lastly, both molecules exhibited identical γ^{t} torsion angles.

The weak antiviral activity displayed for most of the cyclopropane-fused nucleosides suggested that a certain degree of flexibility of the furanose ring is required to exhibit antiviral activity.³² Hence, analogues bearing bigger fused rings have also been explored (Figure 28).

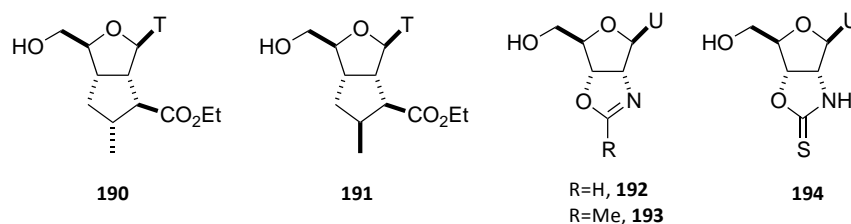


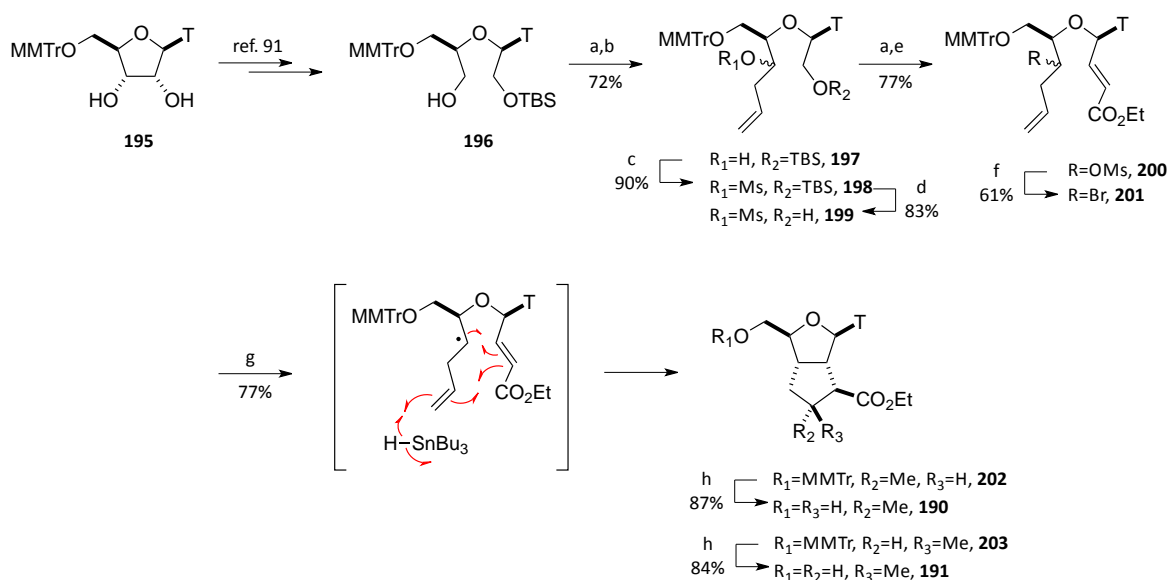
Figure 28. Examples of conformationally restricted nucleosides by the presence of a five-membered ring.

In 1995, Chattopadhyaya and co-workers described the synthesis of the 2',3'-*cis*- α -fused cyclopentane nucleosides **190** and **191** from the 2'-*O*-silylether 2',3'-*seco*-ribothymidine **196** as outlined in Scheme 37.⁹⁰ The bicyclic system was settled up by a free-radical cyclization on the bromo intermediate **201** with Bu_3SnH . The conformational analysis of these nucleosides was

⁸⁹ Gurskaya, G. V.; Bochkarev, A. V.; Zdanov, A. S.; Papchikhin, A. V.; Purygin, P. P.; Krayevsky, A. A. *FEBS Lett.* **1990**, *265*, 63-66.

⁹⁰ Papchikhin, A.; Agback, P.; Plavec, J.; Chattopadhyaya, J. *Tetrahedron* **1995**, *51*, 329-342.

carried out by energy minimization and revealed that the sugar moiety of both compounds adopted an east conformation close to $O4'$ -endo ($P=86^\circ$ and 89°) and a puckering degree v_{\max} of 27° for **190** and 39° for **191**. Moreover, thymine displayed an *anti* torsion angle χ and the orientation across the $C4'$ - $C5'$ bond was γ^+ . Unfortunately, these cyclopentane nucleosides have not been screened for antiviral activity.

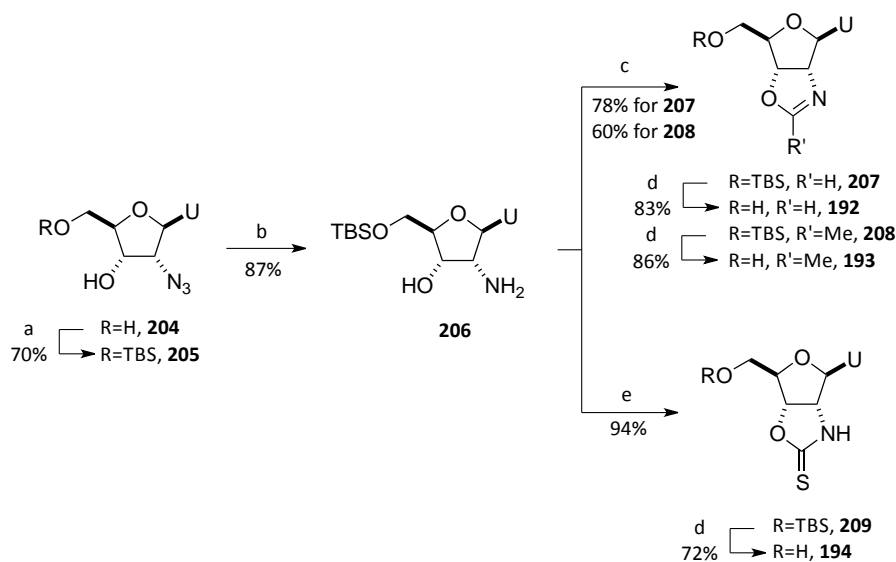


Scheme 37. Synthesis of the cyclopentane-fused nucleosides **190-191**.

Nucleosides bearing oxazole and thiocarbamate rings at their $2',3'$ -positions have also been described (Scheme 38).⁹² The synthetic sequence leading to these compounds started from the $2'$ -azido- $2'$ -deoxyuridine **204**. Cyclization to form the $2',3'$ -oxazole ring in **207** was achieved by treatment with *N,N*-dimethylformamide dimethyl acetal, whereas treatment with the *N,N*-dimethylacetamide reagent delivered **208**. The corresponding thiocarbamate derivative was obtained by reaction of **206** with thiocarbonyldiimidazole. The conformational evaluation of these three nucleosides was performed by theoretical potential energy calculation. Introduction of the oxazole and thiocarbamate rings at the $2',3'$ -position leads the sugar moiety to adopt an east-type conformation ($P=73$ - 110°). The conformation around the glycosidic bond was found to be *anti* and the values of the torsion angle γ were found to be γ^\dagger ($\gamma=180^\circ$) for nucleosides **192** and **194** and γ^+ ($\gamma=60^\circ$) for nucleoside **193**. None of these compounds showed activity against the viral strains tested, as well as no cytotoxicity.

⁹¹ Papchikhin, A.; Chattopadhyaya, J. *Tetrahedron* **1994**, *50*, 5279-5286.

⁹² Kifli, N.; Htar, T. T.; De Clercq, E.; Balzarini, J.; Simons, C. *Bioorg. Med. Chem.* **2004**, *12*, 3247-3257.



a) TBSCl, Im, DMF; b) Ph_3P , THF, H_2O , 60 °C; c) *N,N*-dimethylformamide or *N,N*-dimethylacetamide dimethyl acetal DMF; d) TBAF, THF; e) TCDI, CH_2Cl_2 .

Scheme 38. Synthesis of nucleosides **192-194**.

With regard to nucleoside analogues bearing a fused six-membered ring at the 2',3'-position, bicyclic systems featuring cyclohexene and benzene rings have been reported (Figure 29).

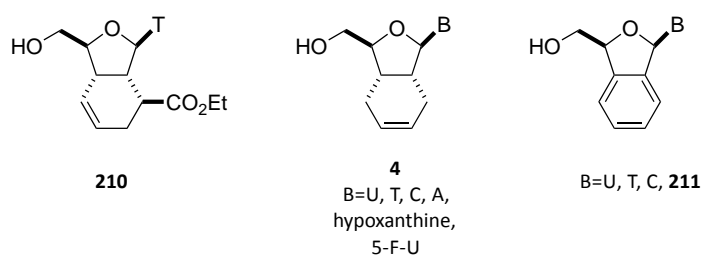
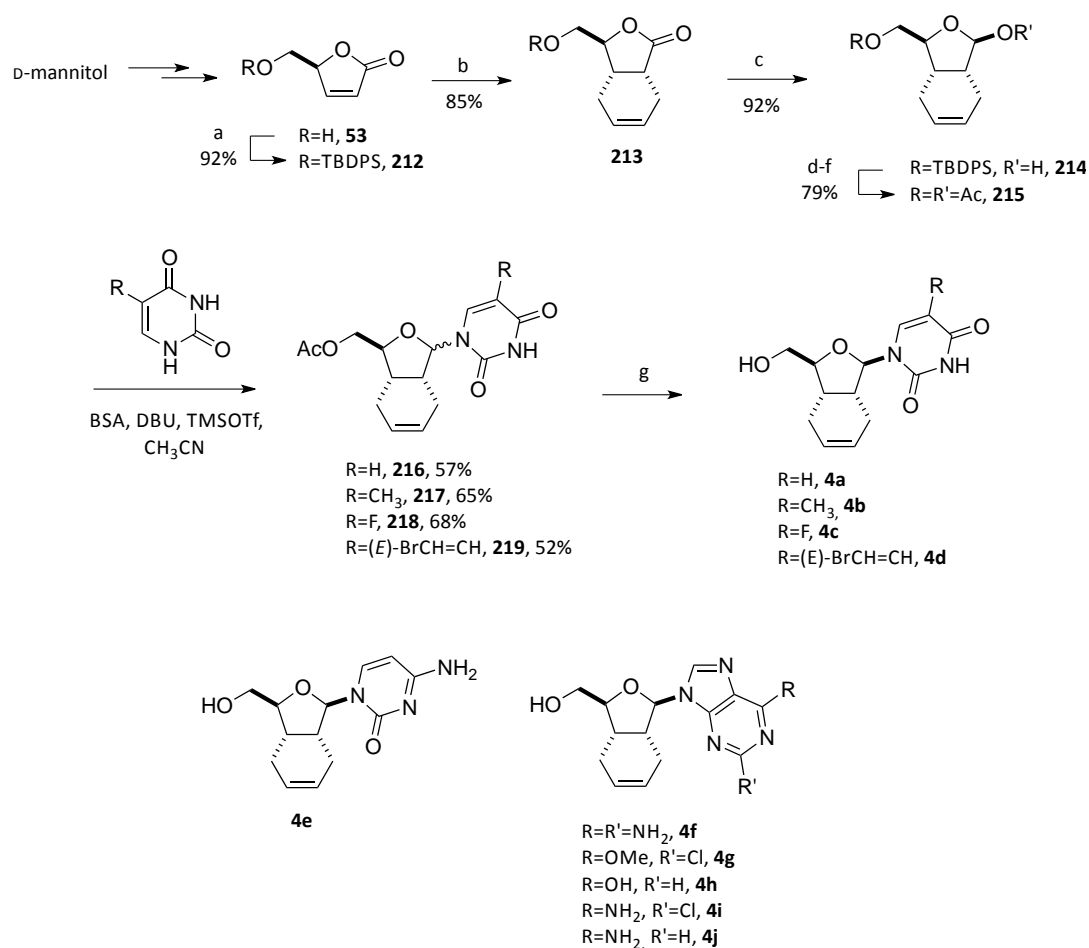


Figure 29. Examples of conformationally restricted nucleosides by the presence of a six-membered ring.

In parallel with their work on cyclopentane bicyclic nucleosides presented in Scheme 37, Chattopadhyaya achieved the synthesis of the cyclohexane nucleoside **210**. The conformational analysis of this compound was carried out by energy minimization and it was found that the furanose moiety adopted a conformation close to O4'-endo-C4'-exo twist ($P=79^\circ$, $\nu_{\text{max}}=27^\circ$), thymine was *anti* ($\chi=-141^\circ$) and orientation across C4'-C5' bond was γ^+ ($\gamma=57^\circ$). As in the case of the cyclopentane derivatives, compound **210** was not screened for antiviral activity.

More recently, Gotor and Theodorakis have described the preparation of the set of cyclohexene derivatives **4**.¹⁹ The synthesis of this family of nucleosides started from the 2(5*H*)-furanone **53** (Scheme 39). The cyclohexene core was installed by a Diels-Alder reaction between the protected lactone **212** and butadiene, providing exclusively the *anti* adduct **213**. Lactone

reduction and acetylation of both hydroxyl groups delivered **215**, an appropriate substrate for the glycosylation reaction. This compound was coupled with different pyrimidine nucleobases giving **216-219** in good yields. Finally, cleavage of the 5'-acetate group by treatment with ammonia afforded nucleosides **4a-d**. Making use of analogous synthetic sequences, the cytidine **4e** and the purine nucleosides **4f-j** could also be reached. These 2',3'-cyclohexene fused analogues were evaluated against HIV and it turned out that only the ddl analogue **4h** exhibited a moderate activity with an EC₅₀ of 12.3 μM. Additionally, the thymine nucleoside **4b** could be crystallized showing a C3'-exo conformation, with a pseudorotational angle *P* of 185.2° and a puckering degree v_{\max} of 39.7°.



a) TBDPSCI, NH₄NO₃, DMF; b) butadiene, AlCl₃, CH₂Cl₂; c) DIBAL-H, CH₂Cl₂; d) Ac₂O, py; e) TBAF, THF; f) Ac₂O, py; g) NH₃, MeOH.

Scheme 39. Synthesis of the cyclohexene-fused nucleosides **4a-j**.

The last group of nucleosides bearing a 2',3'-fused six-membered ring features a benzo[c]furan core (**211**) and have been synthesized by Ewing and co-workers starting from phthalaldehyde.⁹³ So far, neither conformational parameters nor biological properties of these compounds have been reported.

Finally, examples of bicyclo[3.2.0]-fused analogues are shown in Figures 30 and 31. The first example of this series of compounds, **8**, was synthesized by Mikhailopulo and co-workers while working on the synthesis of 3'-substituted nucleoside analogues.²² On the other hand, the synthesis of **220** was described by Wengel and co-workers in 1998.⁹⁴ This nucleoside, featuring a 3'-hydroxyl group, was designed to be implemented into conformationally restricted oligonucleotide chains. Molecular modeling and NMR studies showed that the nucleoside exhibited an O4'-endo (⁰E) conformation.

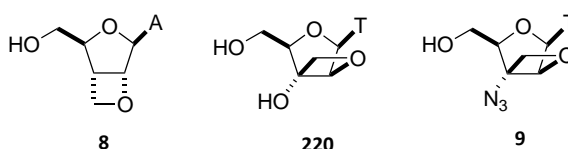


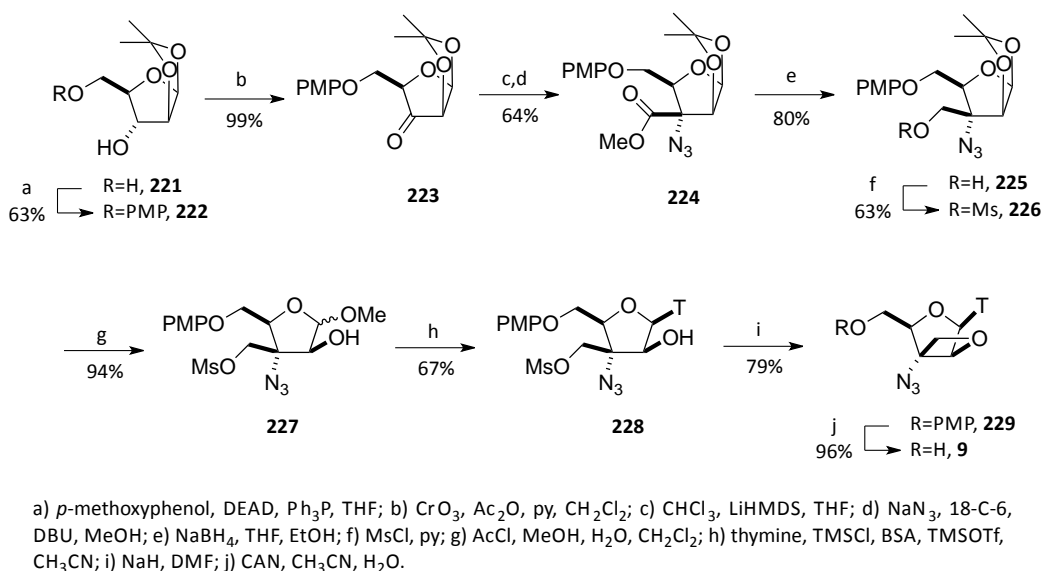
Figure 30. Examples of nucleosides bearing a fused 2',3'-oxetane ring.

Later, Nielsen and co-workers described the synthesis of **9**, a conformationally restricted nucleoside analogue of the anti-HIV drug AZT bearing a 2',3'-fused oxetane ring (Scheme 40).²³ The azide group was introduced by treatment of ketone **223** with the trichloromethyl anion and subsequent modified Corey-Link reaction.⁹⁵ The oxetane ring was constructed by an intramolecular displacement of the mesylate on **228**. Conformational analysis was based on modeling studies and NMR analysis. Thus, a geometry optimization by *ab initio* calculation revealed that the bicyclic nucleoside adopted an east-type conformation (O4'-endo) with $P=91.4^\circ$ and a ν_{\max} of 46.8° . This nucleoside did not show anti-HIV activity in cell culture experiments.

⁹³ Ewing, D. F.; Fahmi, N.-E.; Len, C.; Mackenzie, G.; Pranzo, A. *J. Chem. Soc., Perkin Trans. 1*, **2000**, 3561-3565.

⁹⁴ Christensen, N. K.; Petersen, M.; Nielsen, P.; Jacobsen, J. P.; Olsen, C. E.; Wengel, J. *J. Am. Chem. Soc.* **1998**, *120*, 5458-5463.

⁹⁵ Dominguez, C.; Ezquerro, J.; Baker, S. R.; Borrelly, S.; Prieto, L.; Espada, M.; Pedregal, C. *Tetrahedron Lett.* **1998**, *39*, 9305-9308.



Scheme 40. Synthesis of the AZT analogue 9.

Interestingly, no examples of a C_2 -carbon chain attached to the furanose ring by the 2',3' positions had been published until the synthesis of **10-21** carried out in our laboratories (Figure 31). Crystals of the adenine derivatives **11** and **13** could be grown and their crystallographic data was compared to that of ddA and d4A.^{24,26} The crystallographic data of ddA and d4A could be obtained from the *Cambridge Crystallographic Database*.⁹⁶ The fluorinated α nucleoside **230** could also be crystallized and analyzed by X-ray spectroscopy. All these cyclobutane nucleosides have been evaluated against HIV-1, with the adenine derivatives **11** and **18** showing moderate activity (EC_{50} =17.8 and 22.9 $\mu\text{g}/\text{mL}$, respectively).

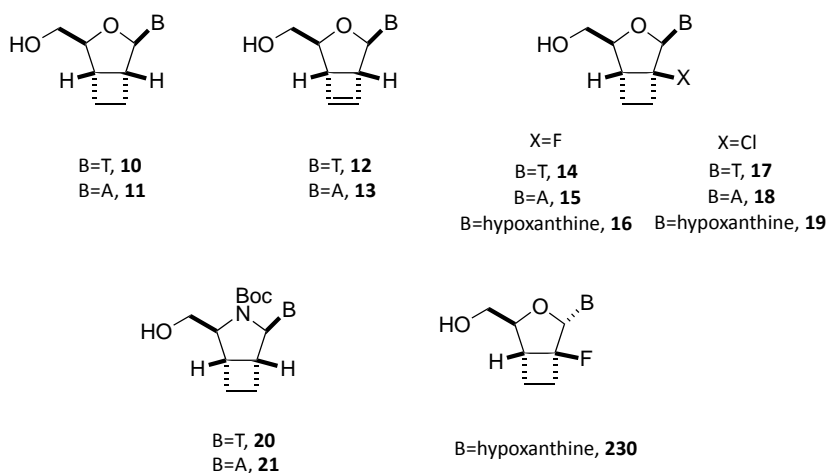


Figure 31. Cyclobutane-fused nucleosides synthesized in our laboratories.

⁹⁶ Allen, F. H. *Acta Crystallogr., Sect. B* **2002**, *58*, 380-388.

The data from compounds **11** and **13** (Table 4) suggests that the introduction of the C₂ chain flattens the sugar ring providing some rigidity (compared to ddA, $v_{\max} \sim 25^\circ$ vs. $v_{\max} \sim 35^\circ$), but at the same time allows a certain degree of flexibility (compared to d4A, $v_{\max} \sim 25^\circ$ vs. $v_{\max} \sim 7^\circ$). The four nucleosides are found on the south-west quadrant of the pseudorotational cycle (Figure 32).

On the other hand, nucleoside **230** shows a C4'-endo (⁴E) pucker with a pseudorotational angle $P=247.1^\circ$ and a puckering amplitude of $v_{\max}=27.5^\circ$. The pucker of this nucleoside lays between **11** and **13**, sharing a ⁴E pucker with the cyclobutane derivative **11**. The torsion angles cannot be compared due to the different configuration of the anomeric center.

Table 4 summarizes the reported conformational information of the nucleosides that appear on this section. Additionally, Figure 32 shows the positioning of these nucleosides on the pseudorotational cycle.

Compound	P^a ($^\circ$)	v_{\max}^b ($^\circ$)	χ^c ($^\circ$)	γ^d ($^\circ$)
ddA	190.4	35.7	-95.9	-178.7
d4A	243.5	7.5	-100.2	179.8
d4T	72.1	0.6	-100.8	52.8
11	228.1	22.9	-157.1	173.8
13	259.8	25.7	-175.5	-75.6
230	247.1	27.5	163.6	56.6
1d	91.7	34.5	-73	177.0
4b	185.2	39.7	160.6	-51.0
5	98.9	29.2	-121.9	-167.7
9	91.4	46.8	nd	nd
169	86.7	8.8	-106.9	-174.7
190	86	27	-154	59
191	89	39	-141	60
192	89	28.6	-135.4	179.9
193	110	41.5	-134.2	60.8
194	73	43.8	-134.7	179.7
210	79	27	-141	57

^a P : pseudorotation angle. ^b v_{\max} : maximum puckering amplitude. ^c χ : torsion angle O4'-C1'-N9-C4 or O4'-C1'-N1-C2. ^d γ : torsion angle O5'-C5'-C4'-C3'.

Table 4. Conformational parameters of conformationally restricted nucleosides.

It is worth to mention that most of the 2',3'-fused bicyclo nucleosides with reported data about their structure are positioned in the east conformation away from the preferred location of the natural nucleosides. Interestingly, our cyclobutane fused ring induces a preferential conformation between west and south.

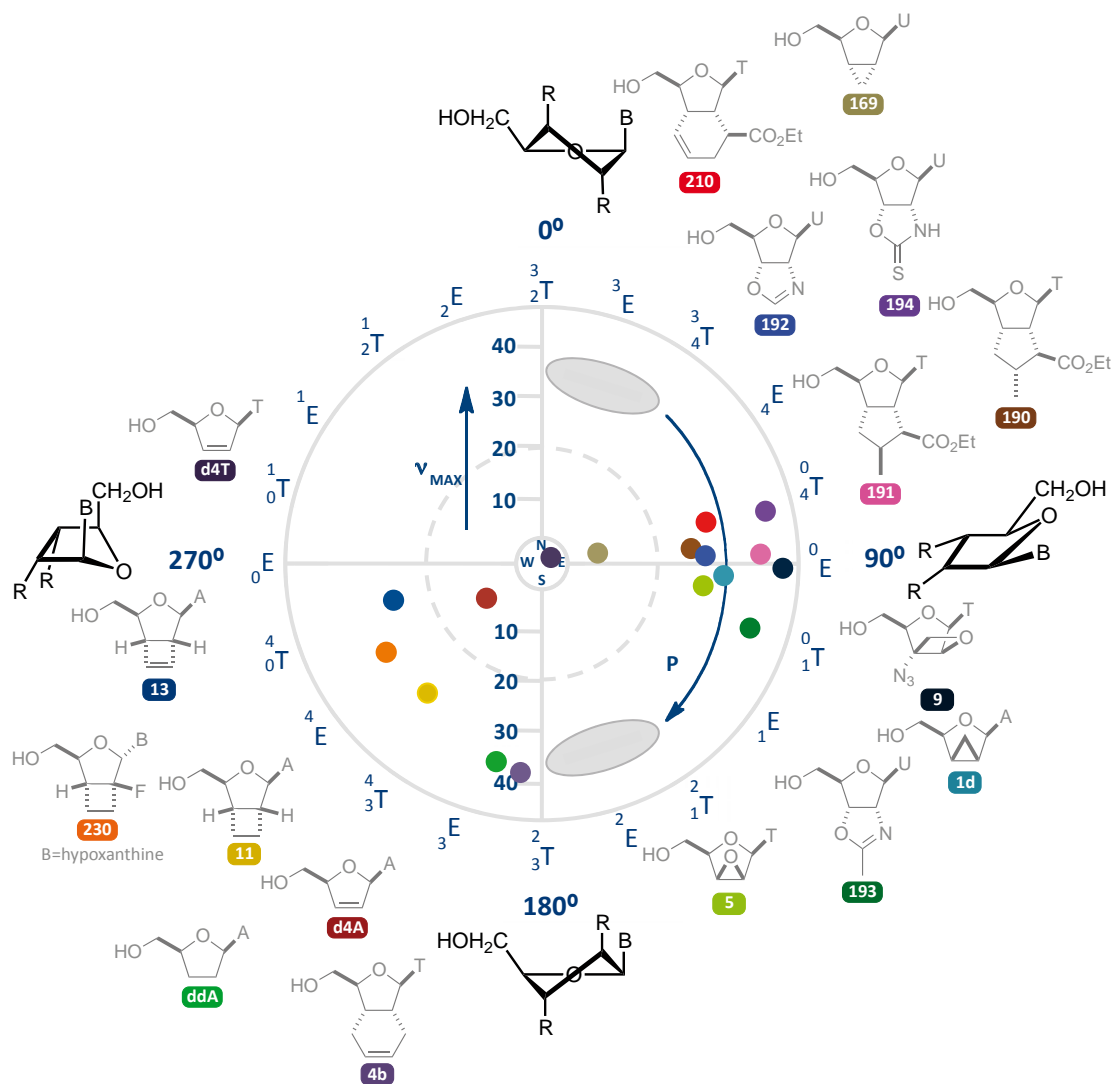


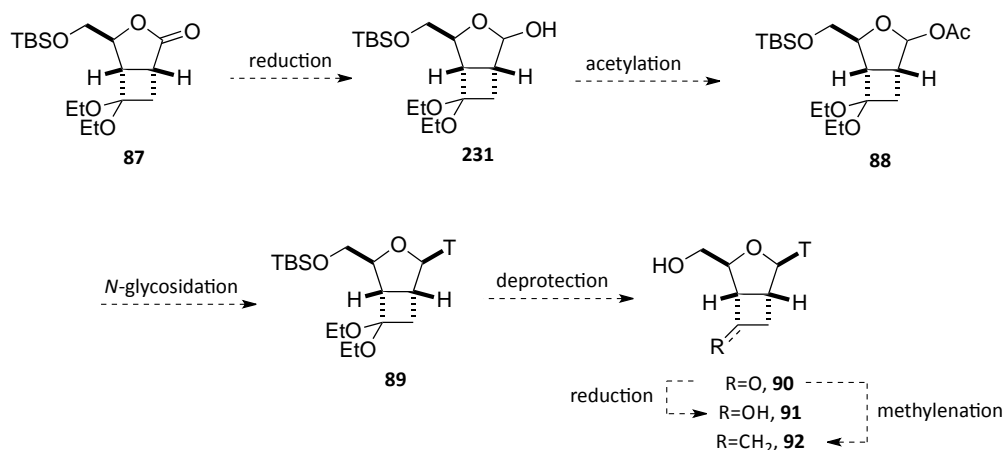
Figure 32. Location of representative conformationally restricted nucleosides on the pseudorotational cycle.

3. SYNTHESIS OF CONFORMATIONALLY RESTRICTED NUCLEOSIDES BEARING A FUNCTIONALIZED CYCLOBUTANE RING

3.1 Synthetic strategy overview

The first objective of the present thesis was the synthesis of a family of novel nucleoside analogues of d4T bearing a fused functionalized cyclobutane ring.

The synthetic strategy started from cycloadduct **87** (Scheme 41). Reduction of the lactone followed by acetylation should provide acetate **88**. This substrate would allow the introduction of the nucleobase using Vorbrüggen's *N*-glycosylation methodology, obtaining the β -anomer **89**. Deprotection of this intermediate would lead to the keto-nucleoside **90**. Finally, this nucleoside would be further transformed into nucleosides **91** and **92**.

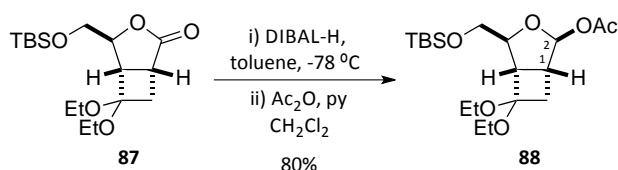


Scheme 41. Planned synthetic strategy to prepare nucleosides **90-92**.

3.2 Synthesis of the conformationally restricted nucleosides **90-92**

3.2.1 Preparation of acetate **88**

Reduction of lactone **87** was accomplished using diisobutylaluminium hydride (DIBAL-H) in toluene at -78 °C (Scheme 42). The resulting lactol was treated directly with acetic anhydride and pyridine in CH₂Cl₂ to afford acetate **88** as a single diastereomer in 80% yield for the two steps.



Scheme 42. Synthesis of acetate **88**.

Determination of the anomeric configuration of the product could be achieved by the value of the coupling constant between H1 and H2, which according to the Karplus equation,⁹⁷ is anticipated to display a high coupling constant value when the dihedral angle is near 0° or 180° (Figure 33). On the other hand, if the angle is close to 90°, the value of the coupling constant should be around 0 Hz.

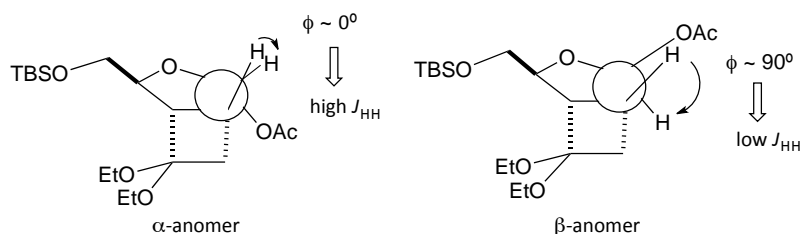


Figure 33. Qualitative determination of $^3J_{\text{HH}}$ between H1 and H2 for the α - and β -anomers.

Since the signal corresponding to H2 appears as a singlet in the $^1\text{H-NMR}$ spectrum, we can assume that $J_{2,1} \approx 0$ Hz, leading to the assignment of a β -configuration of the anomeric center.

3.2.2 Vorbrüggen *N*-glycosylation reaction

3.2.2.1 Reaction mechanism

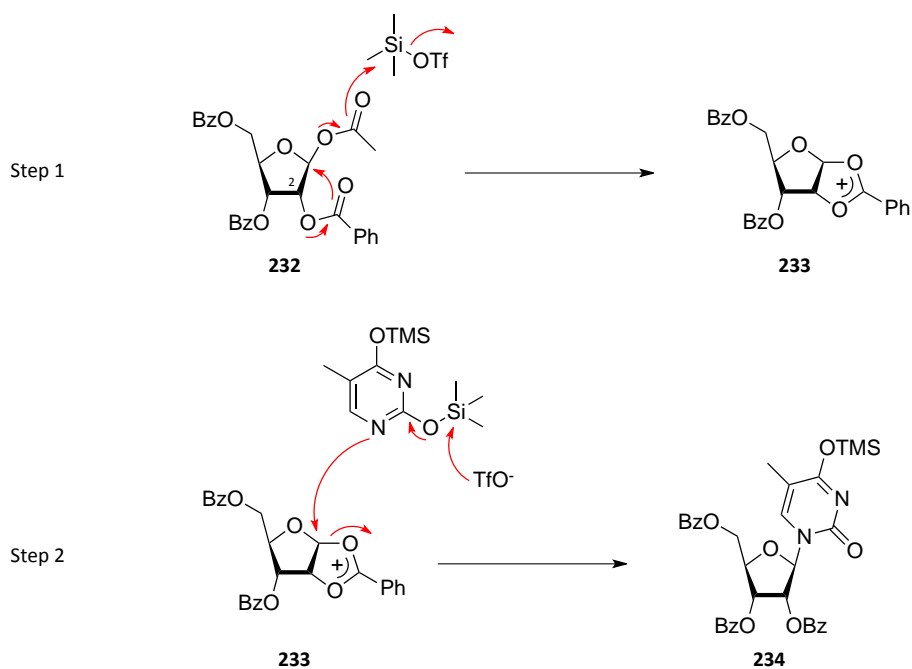
What is nowadays known as the Vorbrüggen *N*-glycosylation reaction is a modification of the silyl-Hilbert-Johnson reaction in which apart from using a silylated nucleobase (enhancing its solubility in organic solvents), a Lewis acid is used to catalytically generate the initial reactive species. Although different Lewis acids have been employed for this purpose (e.g. TiCl_4 , SnCl_4), the use of TMSOTf is currently widespread because of the easy work-up.⁹⁸

According to Vorbrüggen's mechanistic proposal, when the substrate bears an ester-protected hydroxyl group at position 2, the reaction proceeds through a cyclic oxonium cation such as **233** (Scheme 43). Thus, formation of **233** takes place with the participation of the vicinal ester group. This intermediate reacts with the persilylated base to give mainly the β anomer.

Although the catalyst is theoretically recovered, one equivalent of TMSOTf is inactivated during the process due to σ -complex formation with the base. Thus, the use of 1.1-1.3 equivalents of TMSOTf dramatically shortens the reaction time.

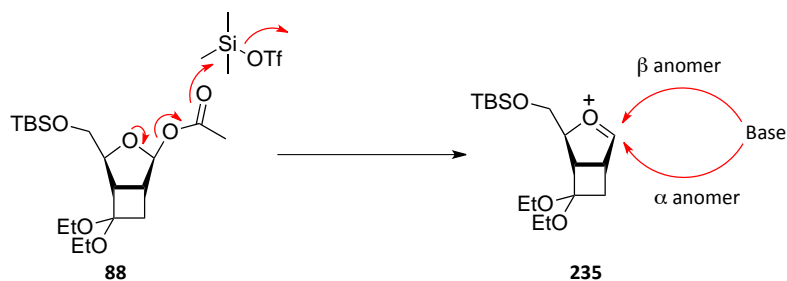
⁹⁷ (a) Karplus, M. J. *Chem. Phys.* **1959**, *30*, 11-15. (b) Karplus, M. J. *Am. Chem. Soc.* **1963**, *85*, 2870-2871.

⁹⁸ (a) Vorbrüggen, H.; Krolkiewicz, K.; Bennua, B. *Chem. Ber.* **1981**, *114*, 1234-1255. (b) Vorbrüggen, H.; Ruh-Pohlenz, C. *Handbook of Nucleoside Synthesis*, John Wiley & Sons: New York, 2001.



Scheme 43. Mechanistic proposal of Vorbrüggen's *N*-glycosylation reaction.

In general, the coupling reaction of 2'-deoxysugars with silylated bases proceeds without selectivity. This is due to the planarity of the intermediate cation, which is not expected to show any significant influence on the approach of the nucleophile. However, in our compound **235**, the presence of the cyclobutane ring may favour the formation of the β -anomer (Scheme 44).



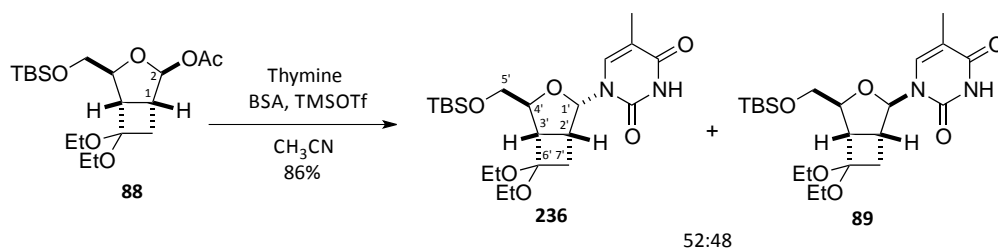
Scheme 44. Mechanistic proposal for the *N*-glycosylation of substrate **88**.

3.2.2.2 *N*-Glycosylation reaction. Introduction of thymine

To carry out the *N*-glycosylation reaction we have followed the one-pot procedure described by Dudycz and Wright,⁹⁹ which uses BSA (*N,O*-Bis(trimethylsilyl)acetamide) as the silylating agent. Thus, reaction of **88** with thymine, BSA and TMSOTf as the Lewis acid in acetonitrile at room temperature, furnished a mixture of anomers **236** and **89** (Scheme 45). The two compounds

⁹⁹ Dudycz, L. W.; Wright, G. E. *Nucleosides Nucleotides* **1984**, *3*, 33-44.

could be separated by column chromatography to afford the pure α - and β -anomers **236** and **89** in 45% and 41% yield, respectively.



Scheme 45. Introduction of thymine on substrate **88**.

The reaction was also carried out using SnCl₄ as the Lewis acid, but neither change in diastereoselectivity (52:48) nor yield (which remained around 80%) was observed. It is worth mentioning that no further attempts to improve the diastereoselectivity of the process were made since evaluation of the antiviral activity of the α analogue was also considered, owing to the significant antiviral activities reported for some α -nucleoside analogues.¹⁰⁰

Assignment of the α/β anomeric configuration was readily achieved by means of the coupling constant values between H1 and H2. Thus, the diastereomer presenting a coupling constant of $J_{1',2'}=5.7$ Hz was assigned as the α -anomer **236**, whereas the compound showing a $J_{1',2'}=2.1$ Hz was designated as the β -anomer **89**. This assignment could be unambiguously confirmed by their NOESY spectra. The α anomer **236** showed cross peaks between H1' and H2' and H6 showed signals with H1', H4' and H7'_{endo} (Figure 34). On the other hand, the β anomer **89** exhibited a signal between H1' and H4' and H6 showed cross peaks with H2', H3' and H5' (Figure 35).

¹⁰⁰ (a) Gosselin, G.; Bergogne, M.-C.; de Rudder, J.; de Clercq, E.; Imbach, J.-L. *J. Med. Chem.* **1986**, *29*, 203-213. (b) Migawa, M. T.; Girardet, J.-L.; Walker, J. A.; Koszalka, G. W.; Chamberlain, S. D.; Drach, J. C.; Townsend, L. B. *J. Med. Chem.* **1998**, *41*, 1242-1251. (c) Yamada, K.; Hayakawa, H.; Sakata, S.; Ashida, N.; Yoshimura, Y. *Bioorg. Med. Chem. Lett.* **2010**, *20*, 6013-6016.

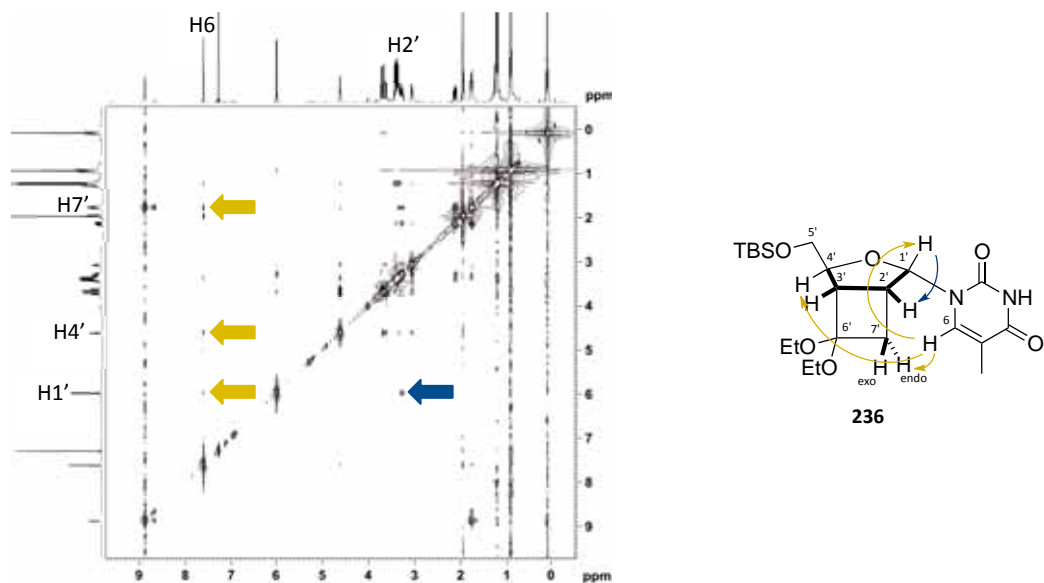


Figure 34. NOESY spectrum (250 MHz, CDCl₃) of 236.

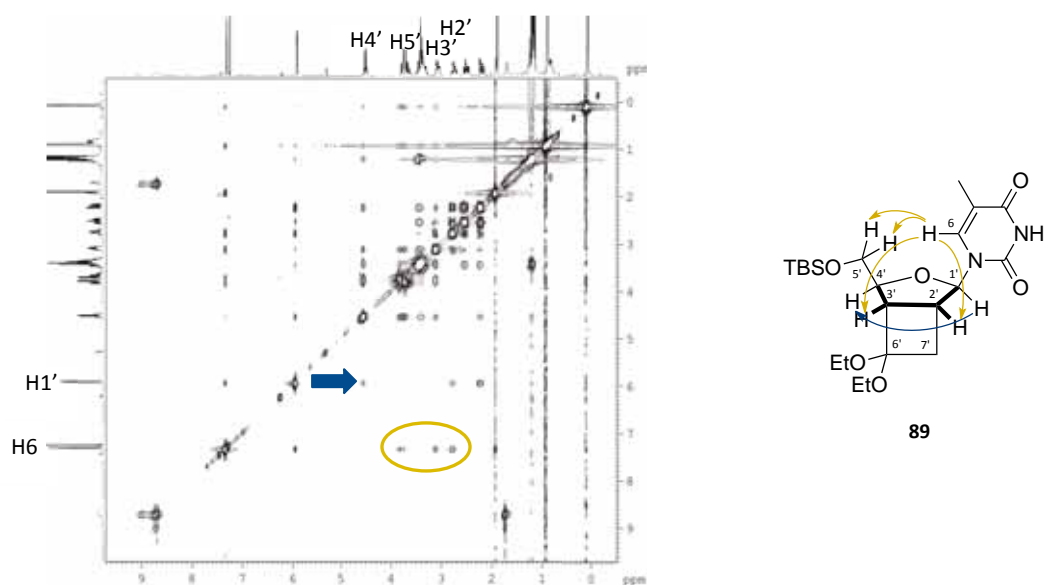
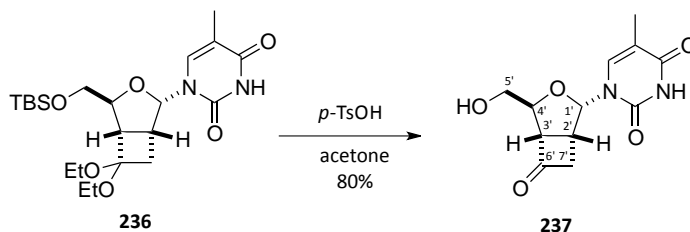


Figure 35. NOESY spectrum (250 MHz, CDCl₃) of 89.

3.2.3 Synthesis of the keto α - and β -nucleosides **237** and **90**.

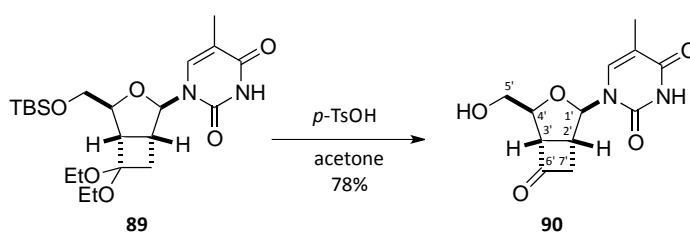
At this point, we turned our attention to the deprotection of adducts **236** and **89** to get the corresponding keto-nucleosides.

First, we considered a selective cleavage of the acetal without deprotection of the 5'-hydroxyl group, in order to carry out the envisioned Wittig reaction. However, reaction of **236** with DMSO/H₂O in dioxane¹⁰¹ only led to the recovery of the unaltered starting material. Other methodologies such as treatment with Amberlyst-15,¹⁰² LiBF₄,¹⁰³ or the acidic clay Montmorillonite K-10,¹⁰⁴ only afforded complex mixtures containing starting material and partly deprotected products. As it was not practical to separate all compounds from these mixtures, we opted for a complete deprotection. Consequently, treatment of acetal **236** with a catalytic amount of *p*-TsOH in acetone at room temperature, led to our first nucleoside analogue, **237**, in 80% yield (Scheme 46).



Scheme 46. Deprotection of **236**.

The same conditions applied to the β anomer **89**, afforded nucleoside **90** in 78% yield (Scheme 47).



Scheme 47. Deprotection of **89**.

¹⁰¹ Kametani, T.; Kondoh, H.; Honda, T.; Ishizone, H.; Suzuki, Y.; Mori, W. *Chem. Lett.* **1981**, *18*, 901-904.

¹⁰² Coppola, G. M. *Synthesis* **1984**, 1021-1023.

¹⁰³ Roush, W. R.; Sciotti, R. J. *J. Am. Chem. Soc.* **1994**, *116*, 6457-6458.

¹⁰⁴ Gautier, E. C. L.; Graham, A. E.; McKillop, A.; Standen, S. P.; Taylor, R. J. K. *Tetrahedron Lett.* **1997**, *38*, 1881-1884.

Deprotection of the carbonyl and hydroxyl groups of both diastereomers could be confirmed by NMR (Figure 36) and IR spectroscopy. Thus, in the proton spectra, protons H7' of **237/90** appear downfield shifted (δ 2.81-3.49) compared to **236/89** (δ 1.73-2.51). Additionally, a new signal at δ 209.6 corresponding to C6' is observed in the ^{13}C -NMR spectra, and a wide absorption in the IR spectra at $3500\text{-}3100\text{ cm}^{-1}$ corresponding to the free hydroxyl group is also observed.

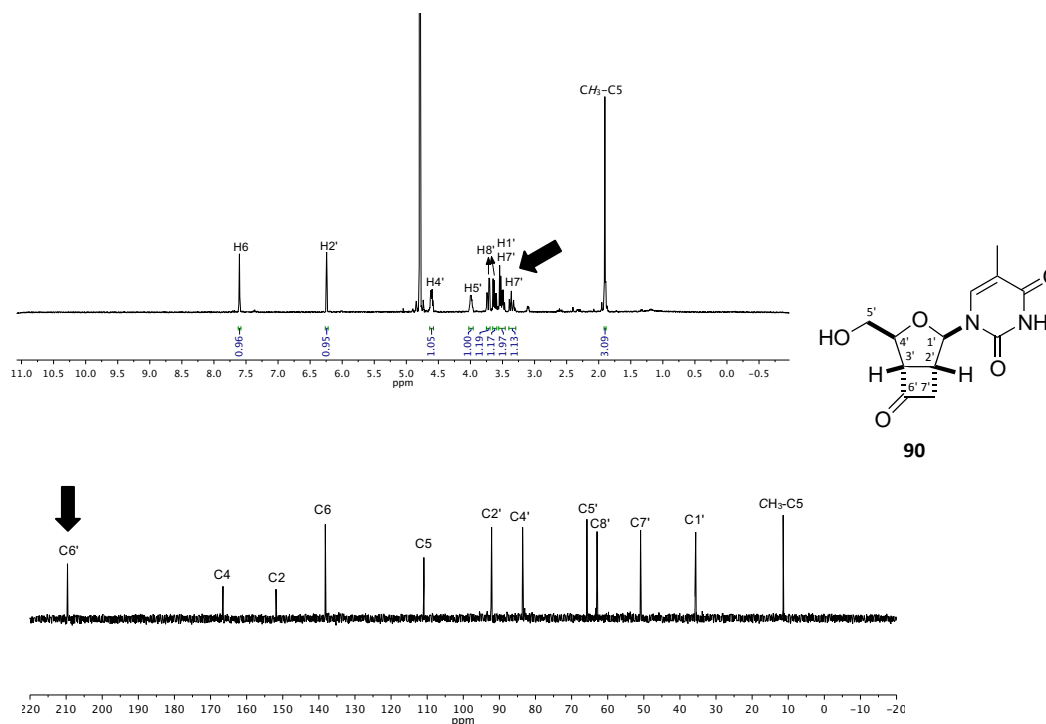


Figure 36. ^1H -NMR (360 MHz, D_2O) and ^{13}C -NMR (90 MHz, D_2O) spectra of **90**.

3.2.4 Synthesis of the hydroxyl and methylene nucleosides **91** and **92**

The presence of the ketone group on compounds **90** and **237** gives them an additional value since they can be further modified to obtain differently functionalized nucleosides. From this point, we decided to focus our efforts on the synthesis of the β derivatives.

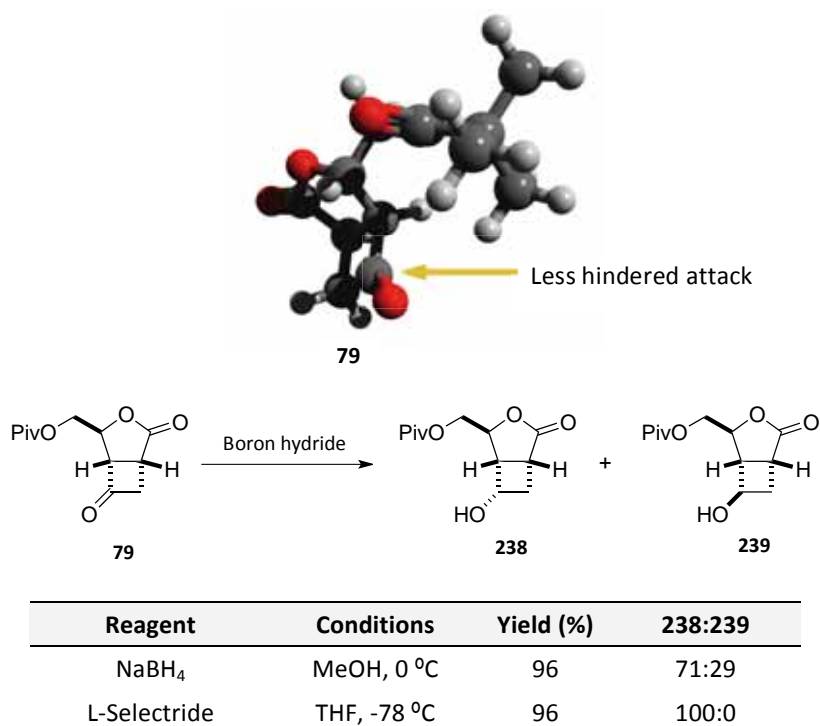
3.2.4.1 Synthesis of the hydroxyl nucleoside **91**

In first place, we undertook the synthesis of the hydroxyl derivative **91** from nucleoside **90**. To carry out this transformation, a stereoselective reduction was necessary.

At this point it should be pointed out that a reduction of a similar cyclobutanone had been previously conducted successfully in our research group by Dr. Albert Rustullet. During his work on the synthesis of Cyclobut-A, he assayed the reduction of **79** with two different boron hydrides.¹⁰⁵

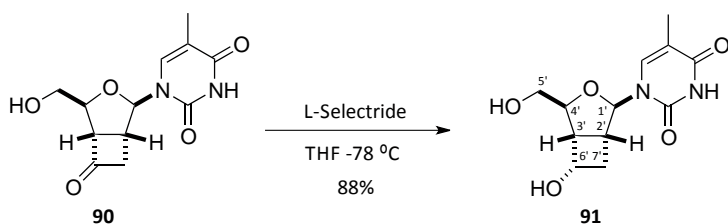
¹⁰⁵ Rustullet, A. *PhD Thesis*, UAB, 2006.

Though the substrate exhibited a notably less congested convex face for hydride attack, a bulky reagent like L-Selectride was necessary to achieve complete diastereoselectivity in an excellent yield (Scheme 48).



Scheme 48. Reduction of **79**.

Taking into account the above results, the reaction of **90** was carried out with L-Selectride in THF at -78 °C delivering nucleoside **91** as a single diastereomer and 88% yield (Scheme 49).



Scheme 49. Reduction of nucleoside **90**.

The stereoselectivity of the hydride attack could be confirmed by the NOESY experiment of **91**, where the newly attached H6' showed cross peaks with H3', H2' and H7'_{exo} (Figure 37).

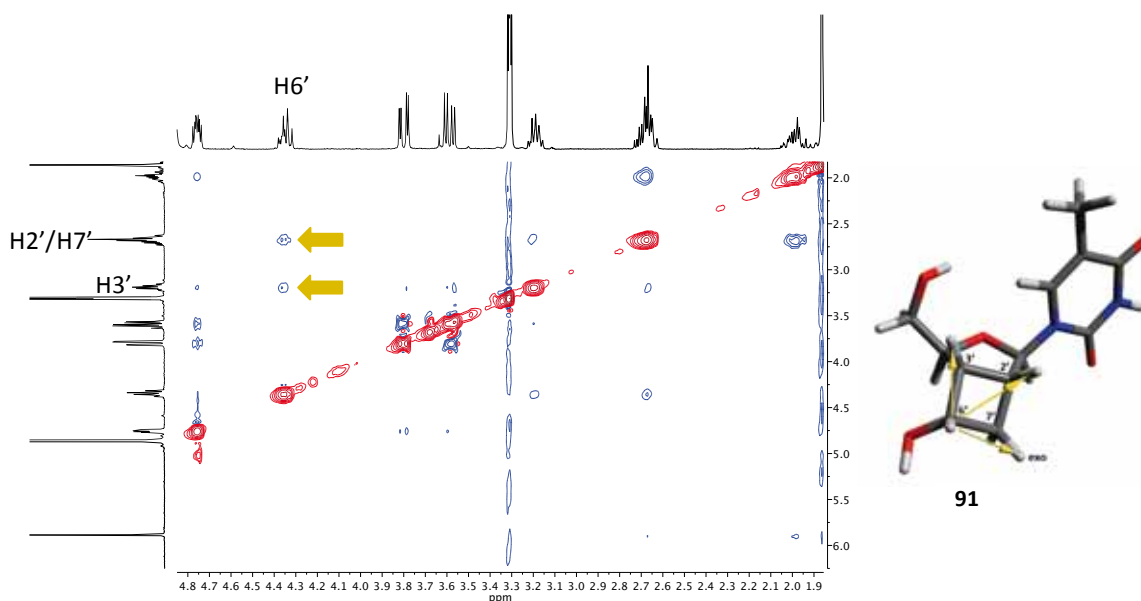
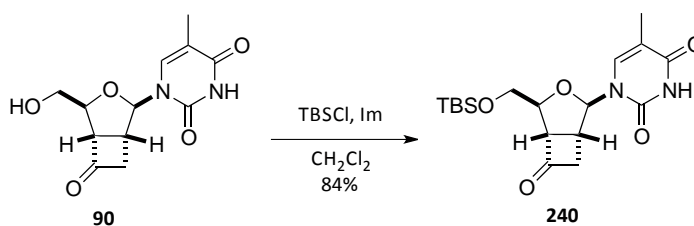


Figure 37. NOESY spectrum (360 MHz, MeOD) of **91**.

The presence of the free 6' hydroxyl group makes compound **91** feasible to explore in a future its possible insertion into conformationally restricted oligonucleotide chains.

3.2.4.2 Synthesis of the methylene nucleoside **92**

After completing the synthesis of **91**, we targeted the preparation of the analogue **92** bearing an exocyclic carbon-carbon double bond. To prepare this analogue, the hydroxyl group of **90** should be previously protected. Thus, treatment of **90** with TBSCl and imidazole in CH_2Cl_2 under standard conditions gave the silyl derivative **240** in 84% yield (Scheme 50).

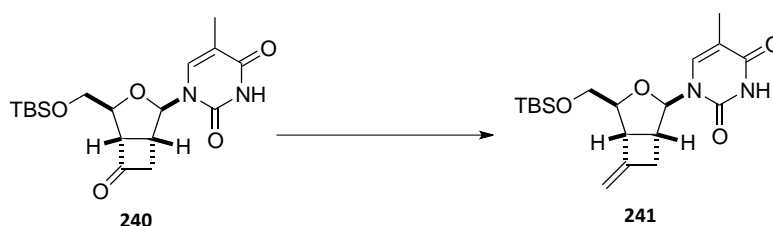


Scheme 50. Protection of **90** as the TBS ether.

With ketone **240** in hands, we moved on to the methylenation reaction, which proved to be more problematic than it was expected. Initially, we tested the standard phosphonium salts $\text{Ph}_3\text{PCH}_3\text{I}$ and $\text{Ph}_3\text{PCH}_3\text{Br}$ together with *n*-BuLi as the base (Scheme 51, entries 1 and 2). However, alkene **241** was obtained in only 44% and 26% yield, respectively, and no other byproducts were

observed. With such moderate results, we decided to explore alternative methodologies.¹⁰⁶ The use of Peterson's methodology¹⁰⁷ also met with failure, providing trace amounts of the β -hydroxy silane intermediate (entry 3).

The combination of TMSCH_2Li and CeCl_3 has been reported as a milder version of the Peterson reaction.¹⁰⁸ However, when this methodology was applied to our substrate, only recovery of the starting material was observed (entry 4). Finally, we attempted the use of organometallic compounds, which have been described to give good results with hindered substrates.¹⁰⁹ However, treatment of **240** with neither the Petasis'¹¹⁰ nor Tebbe's¹¹¹ reagents (entries 5 and 6) improved the preceding results.



Entry	Reagent(s)	Yield (%)
1	$\text{Ph}_3\text{PCH}_3\text{I}$, <i>n</i> -BuLi	44
2	$\text{Ph}_3\text{PCH}_3\text{Br}$, <i>n</i> -BuLi	26
3	TMSCH_2Li	-
4	TMSCH_2Li , CeCl_3	sm
5	Cp_2TiMe_2	sm
6	Tebbe reagent	27

Scheme 51. Methylenation of substrate **240**.

After all, the methodology that gave better results was the use of $\text{Ph}_3\text{PCH}_3\text{I}$ and *n*-BuLi in THF, which delivered alkene **241** in 44% yield.

The new methylene unit could be easily identified in the $^1\text{H-NMR}$ and $^{13}\text{C-NMR}$ spectra. In the former, a new signal corresponding to H1'' appeared at δ 4.91 (Figure 38). In the latter, the C6' peak which in **240** appeared at δ 204.9, was found at higher fields (δ 147.0). Furthermore, a new signal appeared at δ 108.6 corresponding to the methylene carbon C1''.

¹⁰⁶ For a review see: Beadham, I.; Micklefield, J. *Curr. Org. Synth.* **2005**, *2*, 231-259.

¹⁰⁷ Peterson, D. J. *J. Org. Chem.* **1968**, *33*, 780-784.

¹⁰⁸ Johnson, C. R.; Tait, B. D. *J. Org. Chem.* **1987**, *52*, 281-283.

¹⁰⁹ Pine, S. H.; Shen, G. S.; Hoang, H. *Synthesis* **1991**, 165-167.

¹¹⁰ Petasis, N. A.; Bzowej, E. I. *J. Am. Chem. Soc.* **1990**, *112*, 6392-6394.

¹¹¹ Tebbe, F. N.; Parshall, G. W.; Reddy, G. S. *J. Am. Chem. Soc.* **1978**, *100*, 3611-3613.

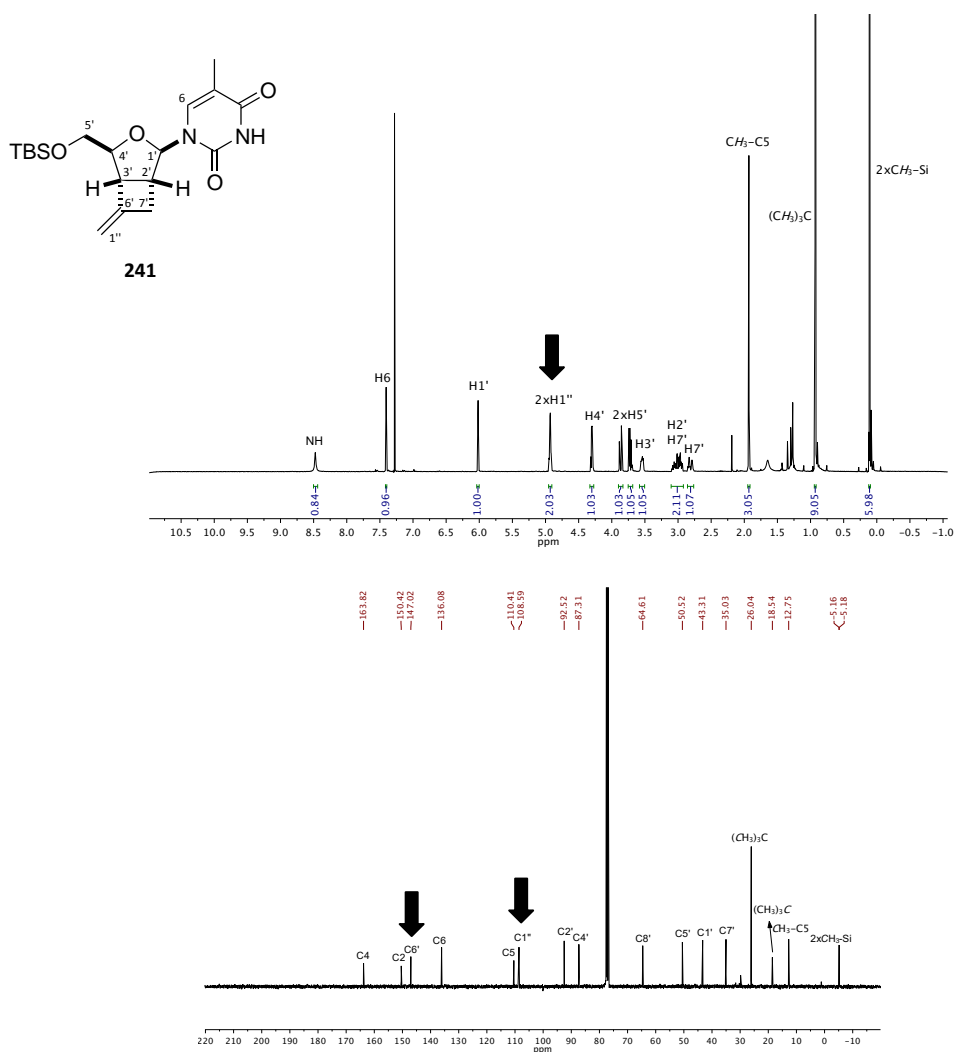
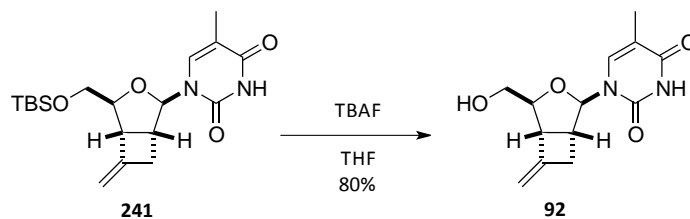


Figure 38. $^1\text{H-NMR}$ (360 MHz, CDCl_3) and $^{13}\text{C-NMR}$ (90 MHz, CDCl_3) spectra of **241**.

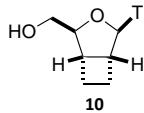
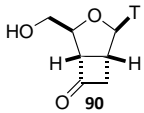
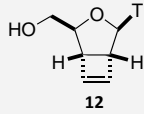
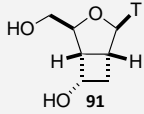
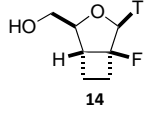
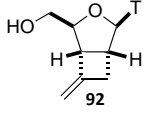
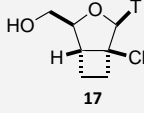
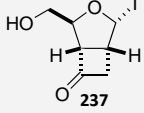
To finish the synthesis of nucleoside **92**, all that remained was the deprotection of the 5'-hydroxyl group. Accordingly, cleavage of the silyl ether was accomplished with standard TBAF treatment, which provided nucleoside **92** in 80% yield (Scheme 52).



Scheme 52. Deprotection of **241**.

4. EVALUATION OF THE ANTIVIRAL ACTIVITY

The anti-HIV activity of all the conformationally restricted d4T analogues prepared by our research group and the ones described in this chapter has been evaluated by the research group leaded by Dr. José A. Esté at the *Laboratori de Retrovirologia de la Fundació IrsiCaixa de l' Hospital Universitari Germans Trias i Pujol* (Table 5). The experiments have been carried out against a HIV-1 NL4-3 wild type strain, using a MT-4 limfoid cellular line (received from the NIH AIDS Reagent Program).¹¹² Measures were performed taking the known antivirals AZT and d4T as reference.

Compound	EC ₅₀ ^b	CC ₅₀ ^c	Compound	EC ₅₀	CC ₅₀
AZT	0.0007	>1	AZT	0.0007	>1
d4T	0.01	>2	d4T	0.01	>2
	>25	>25		>25	>25
	>25	>25		>25	>25
	>25	>25		>25	>25
	>25	>25		>18.3	18.3

All values are in $\mu\text{g/mL}$. Data represent mean values of at least two experiments. ^b EC₅₀: Effective concentration 50 or needed concentration to inhibit 50% HIV-induced cell death, evaluated with the MTT method in MT-4 cells. ^c CC₅₀: Cytotoxic concentration 50 or needed concentration to induce 50% death of non-infected cells, evaluated with the MTT method in MT-4 cells.

Table 5. Evaluation of the anti-HIV activity of conformationally restricted d4T analogues.

The data from Table 5 reveals that despite the structural analogy of the prepared nucleosides with d4T, none of these cyclobutane nucleosides exhibited activity against HIV at concentrations up to 25 $\mu\text{g/mL}$. Besides, the α -anomer **237** was found to be cytotoxic for concentrations above 18.3 $\mu\text{g/mL}$. In order to shed light on the plausible reasons for this lack of activity, a molecular study of the activation process of these nucleosides and their binding with HIV-RT was undertaken.⁷⁸

¹¹² Manetti, F.; Esté, J. A.; Clotet-Codina, I.; Armand-Ugón, M.; Maga, G.; Crespan, E.; Cancio, R.; Mugnani, C.; Bernardini, C.; Togninelli, A.; Carmi, C.; Alongi, M.; Petricci, E.; Massa, S.; Corelli, F.; Botta, M. *J. Med. Chem.* **2005**, *48*, 8000-8008.

Additionally, nucleosides **90-92** and **237** have been evaluated against several viruses by the research group leaded by Prof. Jan Balzarini at the *Katholieke Universiteit Leuven*. The results obtained are summarized in Tables 6-10. Unfortunately, these analogues did not exhibit antiviral activity at concentrations up to 100 $\mu\text{g}/\text{mL}$ except for the methylene derivative **92**. This nucleoside showed weak activity particularly against influenza viruses (Table 10). However, it also exhibited substantial cytotoxicity.

Compound	Min. cytotoxic concentration ^a ($\mu\text{g}/\text{mL}$)	EC ₅₀ ^b ($\mu\text{g}/\text{mL}$)				
		HSV-1 (KOS)	HSV-2 (G)	Vaccinia Virus	Vesicular Stomatitis Virus	HSV-1 TK ⁻ KOS ACV
Brivudin (μM)	>250	0.01	96	1.8	>250	250
Cidofovir (μM)	>250	1.2	0.4	10	>250	2
Acyclovir (μM)	>250	0.4	0.08	>250	>250	126
Ganciclovir (μM)	>100	0.03	0.03	>100	>100	4
90	>100	>100	>100	>100	>100	>100
91	>100	>100	>100	>100	>100	>100
92	>100	>100	>100	>100	>100	>100
237	>100	>100	>100	>100	>100	>100

^a Required to cause a microscopically detectable alteration of normal cell morphology. ^b EC₅₀: Effective concentration 50 or needed concentration to inhibit 50% HIV-induced cell death, evaluated with the MTS assay.

Table 6. Cytotoxicity and antiviral activity of nucleosides **90-92** and **237** in HEL cell cultures.

Compound	Min. cytotoxic concentration ^a ($\mu\text{g}/\text{mL}$)	EC ₅₀ ^b ($\mu\text{g}/\text{mL}$)		
		Vesicular Stomatitis Virus	Coxsackie Virus B4	Respiratory Syncytial Virus
DS-5000	>100	100	100	1.8
(S)-DHPA (μM)	>250	>250	>250	>250
Ribavirin (μM)	>250	22	25	4.5
90	>100	>100	>100	>100
91	>100	>100	>100	>100
92	100	>20	>20	>20
237	>100	>100	>100	>100

^a Required to cause a microscopically detectable alteration of normal cell morphology. ^b EC₅₀: Effective concentration 50 or needed concentration to inhibit 50% HIV-induced cell death, evaluated with the MTS assay.

Table 7. Cytotoxicity and antiviral activity of nucleosides **90-92** and **237** in HeLa cell cultures.

Compound	Minimum cytotoxic concentration ^a (µg/mL)	EC ₅₀ ^b (µg/mL)				
		Para-influenza-3 Virus	Reovirus-1	Sindbis Virus	Coxsackie Virus B4	Punta Toro Virus
DS-5000	>100	>100	>100	100	38	20
(S)-DHPA (µM)	>250	>250	>250	>250	>250	>250
Ribavirin (µM)	>250	29	112	>250	>250	29
90	>100	>100	>100	>100	>100	>100
91	>100	>100	>100	>100	>100	>100
92	≥20	>20	>20	>20	>20	>20
237	>100	>100	>100	>100	>100	>100

^a Required to cause a microscopically detectable alteration of normal cell morphology. ^b EC₅₀: Effective concentration 50 or needed concentration to inhibit 50% HIV-induced cell death, evaluated with the MTS assay.

Table 8. Cytotoxicity and antiviral activity of nucleosides **90-92** and **237** in Vero cell cultures.

Compound	CC ₅₀ ^a (µg/mL)	EC ₅₀ ^b (µg/mL)	
		Feline Corona Virus (FIPV)	Feline Herpes virus
HHA	>100	12.2	18.8
UDA	52.4	0.9	1.6
Ganciclovir (µM)	>100	>100	0.7
90	>100	>100	>100
91	>100	>100	>100
92	>100	>100	>100
237	>100	>100	>100

^a CC₅₀: Cytotoxic concentration 50 or needed concentration to induce 50% death of non-infected cells, evaluated with the MTS assay. ^b EC₅₀: Effective concentration 50 or needed concentration to inhibit 50% HIV-induced cell death, evaluated with the MTS assay.

Table 9. Cytotoxicity and antiviral activity of nucleosides **90-92** and **237** in CRFK cell cultures.

Compound	Cytotoxicity		EC ₅₀ ^c (μg/mL)					
			Influenza A H1N1 subtype		Influenza A H3N2 subtype		Influenza B	
	CC ₅₀ ^a	Min. Cytotoxic Conc. ^b	Visual CPE Score	MTS	Visual CPE Score	MTS	Visual CPE Score	MTS
Oseltamivir carboxylate (μM)	>100	>100	9	12.6	0.8	2.0	20	32.1
Ribavirin (μM)	>100	>100	9	9.6	7	2.6	7	1.9
Amantadine (μM)	>200	>200	>200	>200	0.7	0.4	>200	>200
Rimantadine (μM)	>200	>200	40	48.1	0.7	0.1	>200	>200
90	>100	>100	>100	>100	>100	>100	>100	>100
91	>100	>100	>100	>100	>100	>100	>100	>100
92	32.6	20	>4	>4	>4	>4	>4	>4
237	>100	>100	>100	>100	>100	>100	>100	>100

^a CC₅₀: Cytotoxic concentration 50 or needed concentration to induce 50% death of non-infected cells, evaluated with the MTS assay. ^b Required to cause a microscopically detectable alteration of normal cell morphology. ^c EC₅₀: Effective concentration 50 or needed concentration to inhibit 50% HIV-induced cell death, evaluated with the MTS assay.

Table 10. Cytotoxicity and antiviral activity of nucleosides **90-92** and **237** in MDCK cell cultures.

5. COMPUTATIONAL STUDIES OF CYCLOBUTANE-FUSED NUCLEOSIDES

5.1 Docking study

In order to gain understanding of the biological role of these compounds as well as to provide useful information for future synthetic designs, docking studies of the previously described β -nucleosides **10**, **12**, **14** and **17**, as well as the ones prepared in this work (**90**, **91** and **92**), have been carried out in our university by Rosa Miralles in the research group of Dr. Jean-Didier Maréchal. These studies have consisted on the evaluation of the drug-likeness of these compounds, their modeling in the process of activation by cellular kinases and finally the evaluation of their binding at the HIV-RT active site.⁷⁸

Firstly, the seven nucleosides were evaluated for their drug-likeness and cellular absorption. As expected, the full set of compounds fulfilled *Lipinski's rule of five*,¹¹³ predicting adequate pharmacokinetics and suggesting that the lack of activity observed should be attributed to specific molecular interactions with the protein receptors.

The mechanism of action of 2',3'-dideoxynucleosides involves three steps of phosphorylation prior to their interaction with the viral RT (see Chapter I). For the thymine nucleosides, the three kinases that carry out this activation process are thymidine kinase 1 (TK1), thymidylate kinase (TMK) and nucleoside diphosphate kinase (NDPK). Thus, to determine when our compounds could fail in becoming activated, protein-ligand docking studies for both reactant and product forms of our set of nucleosides were carried out at the active site of TK1, TMK and NDPK, taking dT and d4T as structural and energetic benchmarks.

Docking of these nucleosides at the TK1 binding site (PDB IDs: 1XBT,¹¹⁴ 1W4R¹¹⁵) revealed two different behaviours. Compounds **10**, **12**, **14** and **17** presented binding modes similar to dT and d4T, thus being able to undergo phosphate transfer successfully. On the other hand, compounds **90-92** were required to flip around to fit in the enzyme active site, increasing the energy necessary for the phosphorylation process in ~ 4 kJ/mol (Figure 39). Structural analysis of these three nucleosides showed that the substitution on the cyclobutane ring results in steric clashes between the cyclobutane functionalization and some residues of the active site. For compounds

¹¹³ Lipinski, C. A.; Lombardo, F.; Dominy, B. W.; Feeney, P. J. *Adv. Drug Deliver. Rev.* **1997**, *23*, 3-25.

¹¹⁴ Welin, M.; Kosinska, U.; Mikkelsen, N.-E.; Carnrot, C.; Zhu, C.; Wang, L.; Eriksson, S.; Munch-Petersen, B.; Eklund, H. *Proc. Natl. Acad. Sci.* **2004**, *101*, 17970-17975.

¹¹⁵ Birringer, M. S.; Claus, M. T.; Folkers, G.; Kloer, D. P.; Schulz, G. E.; Scapozza, L. *FEBS Lett.* **2005**, *579*, 1376-1382.

90 and **92**, clashing interactions were observed between the carbonyl or methylene group and Asp58, whereas for compound **91** they occurred with the hydroxyl group and Arg60 (Figure 40).

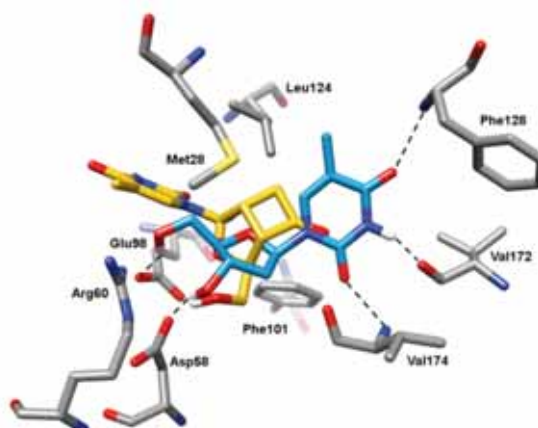


Figure 39. Binding mode of compound **90** (yellow) and dT (blue) in the TK1 binding site. Only the hydrogen bonds for both ligands are shown for clarity. Hydrogen bonds between dT and the residues are depicted as dotted lines.

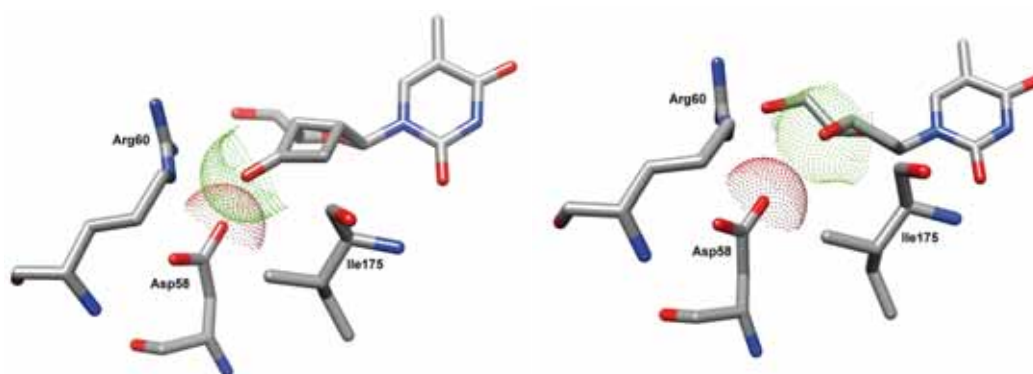


Figure 40. Steric clashes are observed between (a) compound **90** and Asp58 but not between (b) thymidine and Asp58 in the TK1 binding site.

For TMK (PDB IDs: 1E2F,¹¹⁶ 1E9A¹¹⁷), docking calculations on all compounds revealed that the only difference between these compounds and d4TMP and d4TDP were slight displacements of the sugar moiety and the thymine unit (Figure 41). Furthermore, the monophosphorilated derivatives showed close or even better binding energies than those obtained for d4TMP. Therefore, these nucleosides fit adequately on the TMK binding site and should be able to get through the second phosphorylation step successfully.

¹¹⁶ Ostermann, N.; Schlichting, I.; Brundiers, R.; Konrad, M.; Reinstein, J.; Veit, T.; Goody, R. S.; Lavie, A. *Structure* **2000**, *8*, 629-642.

¹¹⁷ Ostermann, N.; Lavie, A.; Padiyar, S.; Brundiers, R.; Veit, T.; Reinstein, J.; Goody, R. S.; Konrad, M.; Schlichting, I. *J. Mol. Biol.* **2000**, *304*, 43-53.

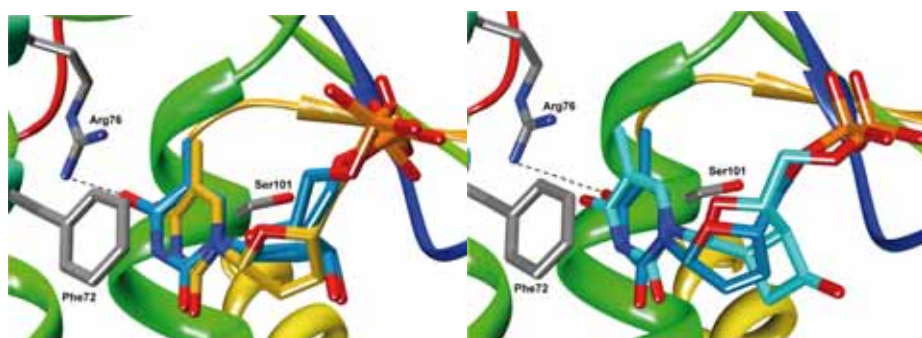


Figure 41. Overlap between (a) the best binding mode of d4TMP (yellow) and dTMP (blue) from the X-ray structure in TMK binding site (b) the best binding mode of monophosphorylated compound **90** (cyan) and d4TMP (blue) in TMK binding site. Hydrogen bonds between dTMP or d4TMP and the residues are depicted in dotted lines. Hydrogen atoms are omitted for clarity.

Evaluation of the third phosphorylation step carried out by NDPK (PDB ID: 1LWX¹¹⁸) showed distinctive behaviours between the synthesized analogues. Compounds **90** and **91** displayed binding orientations similar to those of dTDP and dTTP in terms of energy. Contrarily, for compounds **10**, **12**, **14**, **17** and **92**, none of the lowest-energy binding modes were consistent with the activation process, thus preventing the third activation step. Table 11 summarizes the information obtained from these simulations.

Enzyme-Ligand ^a		dT	d4T	10	12	14	17	90	91	92
TK1	dT	✓	✓	✓	✓	✓	✓	✗	✗	✗
	dTMP	✓	✓	✓	✓	✓	✓	✗	✗	✗
TMK	dTMP	^b	✓	✓	✓	✓	✓	✓	✓	✓
	dTDP	✓	✓	✓	✓	✓	✓	✓	✓	✓
NDPK	dTDP	✓	✓	✗	✗	✗	✗	✓	✓	✗
	dTTP	✓	✗	✗	✓	✗	✗	✓	✓	✗
Activation process		✓	✓	✗	✗	✗	✗	✗	✗	✗

^a TK1: thymidine kinase 1; TMK: thymidylate kinase; NDPK: nucleoside diphosphate kinase. ^b None of the docking solutions is in agreement with the crystal structure.

Table 11. Predicted catalytic pass-through of dT, d4T and compounds **10**, **12**, **14**, **17** and **90-92** for the three enzymes of the activation step.

These docking studies demonstrate that the lack of antiviral activity of our compounds is due to their inefficient interaction with at least one of the three kinases that carry out the activation process. However, to complete the scope of the study, the interaction of these nucleosides with

¹¹⁸ Xu, Y.; Sellam, O.; Morera, S.; Sarfati, S.; Biondi, R.; Veron, M.; Janin, J. *Proc. Natl. Acad. Sci. USA* **1997**, *94*, 7162-7165.

their main target (i.e. HIV-RT) should be analyzed. Thus, docking studies with two different HIV-RT structures were carried out. The first structure corresponds to the binding of the triphosphorylated nucleoside prior to DNA insertion (PDB ID: 1RTD¹¹⁹), while the second corresponds to the monophosphorylated nucleoside bound to the DNA strand (PDB ID: 1N5Y¹²⁰). These calculations disclosed that the presence of the cyclobutane moiety required energetically higher binding modes at the active site of either one (compounds **10**, **12**, **14** and **17**) or both HIV-RT structures (compounds **90-92**).

In summary, the docking study has revealed that the weak antiviral activity of these compounds can be explained in terms of their unfavourable binding interactions at the different stages of phosphorylation as well as with HIV-RT. Specifically, docking of our nucleosides with TK1 has revealed inadequate binding when additional substitution was found on the cyclobutane. TMK has shown little ligand specificity, whereas the binding modes of all nucleosides except **91** and **92** are unable to undertake phosphorylation from NDPK. Finally, the presence of the cyclobutane moiety seems to prevent adequate interaction with HIV-RT.

5.2 Conformational study

To provide further insight into the structure-activity relationships of these nucleosides, their conformational parameters have been calculated (Table 12) and their results are positioned in the pseudorotational cycle (*vide infra*).¹²¹ For compounds **10**, **12**, **14** and **17**, the structures that have been used for these calculations have been obtained in the first phosphorylation step at the TK1 active site, which correspond to energy minima. For compounds **90-92**, the less energetic conformation at the active site is not suitable to undergo phosphorylation. Hence, the first conformation that could go through the activation process has been chosen, even though they were not energy minima. Moreover, for compounds **90-92** and **237** a geometry optimization has been carried out and the conformational parameters of these minimized structures have been calculated and compared with those found from the TK1 active site (Table 13).

¹¹⁹ Huang, H.; Chopra, R.; Verdine, G. L.; Harrison, S. C. *Science* **1998**, *282*, 1669-1675.

¹²⁰ Sarafianos, S. G.; Clark, Jr., A. D.; Das, K.; Tuske, S.; Birktoft, J. J.; Ilankumaran, P.; Ramesha, A. R.; Sayer, J. M.; Jerina, D. M.; Boyer, P. L.; Hughes, S. H.; Arnold, E. *EMBO J.* **2002**, *21*, 6614-6624.

¹²¹ The Altona pseudorotational parameters were calculated by the Pseudo-Rotational Online Service and Interactive Tool (PROSIT) available at <http://cactus.nci.nih.gov/prosit>. Accessed 14/08/2012. See: Sun, G. S.; Voight, J. H.; Filipov, I. V.; Marquez, V. E.; Nicklaus, M. C. *J. Chem. Inf. Comput. Sci.* **2004**, *44*, 1752-1762.

Compound	Pucker	P^a (°)	v_{\max}^b (°)	χ^c (°)	γ^d (°)
d4T^e	O4'-endo	72.1	0.6	-100.8	52.8
d4T-TK1	O4'-endo	91.1	9.3	-158.2	-134.3
10-TK1	C1'-exo	119.3	33.7	-130.6	-53.98
12-TK1	O4'-endo	89.1	19.6	-135.0	-60.1
14-TK1	C1'-exo	114.3	31.8	-172.4	-73.9
17-TK1	C1'-exo	121.8	32.8	-169.0	-53.4
90-TK1	O4'-endo	90.7	30.8	-130.8	-56.8
91-TK1	C4'-exo	63.3	34.12	-171.8	-60.1
92-TK1	O4'-endo	86.8	32.1	-177.3	-63.4

^a P : pseudorotation angle. ^b v_{\max} : maximum puckering amplitude. ^c χ : torsion angle O4'-C1'-N9-C4 or O4'-C1'-N1-C2. ^d γ : torsion angle O5'-C5'-C4'-C3'. ^e Data from the crystal structure.

Table 12. Calculated conformational parameters at the TK1 active site.

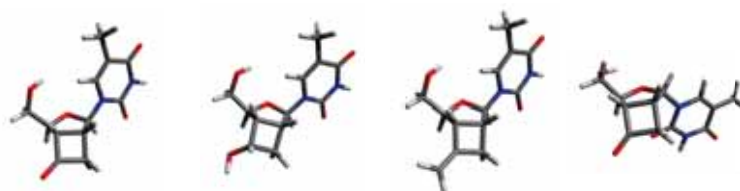
Data from Table 12 shows that all nucleosides display similar conformational parameters with pseudorotation angles comprised between ~ 60 - 120° and the thymine located in an *anti* arrangement (χ). Remarkably, the cyclobutene derivative **12** exhibits the flattest furanose ring, with $v_{\max}=19.6^\circ$. The *-gauche* (γ) disposition around the C4'-C5' bond is adopted in all structures, indicating that this geometry is the appropriate to undergo phosphorylation.

Regarding the energy minimization, nucleosides **90-92** and **237** were built using the molecule editor Avogadro¹²² and their geometry was firstly optimized using the built-in force field MMFF94s.¹²³ Then, using the GAMESS package,¹²⁴ the geometry was further optimized at the RHF/6-31G(d) level. Frequency analyses were performed to ensure that these minimized structures were true minima on the potential energy surface. With the obtained final geometry, the conformational parameters were calculated as summarized in Table 13.

¹²² Avogadro: an open-source molecular builder and visualisation tool. Version 1.0.3. <http://avogadro.openmolecules.net/>. Accessed 14/08/2012.

¹²³ Halgren, T. A. *J. Comput. Chem.* **1999**, *20*, 720-729.

¹²⁴ Schmidt, M. W.; Baldridge, K. K.; Boatz, J. A.; Elbert, S. T.; Gordon, M. S.; Jensen, J. H.; Koseki, S.; Matsunaga, N.; Nguyen, K. A.; Su, S.; Windus, T. L.; Dupuis, M.; Montgomery Jr, J. A. *J. Comput. Chem.* **1993**, *14*, 1347-1363. <http://www.msg.ameslab.gov/gamess/>. Accessed 14/08/2012.



Compound	90	91	92	237
Pucker	C4'-exo	C4'-exo	C4'-exo	O4'-endo
P^a ($^\circ$)	67.1	55.2	66.7	96.2
v_{\max}^b ($^\circ$)	28.8	31.9	29.6	14.3
χ^c ($^\circ$)	-121.3	-122.9	-121.3	-52.5
γ^d ($^\circ$)	60.3	60.3	60.4	175.1

^a P : pseudorotation angle. ^b v_{\max} : maximum puckering amplitude. ^c χ : torsion angle O4'-C1'-N9-C4 or O4'-C1'-N1-C2. ^d γ : torsion angle O5'-C5'-C4'-C3'.

Table 13. Calculated conformational parameters for nucleosides **90-92** and **237**.

The three beta nucleosides show C4'-exo puckers with similar conformational parameters. The +gauche (γ^+) disposition around the C4'-C5' bond has been found to be the most stable in all three cases, with values of γ around 60° .

The alpha nucleoside **237** shows an O4'-endo pucker ($P=96.2^\circ$) with a practically planar sugar ring ($v_{\max}=14.3^\circ$). The torsion angle γ has a value of 175.1° , indicating preference for antiperiplanar disposition (γ^\dagger) around the C4'-C5' bond.

When these structures are compared to the ones obtained from the docking study, the only significant difference is the disposition around the C4'-C5' bond. Thus, although the γ^+ geometry around this bond seems energetically favorable, a 120° twist to the γ^- conformation appears necessary to be activated by cellular kinases.

Representation of these nucleosides in the pseudorotational cycle shows that all of them are found relatively close to each other (Figure 42). However, the derivatives that feature substitution at the cyclobutane (**90-92**) display lower pseudorotational angles (C4'-exo, O4'-endo puckers, $60^\circ \leq P \leq 90^\circ$) than their cyclobutane and cyclobutene counterparts **10**, **12**, **14** and **17** (O4'-endo, C1'-exo puckers, $90^\circ \leq P \leq 120^\circ$).

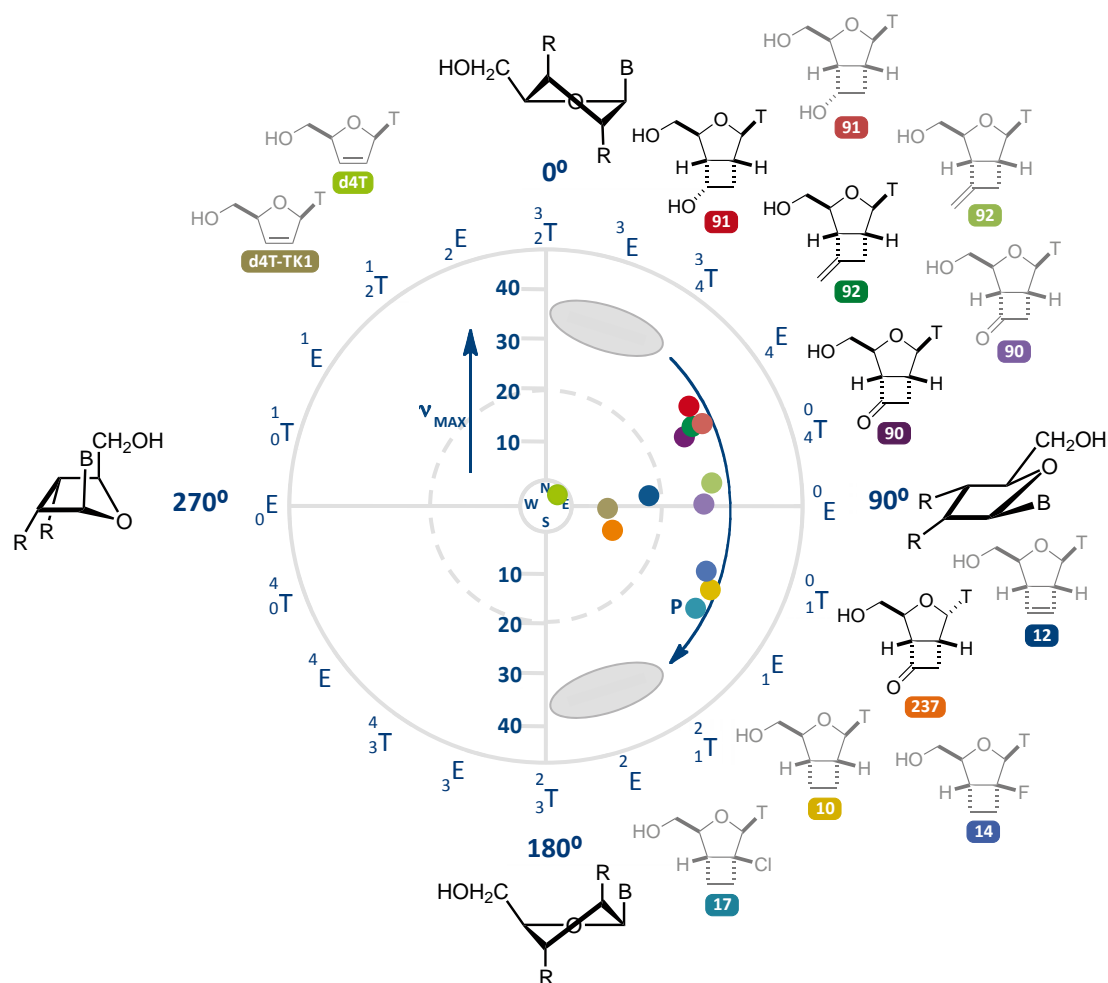
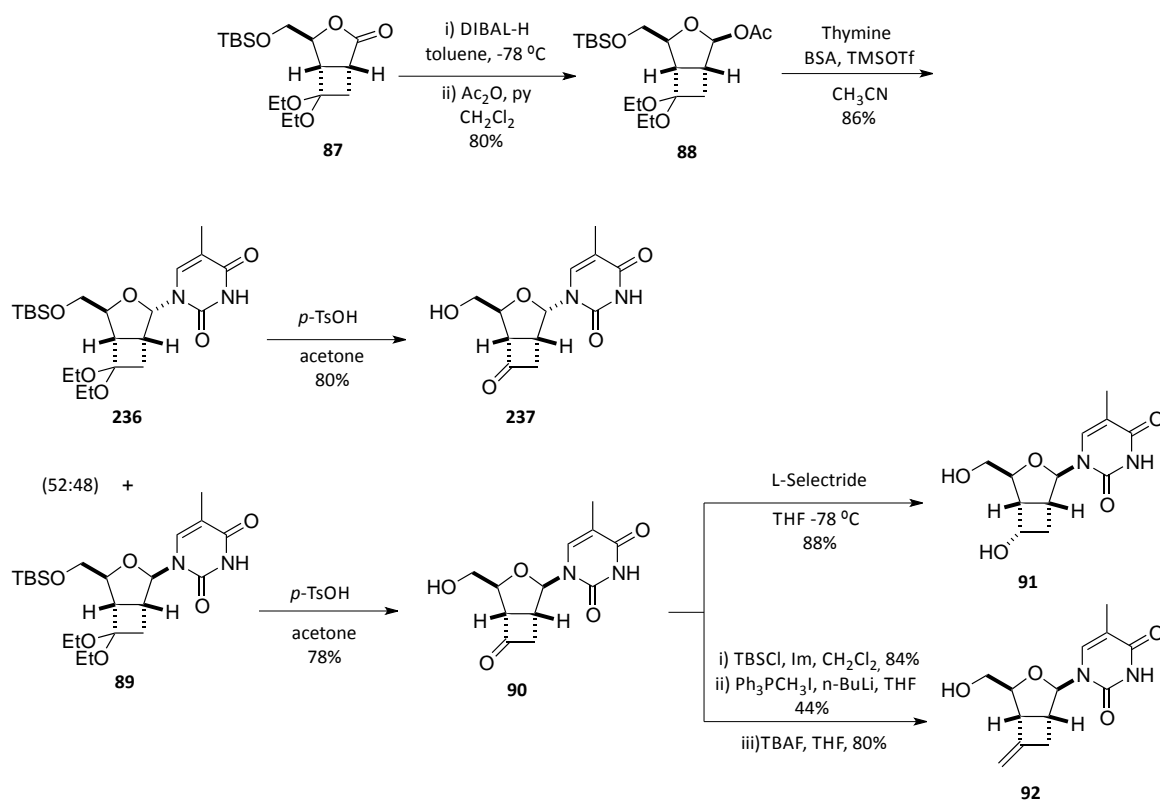


Figure 42. Location of 3-oxabicyclo[3.2.0]heptane-type nucleosides in the pseudorotational cycle. Grey structures indicate that conformational data has been calculated from the structure at the TK1 active site. Black structures indicate that the conformational data has been obtained by energy minimization.

6. CHAPTER III OUTLINE

In this chapter the synthesis of four novel conformationally restricted nucleosides from cycloadduct **87** is described. The cyclobutanone nucleosides **237** and **90** have been obtained in 5 steps and 13% and 12% yield respectively. Nucleoside **91** has been achieved in 6 steps and 10% yield. Finally, nucleoside **92** has been obtained in 8 steps and 4% global yield. The results of their activity evaluation against several viruses have been presented.

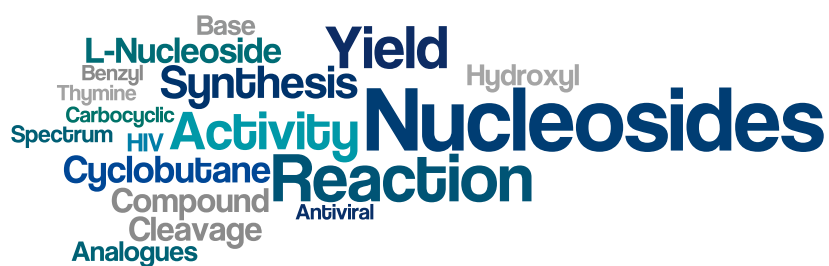
Finally, computational studies have given insight into the interaction of these nucleosides with cellular kinases and HIV-RT as well as their conformational behaviour.



Scheme 53. Chapter III summary.

IV. Cyclobutane L-Nucleosides

Enantiopure Synthesis of Novel
Cyclobutane L-Nucleosides





1. INTRODUCTION

1.1 L-Nucleosides as antiviral agents

L-nucleosides are enantiomers of the naturally occurring D-nucleosides (Figure 43).^{8, 125} Although the preparation of L-thymidine (the first L-nucleoside synthesized) dates from 1964,¹²⁶ this family of compounds was practically ignored for nearly 30 years. However, the impressive anti-HIV activity displayed by Lamivudine (3TC),¹²⁷ triggered the exploration of this type of nucleosides.

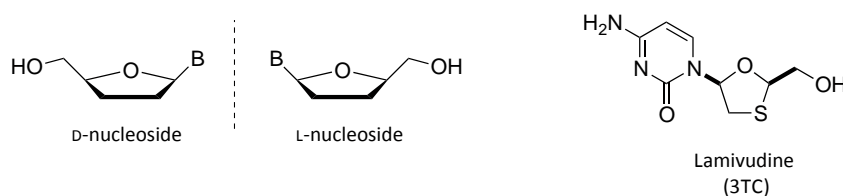


Figure 43. D- and L-nucleosides and the structure of Lamivudine.

Since then, a plethora of L-nucleosides have been synthesized and screened for antiviral activity.⁸ The most successful examples are shown in Figure 44. Apart from the anti-HIV activity of some of these nucleosides, other compounds such as Telbivudine (LdT) and Clevudine (L-FMAU) have been found to be highly active and specific to treat HBV infections. Lamivudine itself is currently used to treat both diseases.

¹²⁵ For additional reviews on this topic see: (a) Nair, V.; Jahnke, T. S. *Antimicrob. Agents Chemother.* **1995**, *39*, 1017-1029. (b) Wang, P.; Hong, J. H.; Cooperwood, J. S.; Chu, C. K. *Antiviral Res.* **1998**, *40*, 19-44. (c) Zemlicka, J. *Pharmacol. Therapeut.* **2000**, *85*, 251-266. (d) Gumina, G.; Song, G.-Y.; Chu, C. K. *FEMS Microbiol. Lett.* **2001**, *202*, 9-15.

¹²⁶ Smejkal, J.; Sorm, F. *Collect. Czech. Chem. Commun.* **1964**, *29*, 2809-2813.

¹²⁷ Schinazi, R. F.; Chu, C. K.; Peck, A.; McMillan, A.; Mathis, R.; Cannon, D.; Jeong, L.-S.; Beach, J. W.; Choi, W.-B.; Yeola, S.; Liotta, D. C. *Antimicrob. Agents Chemother.* **1992**, *36*, 672-676.

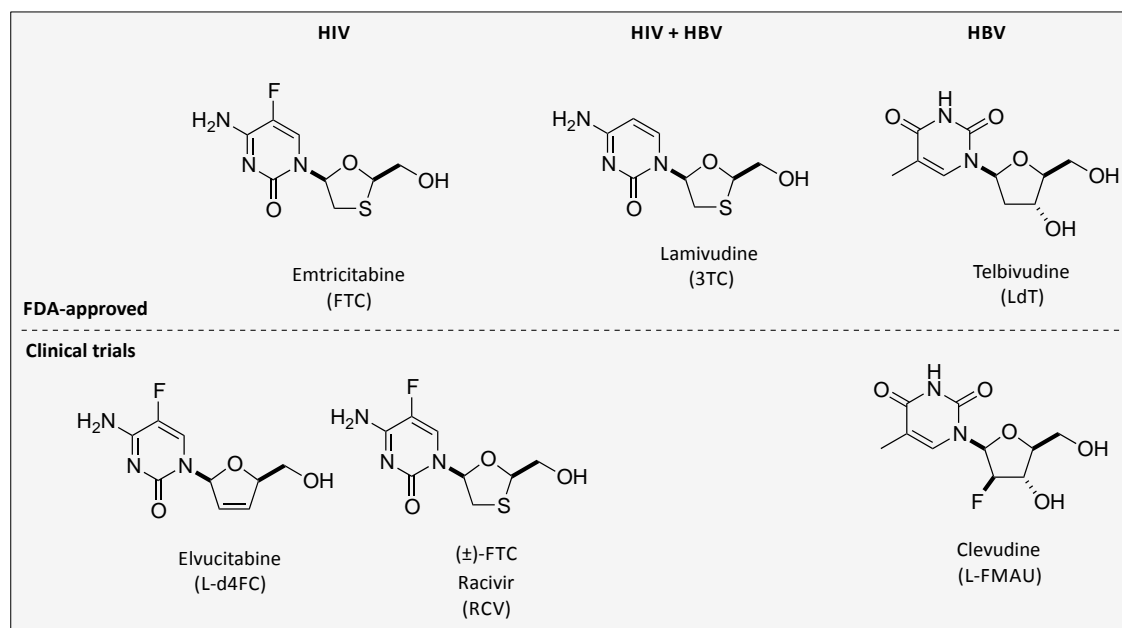


Figure 44. Structure of L-nucleoside analogues approved or in the course of being approved for the treatment of HIV and HBV.

The biological activity of unnatural L-nucleosides has demonstrated that not all enzymes implied in phosphorylation processes are completely enantioselective. Actually, this relaxed enantioselectivity has been perceived as a potential antiviral strategy, favouring the use of L-nucleosides due to their lower cytotoxicity and greater resistance to degradation processes.¹²⁸

1.2 Carbocyclic nucleosides as antiviral agents

Carbocyclic nucleosides are another interesting family of nucleoside analogues that have been mentioned earlier. The main structural feature of these compounds is the substitution of the furanose ring by a carbocycle. As it has been pointed out, this replacement results in higher resistance to hydrolytic processes and enhanced lipophilicity, favouring absorption and penetration through cell membrane.

These nucleosides started being investigated after the discovery of the high bioactivity of the naturally occurring Aristeromycin¹²⁹ and Neplanocin A¹³⁰ (Figure 45). Since then, research on this field has culminated in the synthesis of an assorted array of mainly five-membered ring systems, although three-, four-, and six-membered carbocyclic analogues have also been described.²⁷ Biological evaluation of these compounds has often shown powerful antiviral activity against a

¹²⁸ Maury, G. *Antivir. Chem. Chemother.* **2000**, *11*, 165-190.

¹²⁹ Shealy, Y. F.; Clayton, J. D. *J. Pharm. Sci.* **1973**, *62*, 858-859.

¹³⁰ Yaginuma, S.; Muto, N.; Tsujino, M.; Sudate, Y.; Hayashi, M.; Otani, M. *J. Antibiot.* **1981**, *34*, 359-366.

wide range of viruses such as HIV, HBV, HSV or VZV. Thus, the synthesis of carbocyclic nucleoside analogues with enhanced selectivity and improved activity is still an active research topic.

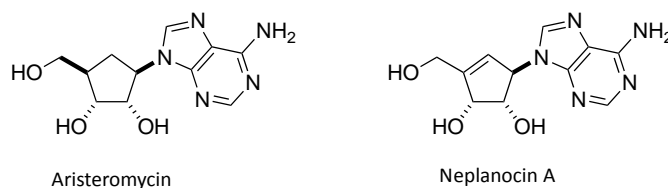


Figure 45. Structure of the carbocyclic nucleosides Aristeromycin and Neplanocin A.

The cyclopentane structural motif is by far the most extensively studied. Despite the high antiviral activity of the natural nucleosides Aristeromycin and Neplanocin A, their therapeutic utility has been limited due to their significant toxicity.¹³¹ Therefore, in an attempt to reduce the toxicity of this class of compounds, synthetic mimics were developed. This search ended up in the synthesis of an overwhelming number of five-membered carbocyclic nucleosides, some displaying interesting biological properties. Among them, Carbovir (CBV), Abacavir and Entecavir (Figure 46) are the most successful examples, showing high activity and low toxicity.

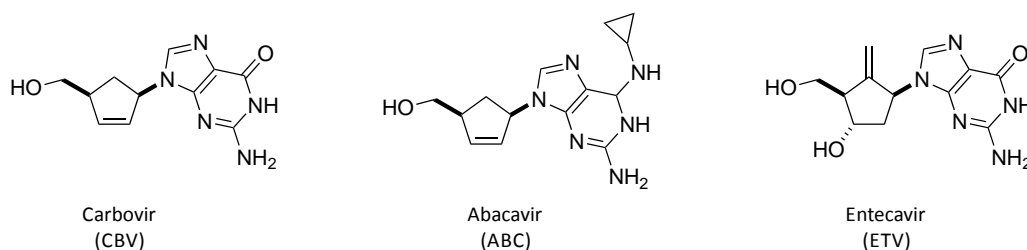


Figure 46. Structure of the five-membered carbocyclic nucleosides Carbovir, Abacavir and Entecavir.

Carbovir was synthesized in 1988 and it was found to exhibit potent anti-HIV activity with low toxicity.¹³² It is noteworthy that although the D-enantiomer was found more active than its L-counterpart, the corresponding triphosphates exhibited equal activity.¹³³ However, its development as a suitable anti-HIV agent was thwarted by a low aqueous solubility, limited oral

¹³¹ Wolfe, M. S.; Lee, Y.; Bartlett, W. J.; Borcharding, D. R.; Borchardt, R. T. *J. Med. Chem.* **1992**, *35*, 1782-1791.

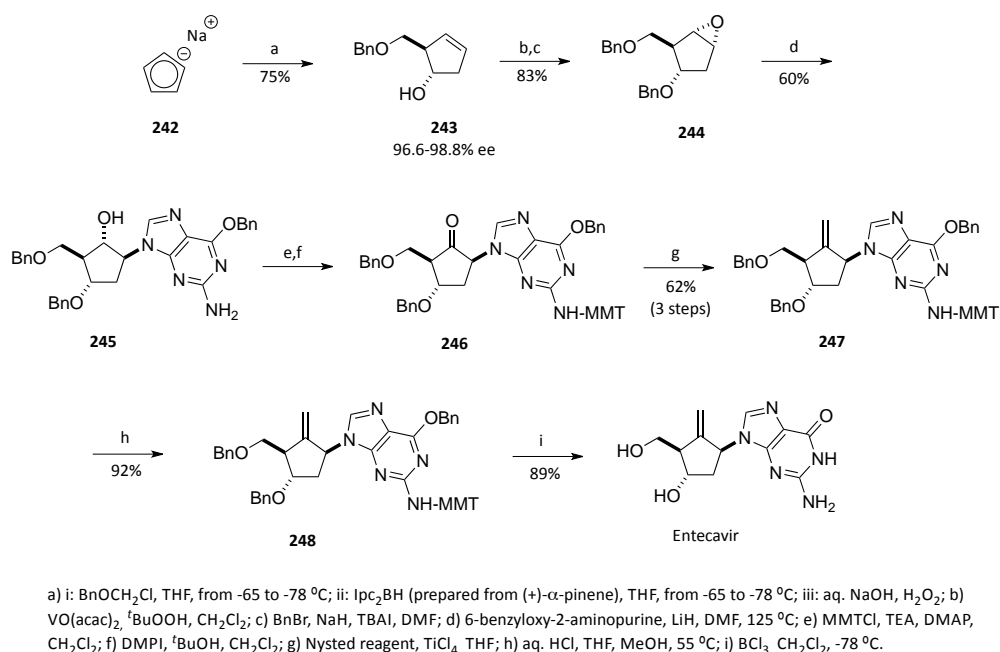
¹³² Vince, R.; Hua, M.; Brownell, J.; Daluge, S.; Lee, F.; Shannon, W. M.; Lavelle, G. C.; Qualls, J.; Weislow, O. S.; Kiser, R.; Canonico, P. G.; Schultz, R. H.; Narayanan, V. L.; Mayo, J. G.; Shoemaker, R. H.; Boyd, M. R. *Biochem. Biophys. Res. Co.* **1988**, *156*, 1046-1053.

¹³³ Miller, W.; Daluge, S.; Garvey, E.; Hopkins, S.; Reardon, J.; Boyd, F.; Miller, R. *J. Biol. Chem.* **1992**, *267*, 21220-21224.

absorption and inefficient central nervous system penetration.¹³⁴ These issues could be solved with the synthesis of the 6-cyclopropylamino derivative, Abacavir.²⁸ Apart from potent anti-HIV activity and low toxicity, this nucleoside displayed excellent pharmacokinetic as well as toxicological profiles, which led the FDA to its approval as an anti-HIV drug in 1998.

Entecavir is another fruitful nucleoside belonging to the five-membered carbocyclic nucleosides. This nucleoside was found to be a potent and selective agent against the hepatitis B virus and in 2005 was approved by the FDA for the treatment of chronic HBV.¹³⁵

As an example, the synthesis of ETV is shown in Scheme 54.²⁹ The synthetic design featured a large-scale preparation of the enantiopure epoxide **244** to introduce different nucleobases. Preparation of this intermediate was accomplished by reaction of commercial sodium cyclopentadienide with benzyl chloromethyl ether followed by a hydroboration-oxidation reaction of the resulting diene using Ipc_2BH as a chiral auxiliary. Then, epoxidation of cyclopentene **243** and protection of the secondary hydroxyl group as a benzyl ether afforded **244**. Reaction of this epoxide with the 6-benzyl derivative of guanine rendered the *N*9 adduct **245** as the major isomer. In order to oxidize the free hydroxyl group, the amino moiety was protected as the monomethoxytrityl derivative. Finally, methylenation using the Nysted reagent and cleavage of all protecting groups delivered ETV.



Scheme 54. Synthesis of Entecavir.

¹³⁴ Daluge, S. M.; Good, S. S.; Faletto, M. B.; Miller, W. H.; St. Clair, M. H.; Boone, L. R.; Tisdale, M.; Parry, N. R.; Reardon, J. E.; Dornsife, R. E.; Averett, D. R.; Krenitsky, T. A. *Antimicrob. Agents Chemother.* **1997**, *41*, 1082-1093.

¹³⁵ Zoulim, F. J. *Clin. Virol.* **2006**, *36*, 8-12.

Carbocyclic nucleosides bearing a cyclopropane unit have also been explored. The synthesis of the series of analogues **249** by Chu and co-workers is among the earliest works that describe the preparation of optically active cyclopropane nucleosides (Figure 47).¹³⁶ However, none of these compounds displayed antiviral activity, suggesting that this lack of activity could be attributed to the short distance between the 5'-OH group and the nucleobase.¹³⁷ For this reason, the synthesis of cyclopropane analogues has been recently directed to the preparation of derivatives featuring a carbon atom between the cyclopropane ring and the nucleobase. These analogues can be considered mimics of the antiviral agents Acyclovir (ACV),¹³⁸ Ganciclovir (GCV)¹³⁹ and Penciclovir (PCV),¹⁴⁰ acyclic nucleosides that show potent activity against HSV, HCMV and VZV.

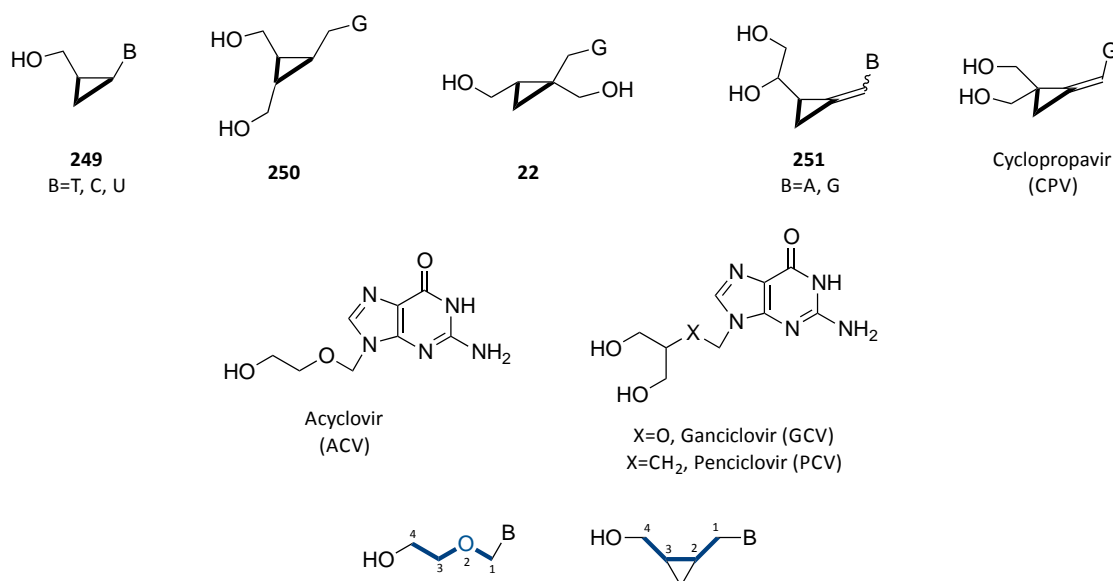


Figure 47. Examples of three-membered carbocyclic nucleosides.

Examples of this class of nucleosides include several analogues bearing two hydroxymethyl groups such as **250** and **22** synthesized by Tsuji and co-workers.¹⁴¹ Biological evaluation of these compounds, which were prepared as racemates, showed potent antiviral activity for compound **22**. Thus, its two enantiomers were synthesized starting from chiral epichlorohydrins. The

¹³⁶ Zhao, Y.; Yang, T.; Lee, M.; Lee, D.; Newton, M. G.; Chu, C. K. *J. Org. Chem.* **1995**, *60*, 5236-5242.

¹³⁷ Pierra, C.; Olgen, S.; Cavalcanti, S. C. H.; Cheng, Y.-C.; Schinazi, R. F.; Chu, C. K. *Nucleosides, Nucleotides & Nucleic Acids* **2000**, *19*, 253-268.

¹³⁸ Elion, G. B.; Furman, P. A.; Fyfe, J. A.; De Miranda, P.; Beauchamp, L.; Schaeffer, H. J. *Proc. Natl. Acad. Sci. USA* **1977**, *74*, 5716-5720.

¹³⁹ Field, A. K.; Davies, M. E.; DeWitt, C.; Perry, H. C.; Liou, R.; Germershausen, J.; Karkas, J. D.; Ashton, W. T.; Johnston, D. B. R.; Tolman, R. L. *Proc. Natl. Acad. Sci. USA* **1983**, *80*, 4139-4143.

¹⁴⁰ Harnden, M. R.; Jarvest, R. L.; Bacon, T. H.; Boyd, M. R. *J. Med. Chem.* **1987**, *30*, 1636-1642.

¹⁴¹ Sekiyama, T.; Hatsuya, S.; Tanaka, Y.; Uchiyama, M.; Ono, M.; Iwayama, S.; Oikawa, M.; Suzuki, K.; Okunishi, M.; Tsuji, T. *J. Med. Chem.* **1998**, *41*, 1284-1298.

(1'S,2'R)-enantiomer showed potent antiviral activity against HSV-1 and HSV-2 compared to ACV and PCV. Moreover, this compound exhibited good selectivity and better activity against VZV than the cited acyclonucleosides.

More recently, Zemlicka and co-workers have described the synthesis of several methylenecyclopropane nucleosides including the set of compounds **251**¹⁴² and Cyclopropavir (CPV),¹⁴³ which has been found to exhibit potent activity against HCMV.¹⁴⁴

Analogues bearing bigger six-membered rings such as **252-254** and **25** have been prepared by Herdewijn and co-workers (Figure 48).¹⁴⁵ Among them, both enantiomers of Cyclohexenyl-G, **25**, were found to exhibit potent and selective anti-herpesvirus (HSV-1 & 2, VZV, CMV) activity,³² comparable to that of ACV and GCV. The high antiviral activity of this cyclohexene derivative prompted our research group to design an approach towards related targets. Since opposite enantiomers usually exhibit different pharmacological and toxicological profiles, an enantiodivergent strategy to synthesize cyclohexenyl nucleosides **26-27** from 1,4-cyclohexanedione was developed.³³ These nucleosides were tested against a HIV-1 wt NL4-3 strain, and although some of them showed weak activity, it was not separated from cytotoxicity.

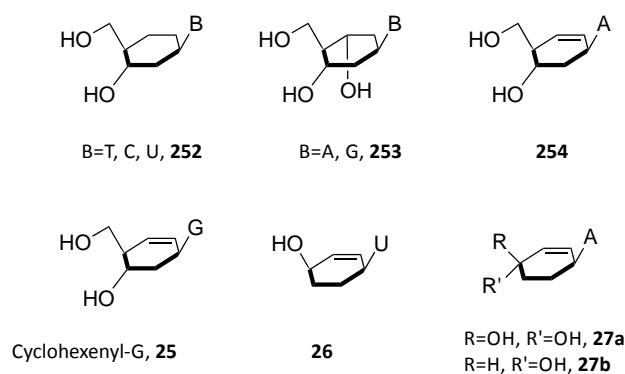


Figure 48. Examples of six-membered carbocyclic nucleosides.

Cyclobutane nucleosides, carbocyclic analogues of oxetanocins and Cyclobut-A have been mainly explored by the group of Huet, which has described the synthesis of the polyhydroxylated

¹⁴² Zhou, S.; Drach, J. C.; Prichard, M. N.; Zemlicka, J. J. *Med. Chem.* **2009**, *52*, 3397-3407.

¹⁴³ Zhou, S.; Breitenbach, J. M.; Borysko, K. Z.; Drach, J. C.; Kern, E. R.; Gullen, E.; Cheng, Y.-C.; Zemlicka, J. J. *Med. Chem.* **2004**, *47*, 566-575.

¹⁴⁴ James, S. H.; Hartline, C. B.; Harden, E. A.; Driebe, E. M.; Schupp, J. M.; Engelthaler, D. M.; Keim, P. S.; Bowlin, T. L.; Kern, E. R.; Prichard, M. N. *Antimicrob. Agents Chemother.* **2011**, *55*, 4682-4691.

¹⁴⁵ (a) Maurinsh, Y.; Schraml, J.; De Winter, H.; Blaton, N.; Peeters, O.; Lescrinier, E.; Rozenski, J.; Van Aerschot, A.; De Clercq, E.; Busson, R.; Herdewijn, P. *J. Org. Chem.* **1997**, *62*, 2861-2871. (b) Wang, J.; Busson, R.; Blaton, N.; Rozenski, J.; Herdewijn, P. *J. Org. Chem.* **1998**, *63*, 3051-3058. (c) Wang, J.; Herdewijn, P. *J. Org. Chem.* **1999**, *64*, 7820-7827.

nucleosides **255-261**¹⁴⁶ and the cyclobutene and methylenecyclobutane analogues **262-267**¹⁴⁷ (Figure 49).

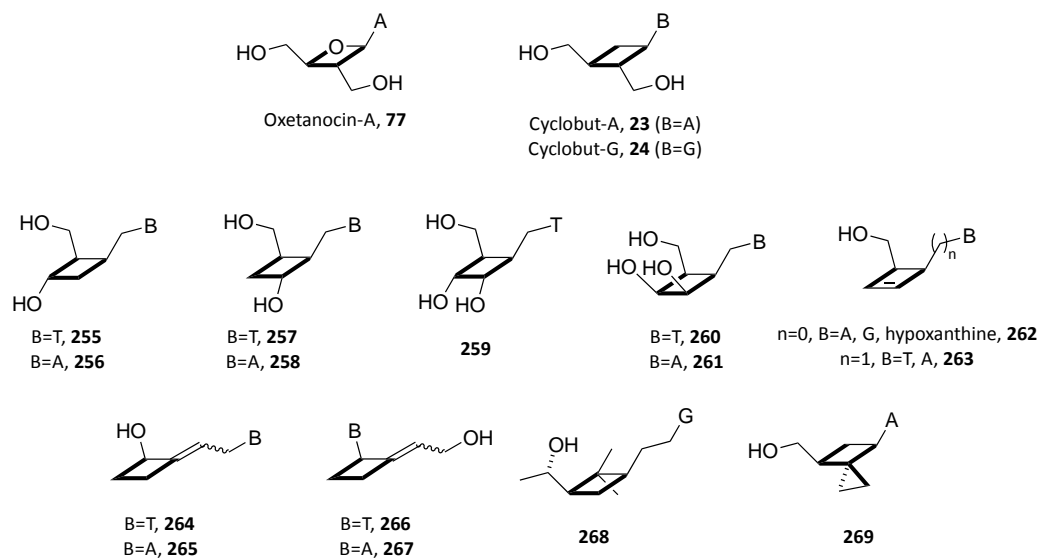


Figure 49. Examples of four-membered carbocyclic nucleosides.

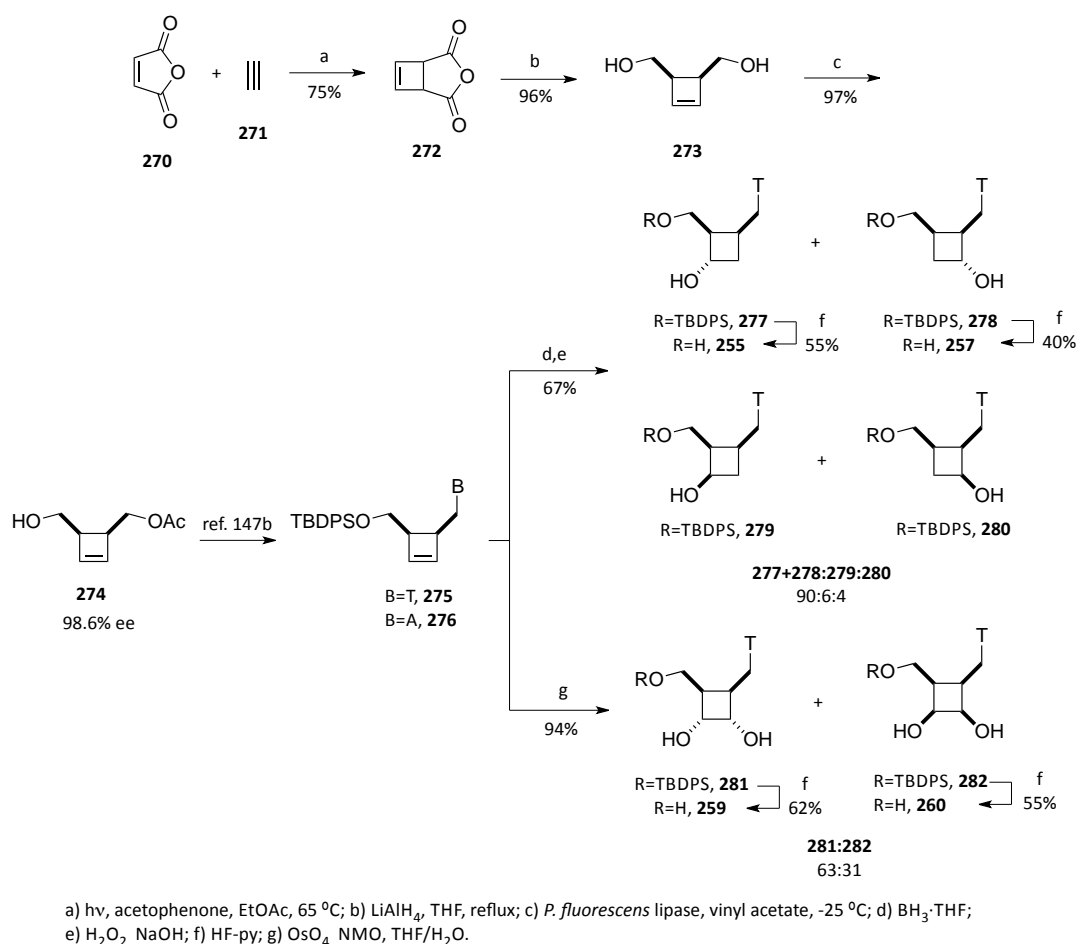
To construct the cyclobutane core of these compounds various methodologies have been developed. For instance, the synthesis of the polyhydroxylated and cyclobutene nucleosides **255-263** employed the [2+2] photocycloaddition of acetylene to maleic anhydride.¹⁴⁶⁻¹⁴⁸ As an example, the preparation of the polyhydroxylated nucleosides **255-261** is shown in Scheme 55. From the photoadduct **272**, reduction with LiAlH₄ afforded diol **273**, which was acetylated by an enzymatic process at low temperature.¹⁴⁹ Then, introduction of the nucleobase using a Mitsunobu reaction afforded intermediates **275-276**.^{147b} From this point, hydroboration of this intermediate provided a mixture of the four products **277-280**. Deprotection of **277** and **278** by treatment with HF-pyridine provided nucleosides **255** and **257**. On the other hand, dihydroxylation of **275** afforded a mixture of products **281** and **282** in excellent yield. Cleavage of the silyl group afforded trihydroxylated nucleosides **259** and **260**. The adenine derivatives **256**, **258** and **261** were synthesized using a parallel approach starting from intermediate **276**. Nucleosides **255-261** were tested against HSV-1 and HIV-1 but they were found inactive.

¹⁴⁶ Marsac, Y.; Nourry, A.; Legoupy, S.; Pipelier, M.; Dubreuil, D.; Aubertin, A.-M.; Bourgognon, N.; Benhida, R.; Huet, F. *Tetrahedron* **2005**, *61*, 7607-7612.

¹⁴⁷ (a) Gurdel-Martin, M.-E.; Huet, F. *Nucleosides Nucleotides* **1999**, *18*, 645-648. (b) Hubert, C.; Alexandre, C.; Aubertin, A.-M.; Huet, F. *Tetrahedron* **2002**, *58*, 3775-3778.

¹⁴⁸ Mévellec, L.; Huet, F. *Tetrahedron* **1994**, *50*, 13145-13154.

¹⁴⁹ Pichon, C.; Hubert, C.; Alexandre, C.; Huet, F. *Tetrahedron: Asymmetry* **2000**, *11*, 2429-2434.

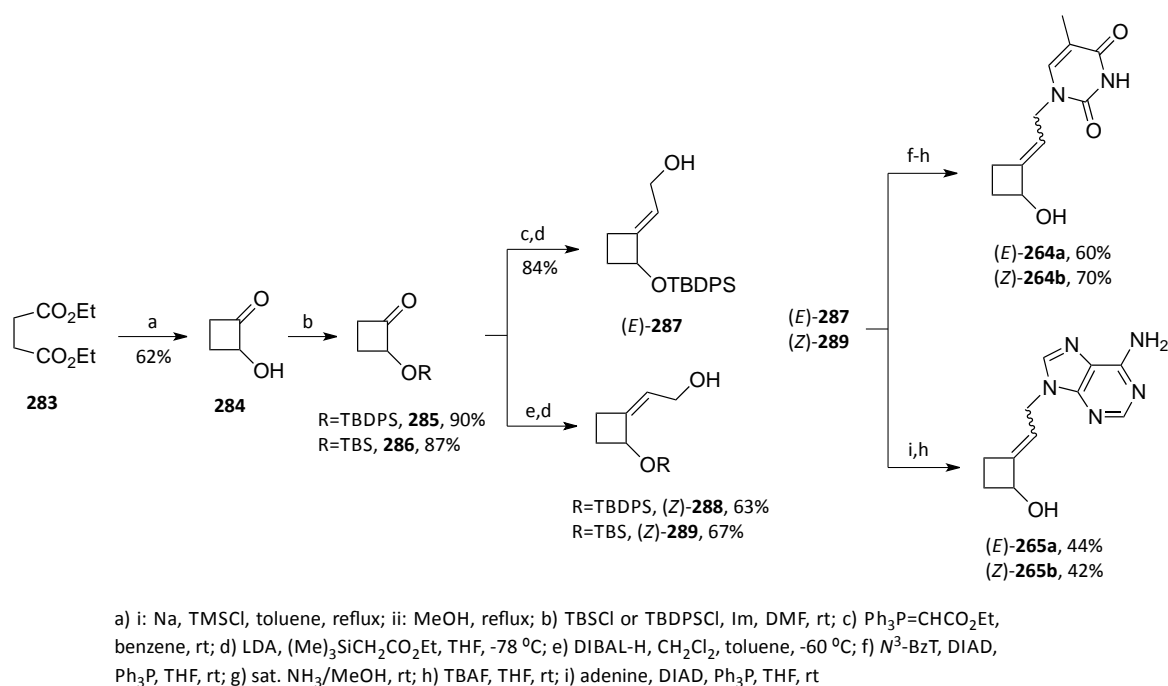


Scheme 55. Synthesis of the polyhydroxylated cyclobutane nucleosides **255**, **257** and **259-260**.

The same research group has also reported the racemic synthesis of the methylenecyclobutane nucleosides **264-267** (Scheme 56).¹⁵⁰ In this case, the cyclobutane core of the α -hydroxyketone **284** was constructed by acyloin condensation of diethyl succinate.¹⁵¹ Protection of the free hydroxyl group as a silyl derivative and Wittig or Peterson olefinations allowed to obtain the *E*- and *Z*-cyclobutenes **287** and **288-289**, respectively. Then, introduction of the base via Mitsunobu reaction and cleavage of the protecting groups delivered nucleosides **264** and **265**. By using an analogous sequence, the authors prepared the methylenecyclobutane nucleosides **266-267**, with the base directly attached to the cyclobutane ring. These methylenecyclobutane nucleosides were tested against HIV-1 and HSV-1, but they did not display significant activity.

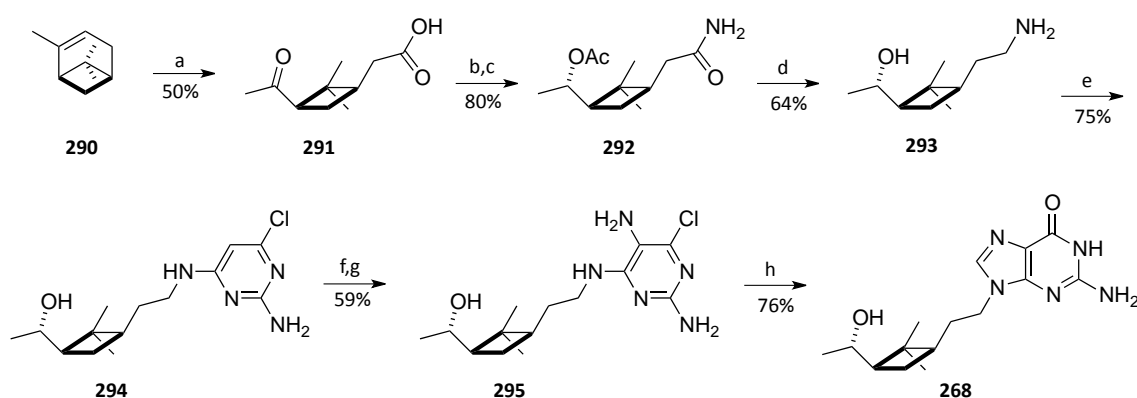
¹⁵⁰ Dannape, S.; Pal, A.; Alexandre, C.; Aubertin, A.-M.; Bourgoignon, N.; Huet, F. *Tetrahedron* **2005**, *61*, 5782-5787.

¹⁵¹ Bloomfield, J. J.; Nelke, J. M. In *Organic syntheses, Collect. Vol. 6*, Wiley: New York, 1988, 167-172.



Scheme 56. Synthesis of the methylenecyclobutane nucleosides **264-265**.

In 2001, Fernández and co-workers described the preparation of the enantiopure cyclobutane nucleoside **268** starting from (1S)- α -pinene, **290** (Scheme 57).¹⁵² Oxidation of this monoterpene with KMnO_4 rendered pinonic acid, **291**. Next, reduction of the ketone, acetylation of the hydroxyl group and conversion of the carboxylic acid into the amide afforded **292**. Then, the amide was reduced to amine **293**, which was used as the substrate to construct the nucleobase present in the nucleoside **268**. This nucleoside was evaluated against several viruses (e.g. HIV-1 & 2, HSV-1 & 2, VZV, CMV) but was found inactive in all the cases.

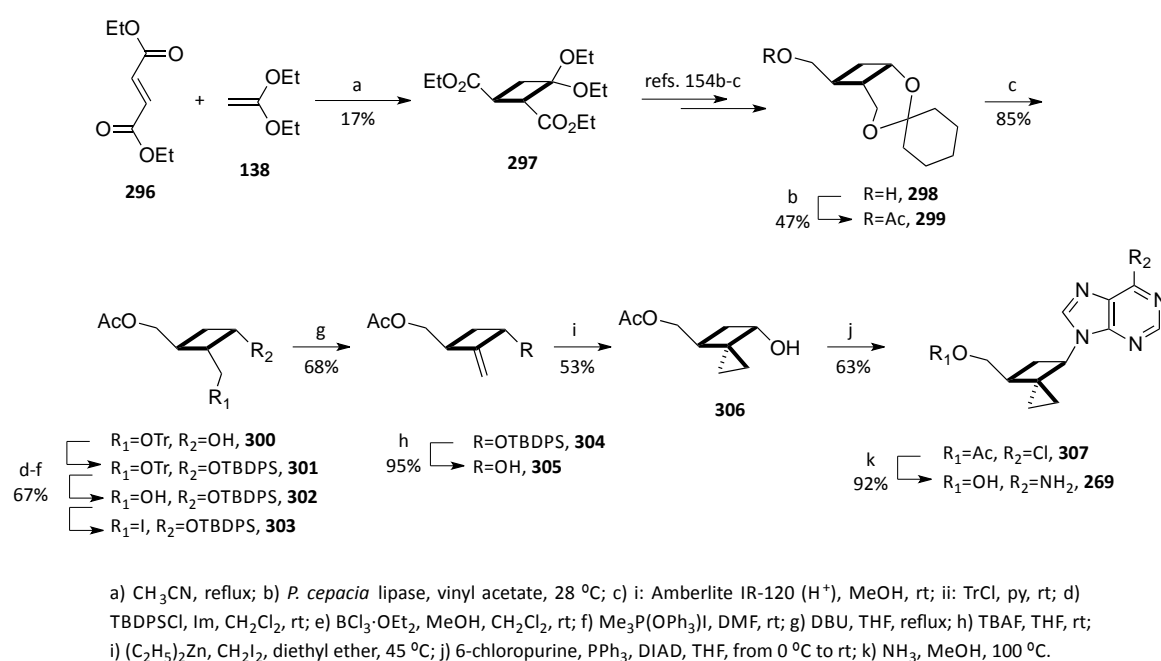


a) KMnO_4 , H_2O ; b) NaBH_4 , EtOH; c) i: Ac_2O , py; ii: ClCO_2Et , Et_3N , NH_3 ; d) LiAlH_4 , THF, e) 4,6-dichloropyrimidin-2-amine, Et_3N , 1-butanol; f) 4- $\text{ClC}_6\text{H}_4\text{N}_2$, H_2O ; g) Zn, AcOH; h) NaNO_2 , 1 M HCl.

Scheme 57. Synthesis of nucleoside **268**.

¹⁵² Fernández, F.; Hergueta, A. R.; López, C.; De Clercq, E.; Balzarini, J. *Nucleosides, Nucleotides & Nucleic Acids* **2001**, *20*, 1129-1131.

Finally, Chu and co-workers reported the synthesis of the spiro[2.3]hexane nucleoside **269** starting from intermediate **298** (Scheme 58).¹⁵³ This intermediate was prepared according to previously described methodologies, using the thermal [2+2] cycloaddition of diethyl fumarate to ketene diethyl acetal to install the cyclobutane core.¹⁵⁴ Next, intermediate **298** was subjected to enzymatic resolution affording acetate **299**. Hydrolysis of the acetal, protecting group exchange and iodination led to compound **303**, which upon DBU-mediated elimination delivered the *exo*-cyclic alkene **304**. Finally, cyclopropanation, base introduction via Mitsunobu reaction and treatment with a saturated solution of ammonia in MeOH afforded nucleoside **269**. This compound was found to exhibit moderate anti-HIV activity ($EC_{50}=22.4 \mu\text{M}$).



Scheme 58. Synthesis of nucleoside **269**.

¹⁵³ Bondada, L.; Gumina, G.; Nair, R.; Ning, X. H.; Schinazi, R. F.; Chu, C. K. *Org. Lett.* **2004**, *6*, 2531-2534.

¹⁵⁴ (a) Brannock, K. C.; Burpitt, R. D.; Thweatt, J. G. *J. Org. Chem.* **1964**, *29*, 940-941. (b) Bisacchi, G. S.; Braitman, A.; Cianci, C. W.; Clark, J. M.; Field, A. K.; Hagen, M. E.; Hockstein, D. R.; Malley, M. F.; Mitt, T.; Slusarchyk, W. A.; Sundeen, J. E.; Terry, B. J.; Tuomari, A. V.; Weaver, E. R.; Young, M. G.; Zahler, R. *J. Med. Chem.* **1991**, *34*, 1415-1421. (c) Maruyama, T.; Hanai, Y.; Sato, Y.; Snoeck, R.; Andrei, G.; Hosoya, M.; Balzarini, J.; De Clercq, E. *Chem. Pharm. Bull.* **1993**, *41*, 516-521.

1.3 Carbocyclic L-nucleosides

The concept of merging the enhanced resistance to degradation from L-nucleosides and the improved lipophilicity of carbocyclic compounds gave rise to the synthesis of several L-nucleoside carbocyclic analogues (Figure 50). Thus, various five-membered cored nucleosides have been prepared.¹⁵⁵ Among them, nucleosides **308** and **309** are the only ones that have been biologically tested, exhibiting significant anti-HIV activity (**308**: EC₅₀=6.76 µg/mL; **309**: B=C, EC₅₀=7.1 µM; B=T, EC₅₀=6.4 µM; B=A, EC₅₀=10.3 µM; B=G, EC₅₀=20.7 µM).

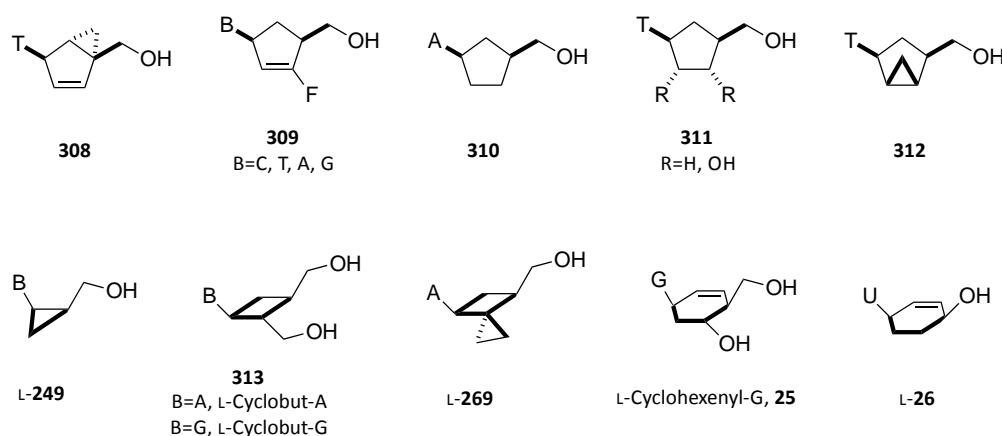


Figure 50. Examples of carbocyclic L-nucleosides.

On the other hand, the three-, four- and six-membered L-carbocyclic nucleosides have remained practically unexplored. In fact, the compounds shown on Figure 50 are among the few examples of this class of compounds. Of all these examples, only the L-enantiomer of Cyclohexenyl G is biologically active, exhibiting significant activity against herpes-viruses.

As illustrated by the scarce number of examples, stereoselective syntheses of unnatural L-nucleoside analogues are very limited. The lack of development of enantiomerically pure routes towards these targets together with their potential biological activities, prompted us to design an enantioselective pathway towards nucleosides **95-100**, analogues that feature an additional carbon atom between the nucleobase and the cyclobutane ring (Figure 51). As it has been mentioned before, this additional atom helps to keep the 1,4-disposition between the base and the hydroxymethyl unit present in natural ribose-based nucleosides.

¹⁵⁵ (a) Park, A.-Y.; Moon, H. R.; Kim, K. R.; Chun, M. W.; Jeong, L. S. *Org. Biomol. Chem.* **2006**, *4*, 4065-4067. (b) Wang, J.; Jin, Y.; Rapp, K. L.; Schinazi, R. F.; Chu, C. K. *J. Med. Chem.* **2007**, *50*, 1828-1839. (c) Marcé, P.; Díaz, Y.; Matheu, M. I.; Castellón, S. *Org. Lett.* **2008**, *10*, 4735-4738. (d) Jessel, S.; Meier, C. *Eur. J. Org. Chem.* **2011**, 1702-1713.

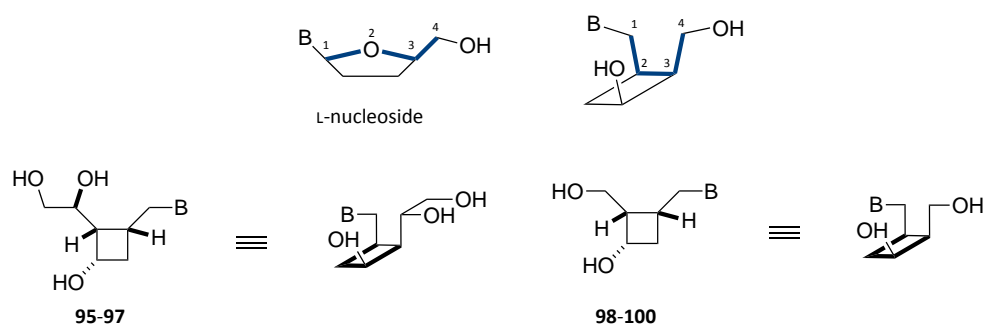
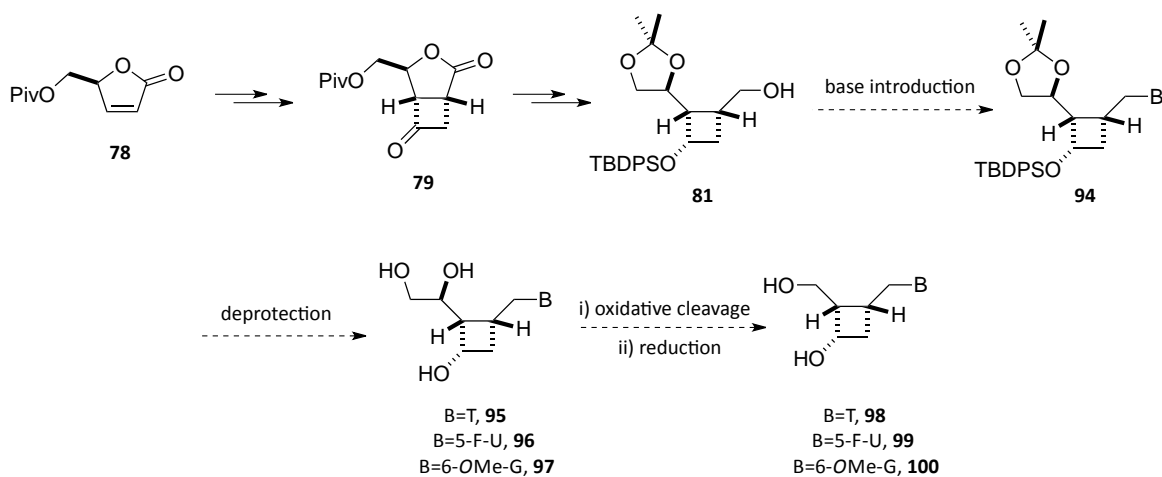


Figure 51. Proposed targets of this work.

2. SYNTHESIS OF CYCLOBUTANE L-NUCLEOSIDE ANALOGUES

2.1 Synthetic strategy overview

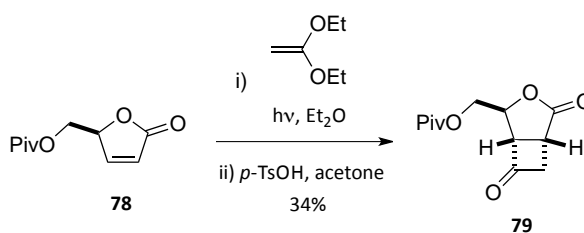
The synthetic pathway to reach the targeted enantiopure L-nucleosides would start from the 5' pivaloyl protected 2(5*H*)-furanone **78**, which would be transformed into the key intermediate **81** following the sequence already used by our research group in the synthesis of Cyclobut-A (Scheme 59).⁴⁷ At this point, coupling of different nucleobases onto **81** would lead to intermediates **94**. Deprotection of the base and the three hydroxyl groups should afford the first family of cyclobutane L-nucleosides **95-97**. Finally, oxidative cleavage and subsequent reduction would afford a second family of nucleosides featuring only two hydroxyl groups, **98-100**.

Scheme 59. Planned strategy for the synthesis of nucleosides **95-100**.

2.2 Synthesis of the cyclobutane L-nucleosides 95-97

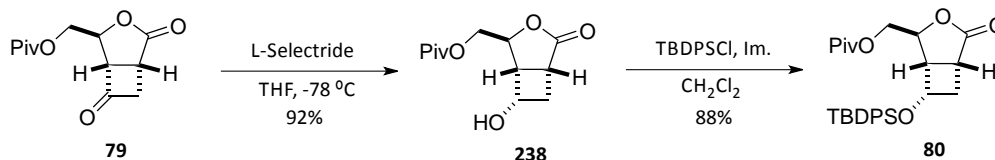
2.2.1 Synthesis of the common intermediate **81**

The synthesis of **81** started with the [2+2] photocycloaddition of ketene diethyl ketal to the pivaloyl-protected 2(5*H*)-furanone **78** as described in Chapter 2 (Scheme 60). This reaction yielded a crude containing a mixture of the four possible cycloadducts, which were treated without further purification with a catalytic amount of *p*-TsOH in acetone. These conditions allowed the isolation of the major HT cycloadduct **79** in 34% overall yield.



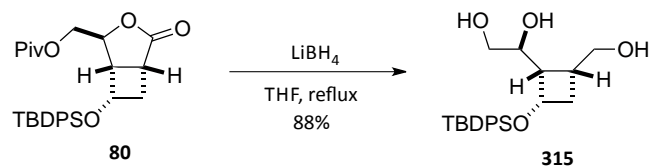
Scheme 60. Synthesis of cyclobutanone **79**.

The stereoselective reduction of the ketone group of **79** was achieved by treatment with L-Selectride in THF. This reaction yielded the hydroxyl derivative **238** in 92% yield as a single diastereomer (Scheme 61). Protection of the resulting cyclobutanol with TBDPSCI and imidazole delivered the silyl derivative **80** in 88% yield.

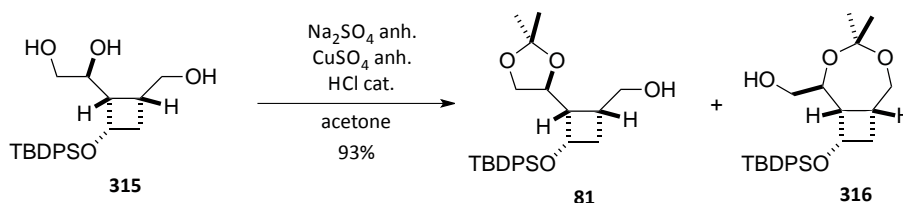


Scheme 61. Synthesis of the protected intermediate **80**.

Formation of triol **315** by complete reduction of **80** had been previously accomplished using LiAlH_4 in THF at 0 °C with yields around 88%. However, the yields obtained using this methodology were barely reproducible. As the use of different reaction conditions and/or work-ups did not improve the results, alternative reducing agents were considered. To our delight, it turned out that using LiBH_4 the reaction proceeded smoothly with highly reproducible results and comparable yields. Thus, treatment of lactone **80** with lithium borohydride in THF at reflux temperature provided triol **315** in 88% yield (Scheme 62).

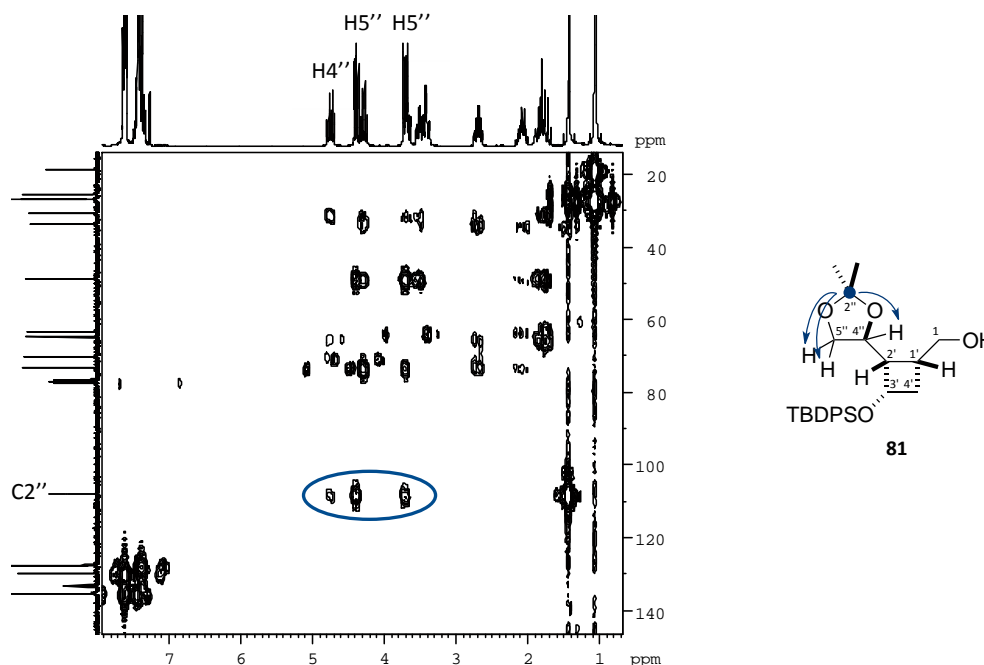
Scheme 62. Reduction of **80**.

Subsequent protection of the 1,2-diol moiety was accomplished by treatment of **315** with acetone and acid catalysis. Addition of CuSO_4 minimized the formation of the seven-membered ring acetal,¹⁵⁶ allowing to obtain the five-membered acetonide in a *ca.* 9:1 ratio (Scheme 63).



Scheme 63. Protection of the 1,2-diol group as an acetonide.

To determine whether the compounds presented the dioxolane or the dioxepane ring, HMBC spectra were registered. Hence, the HMBC spectrum of **81** showed cross peaks between $\text{C}2''$ and the protons $\text{H}4''$ and $\text{H}5''$ (Figure 52), while the spectrum of compound **316** revealed correlation between $\text{C}4$ and protons $\text{H}2$ and $\text{H}6$ (Figure 53).

Figure 52. HMBC spectrum (250 MHz, CDCl_3) of **81**.

¹⁵⁶ Kotecha, N. R.; Ley, S. V.; Mantegani, S. *Synlett* **1992**, 395-399.

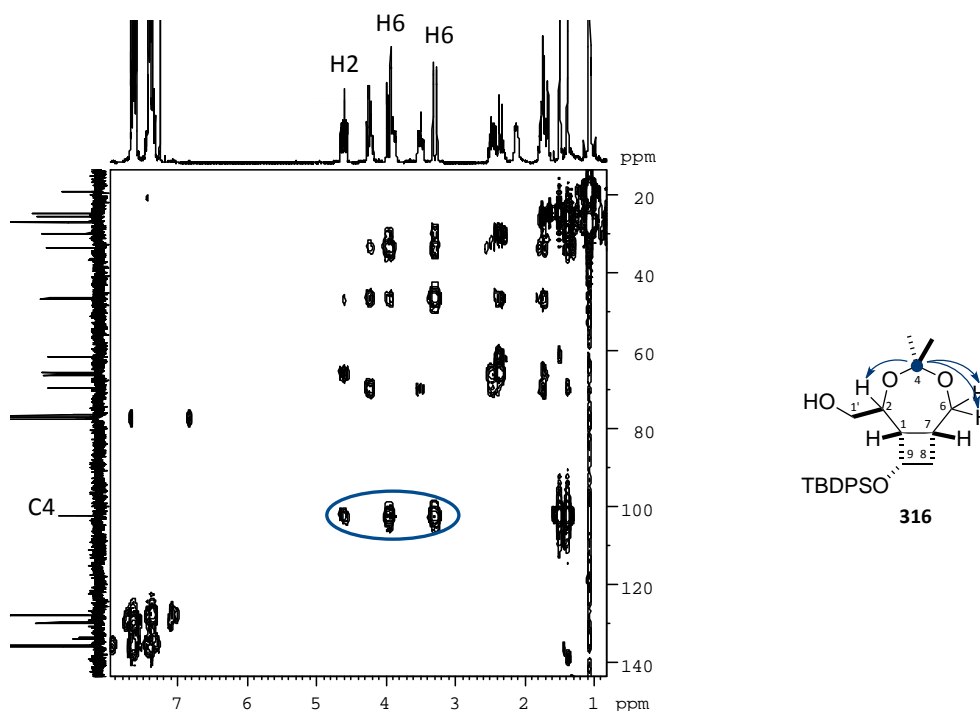


Figure 53. HMBC spectrum (250 MHz, CDCl_3) of **316**.

2.2.2 Introduction of the nucleobase

Alcohol **81** is an ideal substrate for the introduction of the nucleobase. With this purpose in mind, two methodologies were studied: the Mitsunobu reaction¹⁵⁷ and mesylate displacement.

2.2.2.1 The Mitsunobu reaction

The currently accepted mechanism for the Mitsunobu reaction is depicted in Figure 54.¹⁵⁸ The reaction starts with the nucleophilic attack of triphenylphosphine to the azodicarboxylate **II** to form the betaine **III**. This betaine can react by two competitive pathways: in the pathway a, the betaine is protonated to deliver intermediate **IV**, which after addition of one equivalent of alcohol affords the alkoxyphosphonium salt **VII**; in the pathway b, the betaine reacts with two equivalents of alcohol to form the dialkoxyphosphorane **V** and the corresponding hydrazine, **VI**. Reaction of **V** with an equivalent of acid leads to the formation of **VII**. Finally, the alkoxyphosphonium salt **VII** undergoes a substitution reaction to give product **IX** with inversion of configuration. This product is clearly favoured, and, although possible, formation of the retention product is rarely observed. If the alcohol is sterically hindered and the nucleophile is weak, the

¹⁵⁷ For recent reviews see: (a) Dembinski, R. *Eur. J. Org. Chem.* **2004**, 2763-2772. (b) But, T. Y. S.; Toy, P. H. *Chem. Asian J.* **2007**, *2*, 1340-1355. (c) Reynolds A. J.; Kassiou M. *Curr. Org. Chem.* **2009**, *13*, 1610-1632. (d) Swamy, K. C. K.; Kumar, N. N. B.; Balaraman, E.; Kumar, K. V. P. *Chem. Rev.* **2009**, *109*, 2551-2651.

¹⁵⁸ Schenk, S.; Weston, J.; Anders, E. J. *Am. Chem. Soc.* **2005**, *127*, 12566-12576.

latter can compete with the alcohol for the alkoxyphosphonium salt **VII**, giving rise to undesired side reactions.

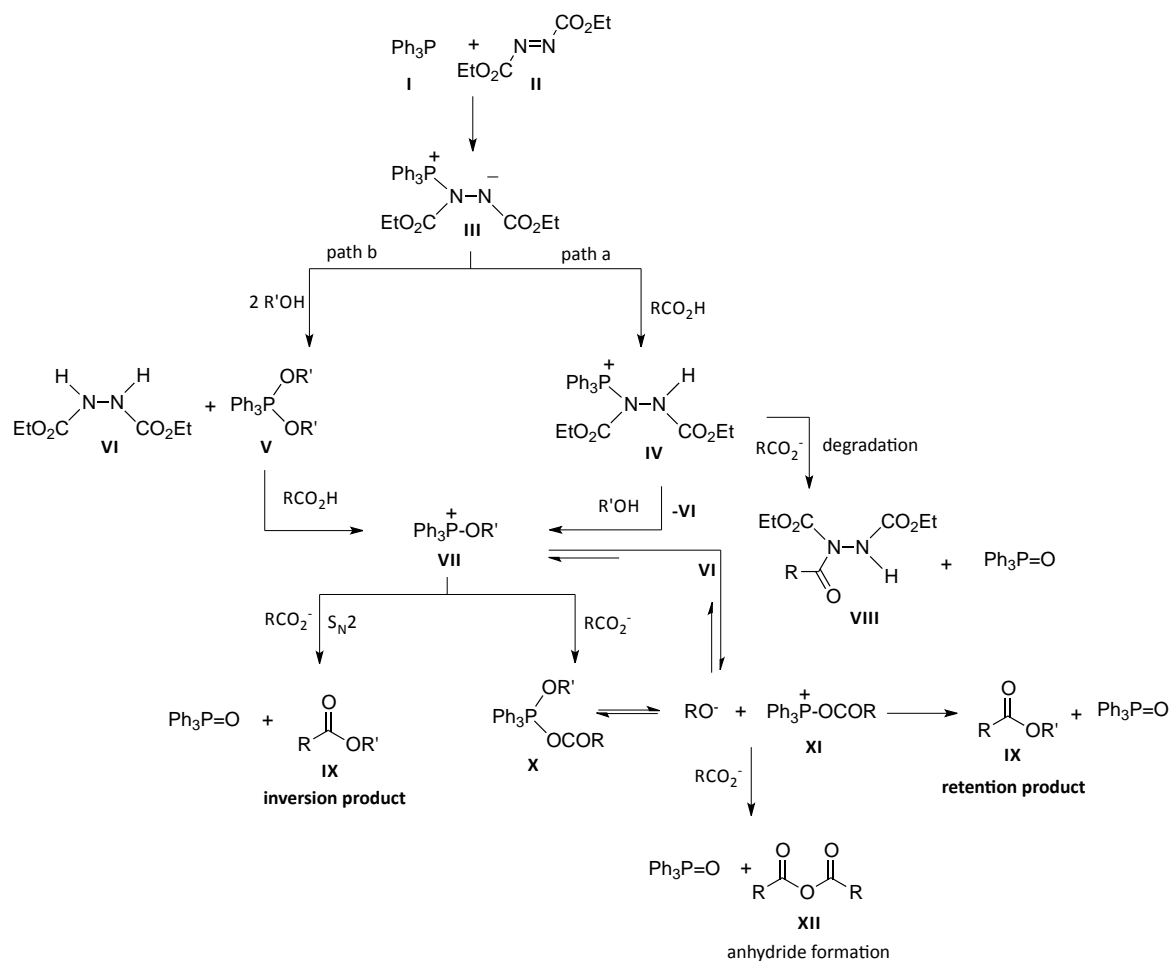
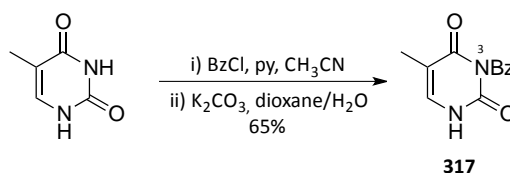


Figure 54. General mechanism of the Mitsunobu reaction.

2.2.2.1.1 Introduction of thymine

Initially, we chose thymine as the initial base to optimize the reaction. Since both *N*1 and *N*3 nitrogen atoms of thymine can act as nucleophiles, protection of the *N*3 position should be performed. Thus, *N*³-benzoylthymine, **317**, was prepared in a two-step sequence involving dibenzoylation and subsequent pH-controlled cleavage of the *N*¹-benzoyl group (Scheme 64).¹⁵⁹

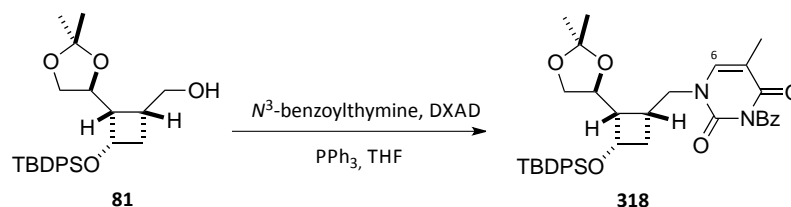
¹⁵⁹ Frieden, M.; Giraud, M.; Reese, C. B.; Song, Q. *J. Chem. Soc., Perkin Trans. 1*, **1998**, 2827-2832.



Scheme 64. Synthesis of N^3 -benzoylthymine, **317**.

Next, we explored the Mitsunobu reaction of **81** with **317**. Our first attempt involved the use of triphenylphosphine and DBAD as the azodicarboxylate at room temperature. These conditions led to **318** in 63% yield (Scheme 65, entry 1). Nevertheless, separation of the reaction product from triphenylphosphine oxide turned out to be a tedious process. Hence, we studied the use of polymer-bound triphenylphosphine. This polymer, which can be filtered off from the reaction crude, proved to be useful in terms of purification of the product, but the yield of the reaction decreased notably (entry 2). However, by increasing the temperature the amount of obtained product was nearly doubled (entry 3). This result prompted us to increase the temperature using standard PPh_3 , rising the yield up to 73% (entry 4).

Finally, we screened different azodicarboxylates looking for better yields and/or easier purification processes (entries 5 and 6). Unfortunately, although product **318** was formed, we were not able to separate it from the hydrazines derived from the corresponding azodicarboxylates. Hence, we decided to apply the conditions described on entry 4 that delivered **318** in 73% yield.



Entry	DXAD	PPh_3 source	Temperature	Yield
1	DBAD	PPh_3	rt	63
2	DBAD	$\bullet\text{PPh}_3$	rt	30
3	DBAD	$\bullet\text{PPh}_3$	reflux	58
4	DBAD	PPh_3	reflux	73
5	DEAD	$\bullet\text{PPh}_3$	reflux	- ^a
6	DIAD	$\bullet\text{PPh}_3$	reflux	- ^a

DBAD: di-*tert*-butyl azodicarboxylate. DEAD: diethyl azodicarboxylate. DIAD: diisopropyl azodicarboxylate. $\bullet\text{PPh}_3$: polymer-bound triphenylphosphine. ^a The reaction product could not be separated from the corresponding hydrazine.

Scheme 65. Introduction of thymine on alcohol **81**.

Introduction of the nucleobase on substrate **81** was established by the appearance of extra signals on the ^1H and ^{13}C spectra. Thus, the proton spectrum features six additional protons in the area comprised between 7.00-8.00 ppm corresponding to H6 and the benzoyl group (Figure 55), while the carbon spectrum shows additional signals at δ 109.7 and δ 145.0-165.0 corresponding to the thymine sp^2 carbons.

Also, the IR spectrum shows three strong absorptions at 1653, 1698 and 1746 cm^{-1} corresponding to the C=O groups of the nucleobase and the benzoyl protecting group.

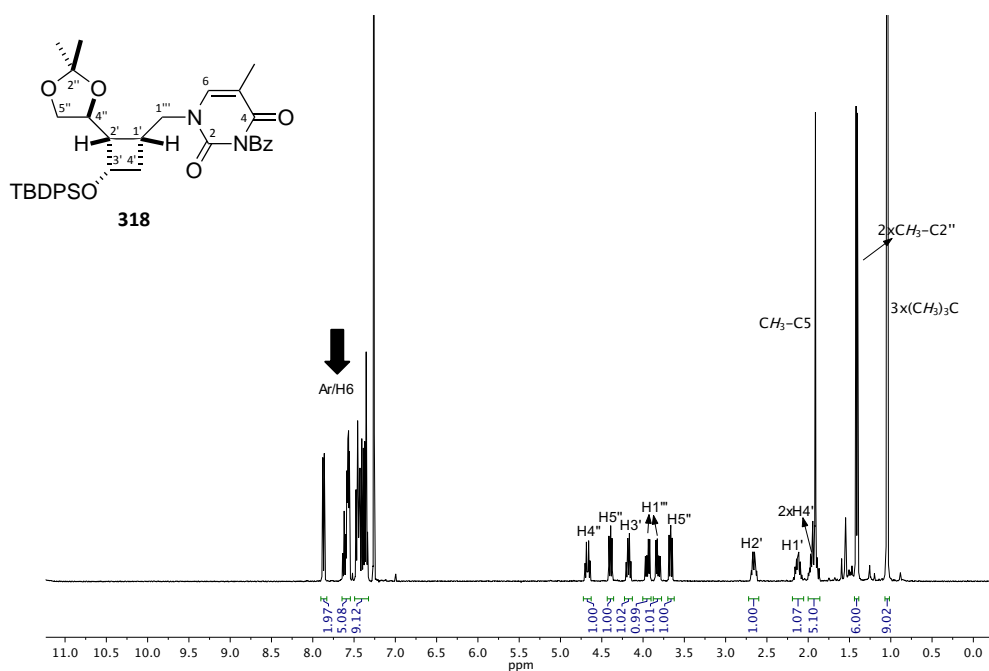


Figure 55. ^1H -NMR spectrum (400 MHz, CDCl_3) of **318**.

In addition, the union of thymine through N1 could be further confirmed by the HMBC spectrum, which showed correlation between $\text{H1}'''$ and both C2 and C6 along with correlation between $\text{C1}'''$ and H6 (Figure 56).

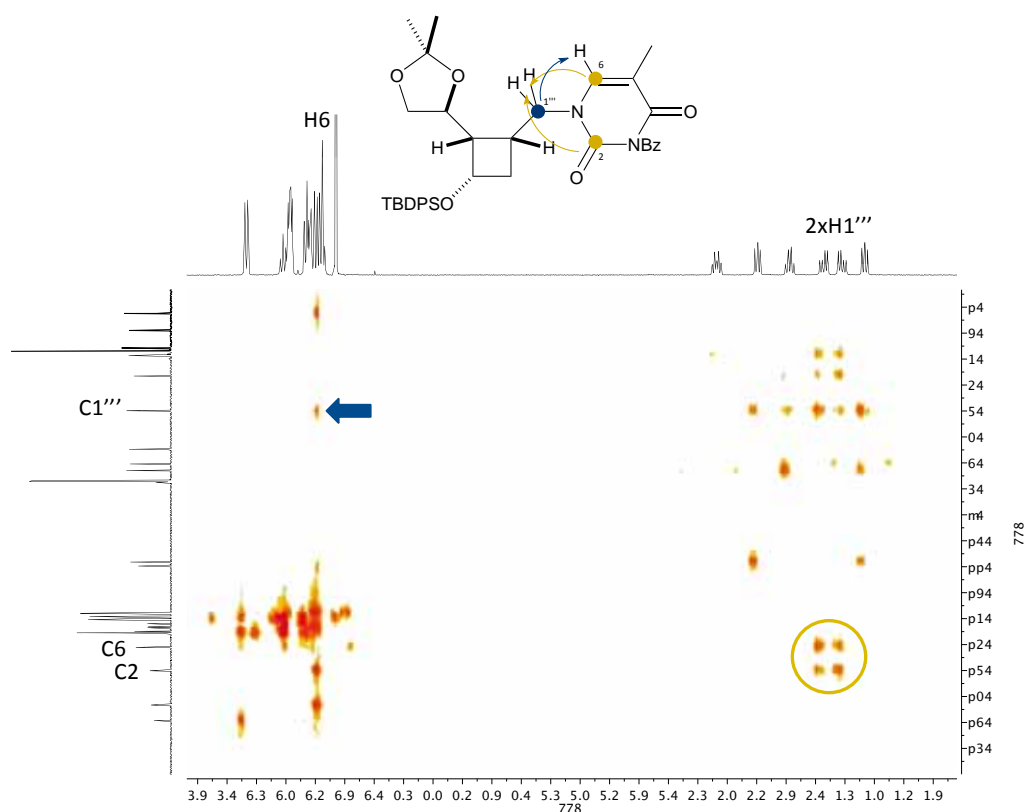


Figure 56. HMBC spectrum (400 MHz, CDCl_3) of **318**.

Using the conditions described above, we planned to introduce two additional bases: 5-fluorouracil and the purine base 2-amino-6-chloropurine, which can be converted into 6-*O*-methylguanine.

2.2.2.1.2 Introduction of 5-fluorouracil

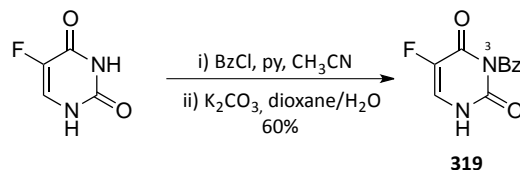
Since the discovery of the tumour-inhibiting activity of 5-fluorouracil,¹⁶⁰ fluorine-containing nucleosides have been widely investigated in medicinal chemistry.¹⁶¹ In recent years, many fluoro nucleosides have been synthesized and evaluated as potential antiviral agents, with some of them showing interesting biological properties (see Chapter I, section 1).

Taking these results into account, we decided to study the incorporation of 5-fluorouracil into compound **81**. Its structural analogy with thymine was expected to grant similar behaviour in the

¹⁶⁰ Heidelberger, C.; Chaudhuri, N. K.; Danneberg, P.; Mooren, D.; Griesbach, L.; Duschinsky, R.; Schnitzer, R. J.; Plevin, E.; Scheiner, J. *Nature* **1957**, *179*, 663-666.

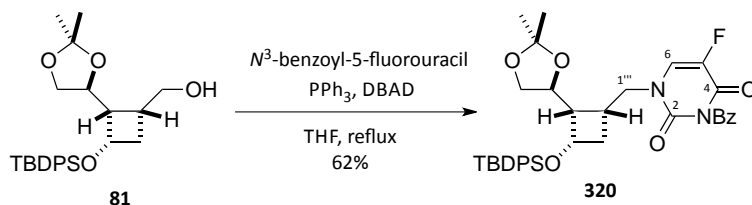
¹⁶¹ (a) Maruyama, T.; Ikejiri, M.; Izawa, K.; Onishi, T. In *Fluorine in medicinal chemistry and chemical biology*, Wiley-Blackwell: Chichester, UK, 2009, Chapter 7, 165-198. (b) Filler, R.; Saha, R. *Future Med. Chem.* **2009**, *1*, 777-791.

Mitsunobu reaction. Prior to this reaction, the 5-fluorouracil unit was N^3 -benzoylated using the same procedure as in the case of thymine (Scheme 66).



Scheme 66. Synthesis of N^3 -benzoyl-5-fluorouracil, **319**.

Then, treatment of the alcohol **81** with **319**, PPh_3 , and DBAD in THF, under the same reaction conditions previously optimized, produced adduct **320** in 62% yield (Scheme 67).



Scheme 67. Introduction of N^3 -benzoyl-5-fluorouracil on alcohol **81**.

The presence of the fluorine atom led to the utilization of ^{19}F -NMR spectroscopy for the characterization of **320**. Thus, the fluorine atom appears as a doublet at δ -167.3 with a coupling constant of $J_{\text{F},6}=6.1$ Hz (Figure 57). The presence of the fluorine atom was also evidenced by the multiplicity of the surrounding carbon atoms. Thus, C4, C5 and C6 appear as doublets in the ^{13}C -NMR spectrum, with coupling constants of $J_{4,\text{F}}=27.0$ Hz, $J_{5,\text{F}}=237.3$ Hz, and $J_{6,\text{F}}=33.5$ Hz.

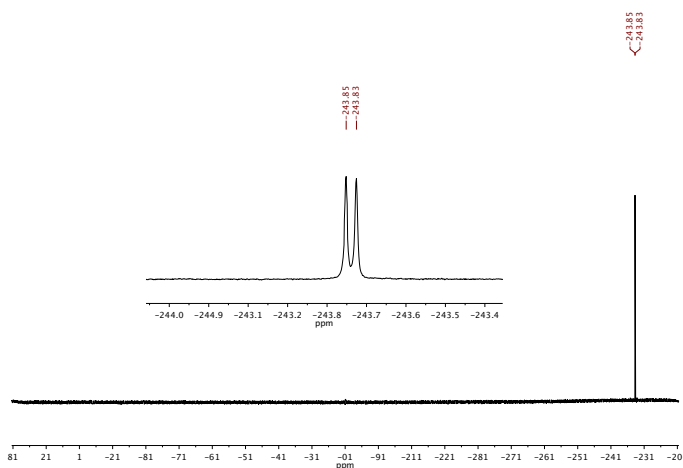


Figure 57. ^{19}F -NMR spectrum (235 MHz, CDCl_3) of **320**.

As before, the connectivity of the base with the cyclobutane could be established through the HMBC spectrum, where the same correlation signals for C2, C6 and C1''' and protons H1''' and H6 as in the case of the thymine derivative **318** are observed.

2.2.2.1.3 Introduction of 2-amino-6-chloropurine

Having introduced two pyrimidine bases, we next aimed at the introduction of a purine base. We chose 2-amino-6-chloropurine because of its easy conversion into either guanine¹⁶² or its 6-*O*-methyl derivative.^{163,164} Specifically, we targeted the synthesis of the *O*⁶-substituted derivative due to its higher lipophilicity, which can result in an improved cellular uptake.^{163,165} Furthermore, several guanosine prodrugs such as **321-322**, which feature 6-alkoxy groups, are in clinical or preclinical development as anti-HCV agents (Figure 58).¹⁶⁶

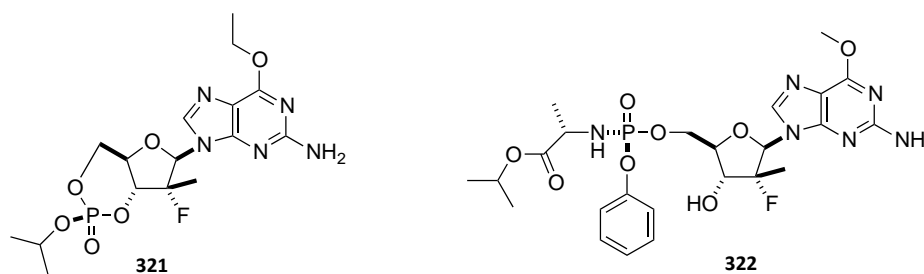


Figure 58. 6-alkoxy-substituted guanosine prodrugs under development as anti-HCV agents.

Mitsunobu reaction of purines usually renders mixtures of both *N*7 and *N*9 regioisomers.^{33,167} However, while formation of the *N*9 regioisomer is predominant, the proportion of *N*7 is highly variable, being obtained in small amounts¹⁶⁸ or being even inexistent.¹⁶⁹

¹⁶² (a) Mullah, K. B.; Bentrude, W. G. *J. Org. Chem.* **1991**, *56*, 7218-7224. (b) Paquette, L. A.; Kahane, A. L.; Seekamp, C. K. *J. Org. Chem.* **2004**, *69*, 5555-5562. (c) Zhou, S.; Zemlicka, J. *Tetrahedron* **2005**, *61*, 7112-7116. (d) Jacobsen, M. F.; Knudsen, M. M.; Gothelf, K. V. *J. Org. Chem.* **2006**, *71*, 9183-9190.

¹⁶³ McGuigan, C.; Madela, K.; Aljarah, M.; Gilles, A.; Brancala, A.; Zonta, N.; Chamberlain, S.; Vernachio, J.; Hutchins, J.; Hall, A.; Ames, B.; Gorovits, E.; Ganguly, B.; Kolykhalov, A.; Wang, J.; Muhammad, J.; Patti, J. M.; Henson, G. *Bioorg. Med. Chem. Lett.* **2010**, *20*, 4850-4854.

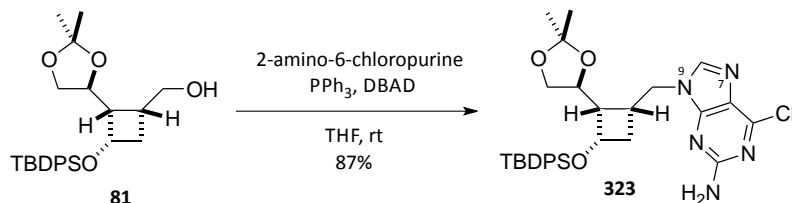
¹⁶⁴ For a recent review on the functionalization of purines see: Legraverend, M. *Tetrahedron* **2008**, *64*, 8585-8603.

¹⁶⁵ (a) Reddy, P. G.; Bao, D.; Chang, W.; Chun, B.-K.; Du, J.; Nagarathnam, D.; Rachakonda, S.; Ross, B. S.; Zhang, H.-R.; Bansal, S.; Espiritu, C. L.; Keilman, M.; Lam, A. M.; Niu, C.; Steuer, H. M.; Furman, P. A.; Otto, M. J.; Sofia, M. J. *Bioorg. Med. Chem. Lett.* **2010**, *20*, 7376-7380. (b) McGuigan, C.; Madela, K.; Aljarah, M.; Gilles, A.; Battina, S. K.; Ramamurty, C. V. S.; Rao, C. S.; Vernachio, J.; Hutchins, J.; Hall, A.; Kolykhalov, A.; Henson, G.; Chamberlain, S. *Bioorg. Med. Chem. Lett.* **2011**, *21*, 6007-6012.

¹⁶⁶ Murakami, E.; Bao, H.; Mosley, R. T.; Du, J.; Sofia, M. J.; Furman, P. A. *J. Med. Chem.* **2011**, *54*, 5902-5914.

¹⁶⁷ See for example: Núñez, M. C.; Pavani, M. G.; Díaz-Gavilán, M.; Rodríguez-Serrano, F.; Gómez-Vidal, J. A.; Marchal, J. A.; Aránega, A.; Gallo, M. A.; Espinosa, A.; Campos, J. M. *Tetrahedron* **2006**, *62*, 11724-11733.

Interestingly, reaction of the alcohol **81** with 2-amino-6-chloropurine, PPh₃ and DBAD in THF afforded uniquely the *N9* regioisomer, **323**, in excellent yield (Scheme 68).



Scheme 68. Introduction of 2-amino-6-chloropurine on alcohol **81**.

Base attachment could be corroborated by the ¹H-NMR spectrum of this compound, where new signals corresponding to H8 and NH₂ appeared (Figure 59).

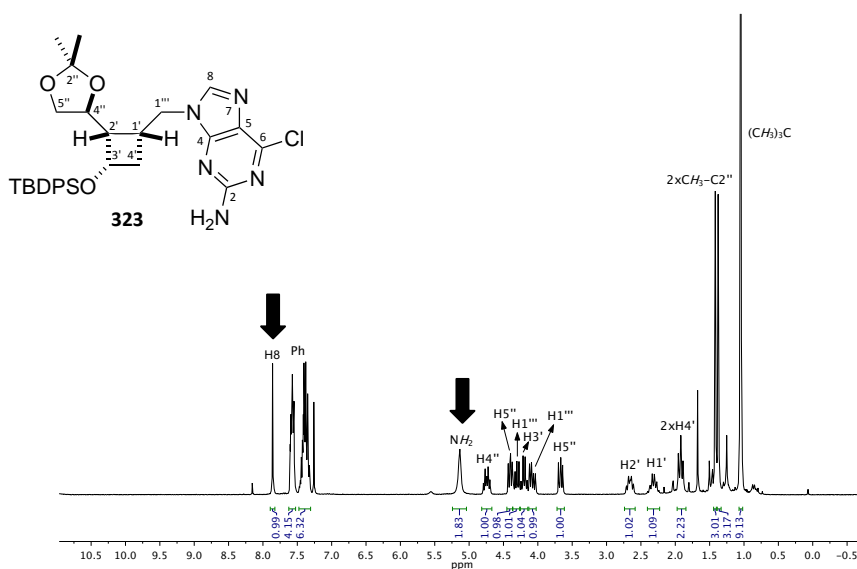


Figure 59. ¹H-NMR spectrum (250 MHz, CDCl₃) of **323**.

To check whether the obtained compound was the *N7* or the *N9* regioisomer, an HMBC experiment was registered. The spectrum revealed correlation between carbons C4 and H1''', thus confirming the desired *N9* regioisomery (Figure 60).

¹⁶⁸ Fletcher, S.; Shahani, V. M.; Lough, A. J.; Gunning, P. T. *Tetrahedron* **2010**, *66*, 4621-4632.

¹⁶⁹ Aubin, Y.; Audran, G.; Vanthuyne, N.; Monti, H. *Tetrahedron* **2007**, *63*, 5050-5055.

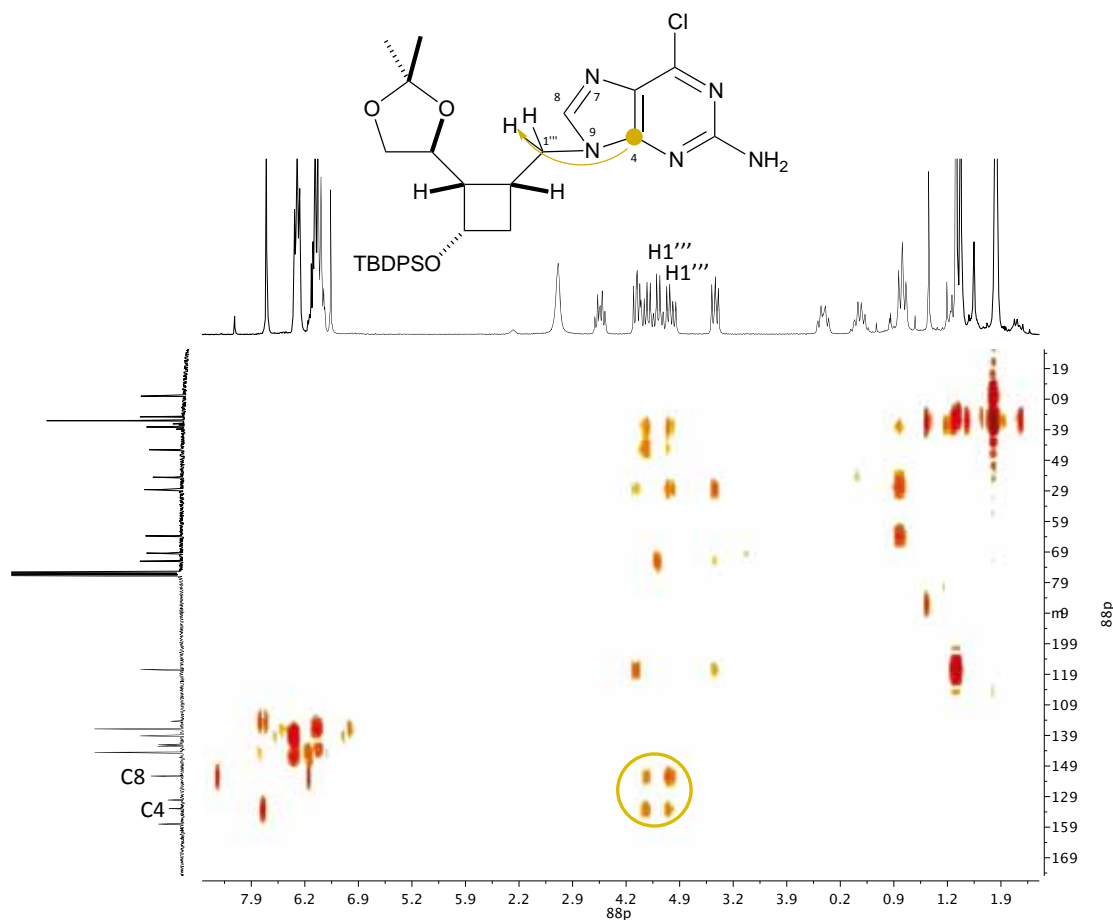


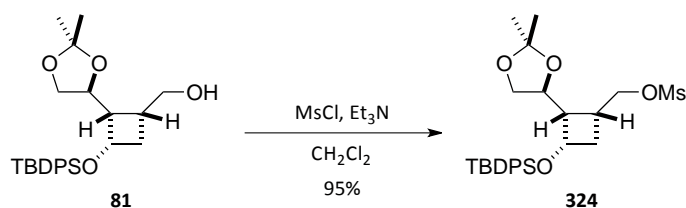
Figure 60. HMBC spectrum (250 MHz, CDCl_3) of **323**.

2.2.2.2 Mesylate displacement

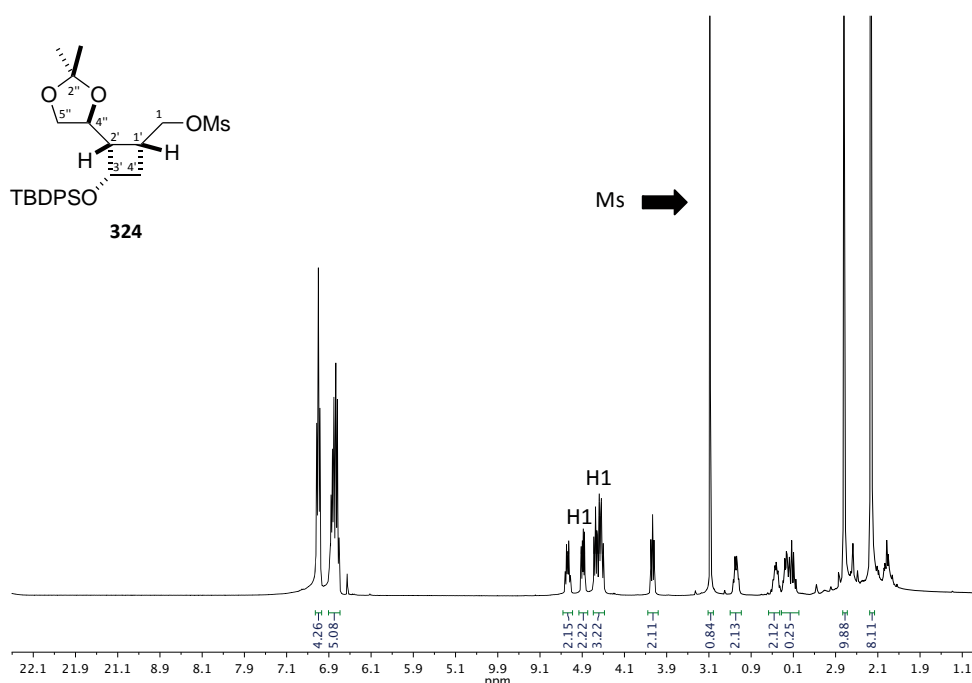
The coupling of nucleobases with glycones using the Mitsunobu reaction has been described to give appreciable better yields than classical substitutions.¹⁷⁰ However, to compare both methodologies, we decided to attempt the introduction of the nucleobase by mesylate displacement.

In order to convert the hydroxyl group into the corresponding mesylate, compound **81** was treated with MsCl and triethylamine in CH_2Cl_2 to afford mesylate **324** in 95% yield (Scheme 69).

¹⁷⁰ Fernández, F.; García-Mera, X.; López, C.; Morales, M.; Rodríguez-Borges, J. E. *Synthesis* **2005**, 3549-3554.

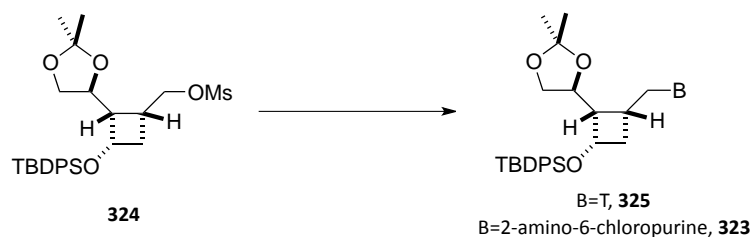
Scheme 69. Mesylation of **81**.

The product was found to be rather unstable, requiring freezer storage. Its formation was confirmed by $^1\text{H-NMR}$ spectroscopy, where the methyl of the mesylate group appeared around $\delta \sim 3.00$ and the signal of protons H1 appeared downfield shifted compared to **81** ($\delta \sim 3.50$ vs. $\delta \sim 4.40$) (Figure 61). The same trend was observed for C1 in the $^{13}\text{C-NMR}$ spectrum (δ 63.6 vs. δ 71.9).

Figure 61. $^1\text{H-NMR}$ spectrum (400 MHz, CDCl_3) of **317**.

With the mesylate on hand, we turned our attention to nucleobase introduction. First, the coupling of thymine employing our previously described conditions was attempted.⁴⁷ As the basic reaction medium could cleave the *N*-protecting groups, the use of unprotected thymine was preferred. Accordingly, mesylate **324** was treated with K_2CO_3 , 18-crown-6 and thymine in DMF at 120 °C (Scheme 70, entry 1). Under these conditions, the expected thymine adduct was obtained, albeit in 24% yield. Analogously to the case of **318**, correlation between H1''' and both C2 and C6 along with correlation between C1''' and H6 allowed to confirm base attachment through N1.

Treatment of **324** with cesium carbonate did not improve the results, providing **325** in 26% yield (entry 2). Finally, we tried the introduction of 2-amino-6-chloropurine using a strong base to achieve **323**, but in this case the yield was even lower (15%) (entry 3).



Entry	Conditions	Base	Yield
1	K ₂ CO ₃ , 18-C-6, DMF	thymine	24
2	Cs ₂ CO ₃ , DMF	thymine	26
3	NaH, DMF	2-amino-6-chloropurine	15

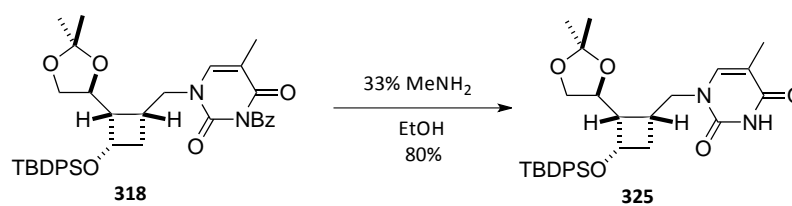
Scheme 70. Nucleobase introduction by nucleophilic substitution on the mesylate **324**.

Despite the poor yields obtained, these results are in accordance with previously reported works in which the yield for such reactions is around 30-40%.^{170,171}

2.2.3 Synthesis of the thymine nucleoside **95**

To achieve the synthesis of the thymine nucleoside **95**, deprotection of N3 and the three hydroxyl groups of **318** was required.

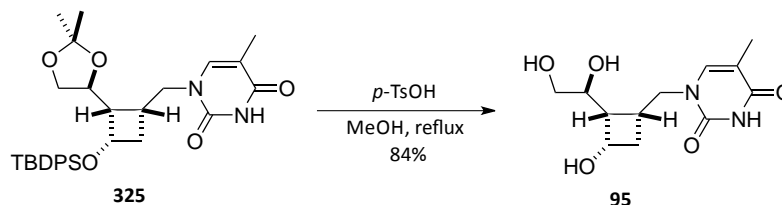
First, cleavage of the N³-protecting group was achieved by treatment of **318** with a 33% MeNH₂ solution in ethanol.¹⁵⁹ The reaction proceeded smoothly at room temperature, giving **325** in 80% yield (Scheme 71).



Scheme 71. Deprotection of the N³-benzoyl group of **318**.

¹⁷¹ (a) Brückner, A. M.; Garcia, M.; Marsh, A.; Gellman, S. H.; Diederichsen, U. *Eur. J. Org. Chem.* **2003**, 3555-3561. (b) Kim, A.; Hong, J. H. *Nucleosides, Nucleotides & Nucleic Acids* **2006**, *25*, 941-950. (c) Oh, C. H.; Hong, J. H. *Nucleosides, Nucleotides & Nucleic Acids* **2008**, *27*, 186-195.

The following deprotection of the hydroxyl groups, would lead to the target cyclobutane L-nucleoside **95**. Hence, cleavage of the acetonide and the silyl ether was achieved in one step by treatment of **325** with *p*-TsOH in MeOH at reflux temperature, furnishing nucleoside **95** in 84% yield (Scheme 72).



Scheme 72. Synthesis of nucleoside **95**.

Due to similar polarities, purification of **95** by column chromatography was not sufficient in order to separate the title nucleoside from *p*-TsOH. Fortunately, filtration through a short path of the basic resin DOWEX 1x8 retained the acid providing pure **95**.¹⁷² Figure 62 shows its proton spectrum, where the acetal and silyl signals are no longer observed.

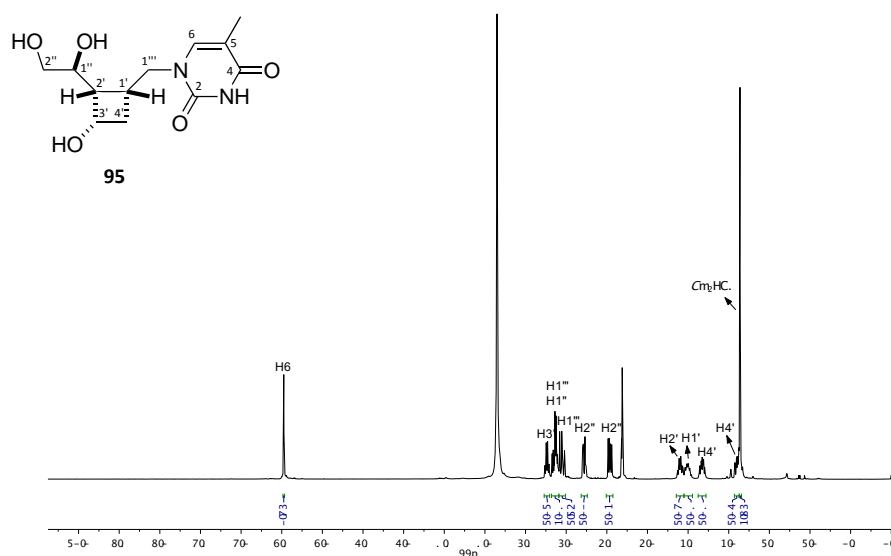


Figure 62. ¹H-NMR spectrum (400 MHz, MeOD) of nucleoside **95**.

The NOESY spectrum of **95** evidences the stereochemistry of the cyclobutane ring. While H2' shows cross peaks with H2'' and H3', H1' shows interaction with H1'', H6, H3' and H4'_{exo} (Figure 63).

¹⁷² Dow fine mesh resins. www.dowwaterandprocess.com/products/fine_mesh.htm. Accessed 14/08/2012.

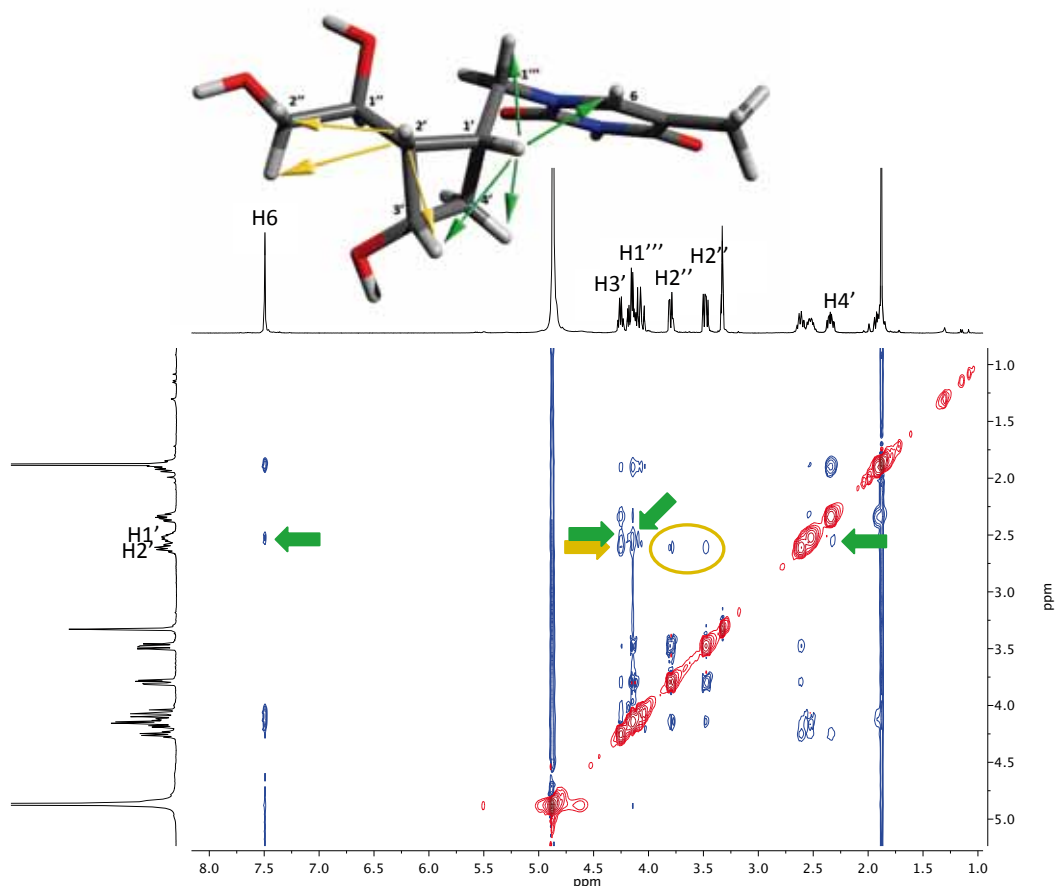
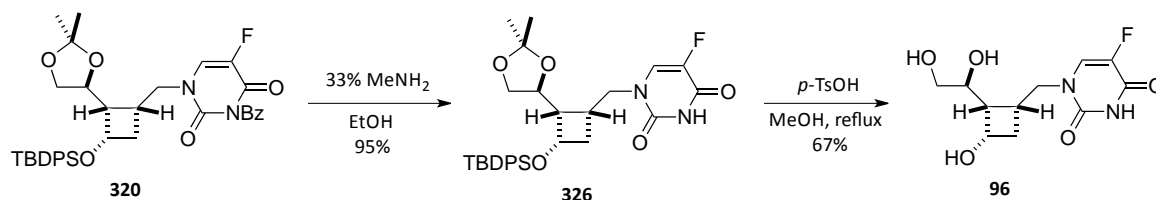


Figure 63. 3D model of **95** showing n.O.e relationships and the corresponding NOESY spectrum (400 MHz, MeOD).

2.2.4 Synthesis of the 5-fluorouracil nucleoside **96**

The synthesis of the fluorouracil nucleoside **96**, was carried out in an analogous manner. First, the benzoyl group of the base was cleaved and then the hydroxyl groups were deprotected.

Accordingly, reaction of **320** with MeNH₂ in EtOH afforded intermediate **326** in 95% yield (Scheme 73). Complete deprotection of **326** by treatment with *p*-TsOH in MeOH and purification following the same procedure described above afforded the fluorine nucleoside **96** in 67% yield.



Scheme 73. Synthesis of nucleoside **96**.

As before, the presence of the fluorine atom was determined by ^1H -, ^{13}C - and ^{19}F -NMR. Thus, a coupling constant of $J_{6,\text{F}}=6.3$ Hz was observed between H6 and the fluorine atom, while carbons C4, C5 and C6 appeared as doublets, with coupling constants of $J_{4,\text{F}}=25.7$ Hz, $J_{5,\text{F}}=231.5$ Hz, and $J_{6,\text{F}}=33.1$ Hz, respectively (Figure 64).

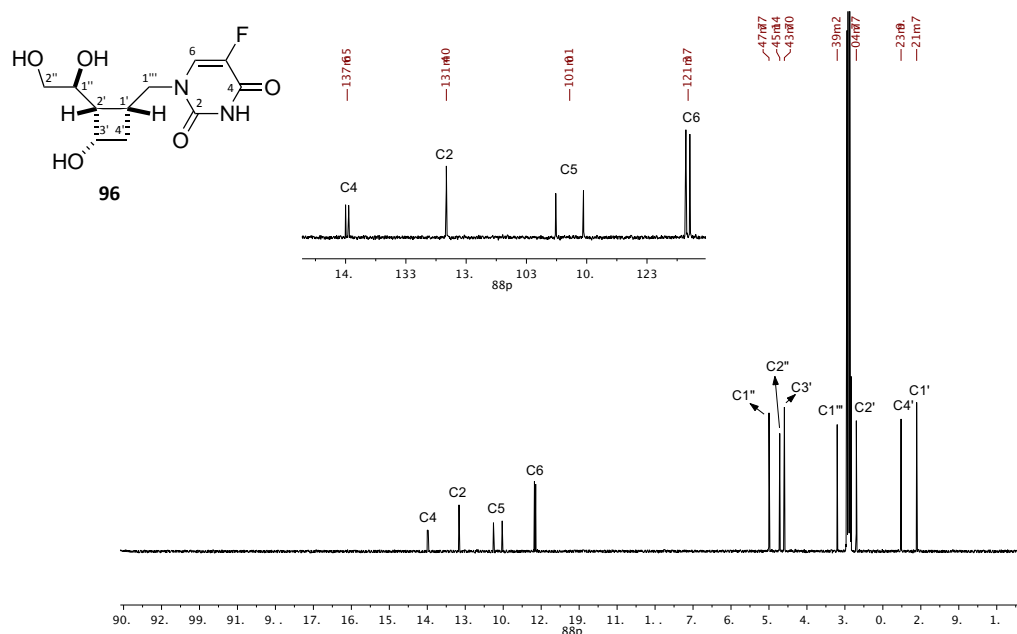


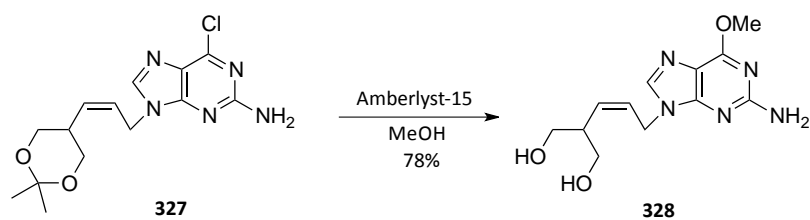
Figure 64. ^{13}C -NMR spectrum (100 MHz, MeOD) of **96**.

2.2.5 Synthesis of the O^6 -methylguanine nucleoside **97**

Next, we considered the synthesis of the O^6 -methylguanine nucleoside **97**. The conversion of the 2-amino-6-chloropurine unit into the O^6 -substituted derivative has been typically performed by substitution of the 6-chlorine atom by the corresponding alkoxide.^{143,163,165,173} However, Vince and co-workers in their work towards the synthesis of acyclic analogues of cyclohexene nucleosides,¹⁷⁴ while carrying out the deprotection of **327** with the acidic resin Amberlyst-15 in MeOH, found out the unexpected substitution at C6 affording compound **328** (Scheme 74).

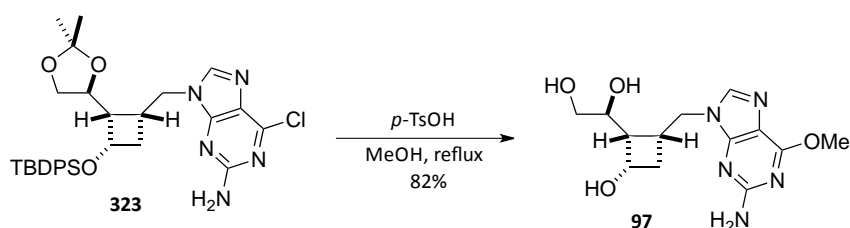
¹⁷³ (a) Coe, D. M.; Roberts, S. M.; Storer, R. *J. Chem. Soc., Perkin Trans. 1*, **1992**, 2695-2704. (b) Zhou, S.; Kern, E. R.; Gullen, E.; Cheng, Y.-C.; Drach, J. C.; Matsumi, S.; Mitsuya, H.; Zemlicka, J. *J. Med. Chem.* **2004**, *47*, 6964-6972.

¹⁷⁴ Tang, Y.; Muthyala, R.; Vince, R. *Bioorg. Med. Chem.* **2006**, *14*, 5866-5875.



Scheme 74. Reaction of **327** with Amberlyst-15 in MeOH.

Taking these results into account, a similar deprotection-substitution step was envisioned. Thus, when compound **323** was treated with *p*-TsOH in MeOH, nucleoside **97** was directly obtained in 82% yield as the sole product (Scheme 75).



Scheme 75. Synthesis of the 6-*O*-methylguanine nucleoside **97**.

The presence of the methoxy moiety could be detected by ^1H - and ^{13}C -NMR spectroscopy, where a new signal appeared at δ 4.04 and at δ 54.1, respectively (Figures 65 and 66).

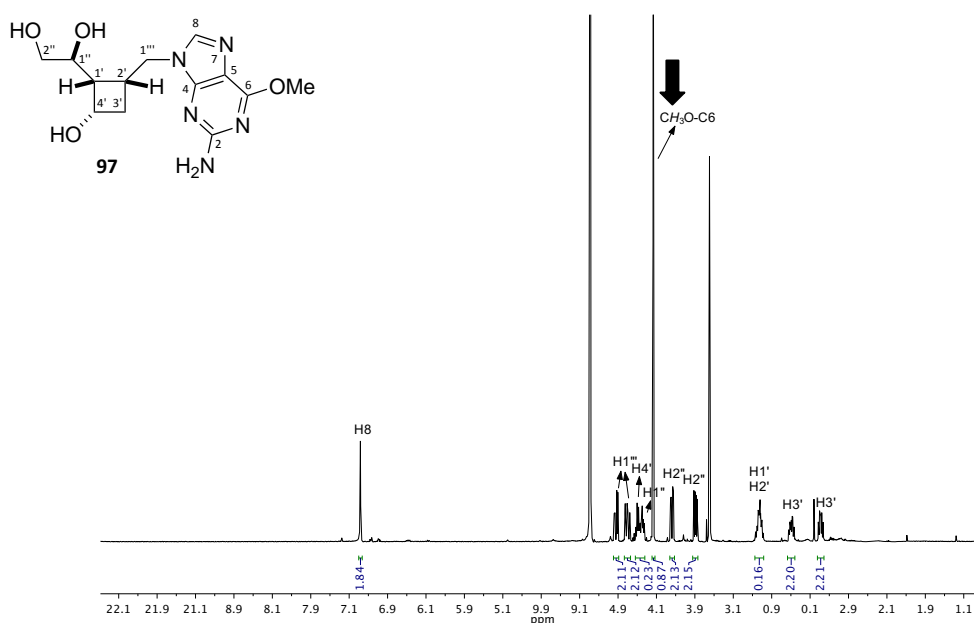


Figure 65. ^1H -NMR spectrum (400 MHz, MeOD) of **97**.

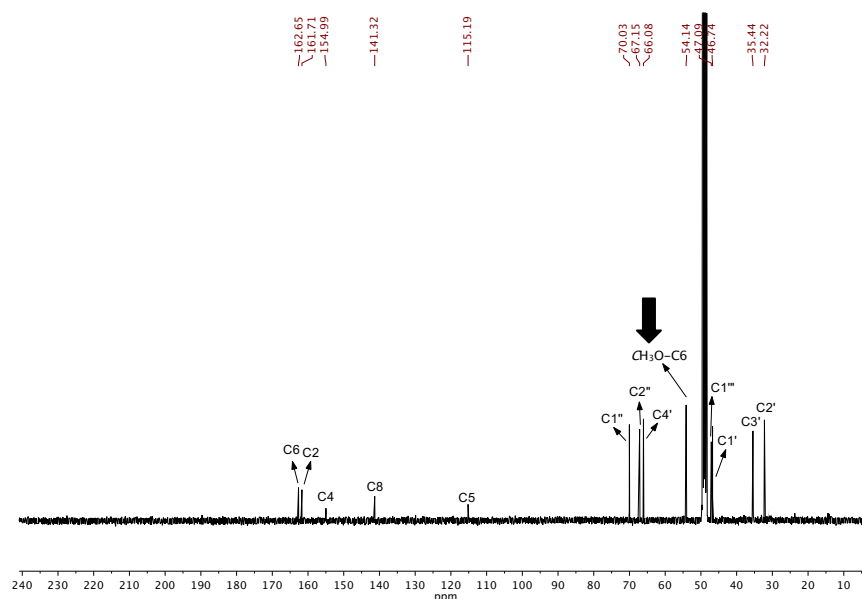


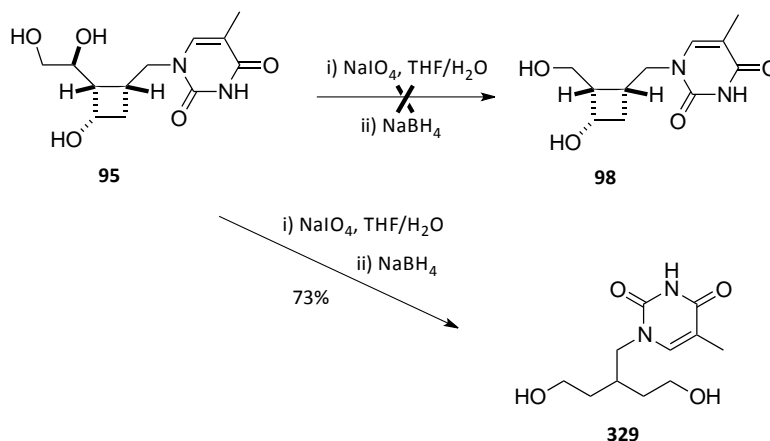
Figure 66. ^{13}C -NMR spectrum (100 MHz, MeOD) of **97**.

2.3 Synthesis of the thymine nucleoside **98**

With nucleoside **95** in hand, we targeted the synthesis of the hydroxymethyl derivative **98**. The synthesis of this compound would involve an oxidative cleavage of the diol present in **95** followed by reduction of the corresponding aldehyde.

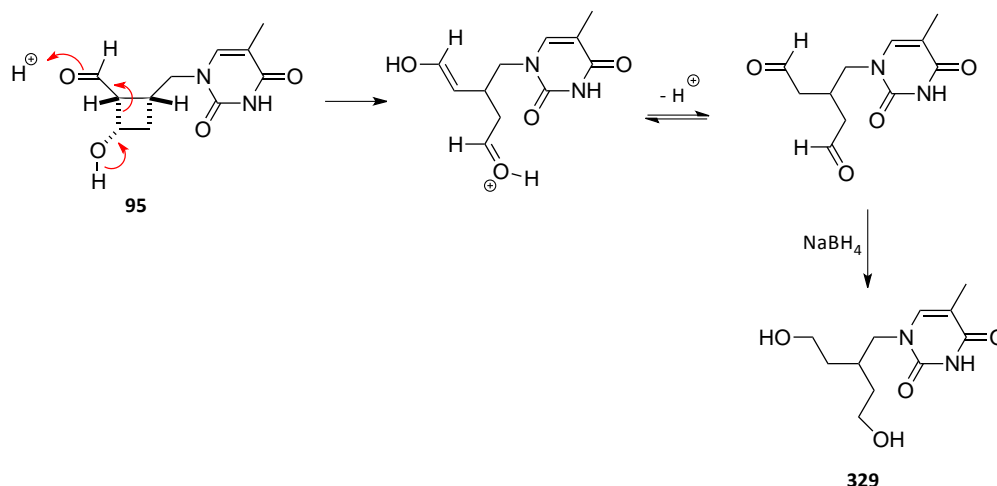
2.3.1 Oxidative cleavage of nucleoside **95**

However, when the thymine nucleoside analogue **95** was submitted to standard oxidative cleavage/reduction conditions, we isolated a product which spectra exhibited less signals than the ones predicted, suggesting the existence of some kind of symmetry in the molecule (Scheme 76). This fact is in accordance with the opening of the cyclobutane to form **329**.



Scheme 76. Failed attempt to obtain nucleoside **98** from **95**.

The formation of this acyclic product can be rationalized in terms of a retro-aldol reaction followed by the reduction of both aldehyde groups (Scheme 77).



Scheme 77. Possible mechanistic pathway leading to **329**.

In order to avoid the formation of this acyclic product, other oxidative cleavage methodologies were explored. First, diol cleavage of **95** with $\text{Pb}(\text{OAc})_4$ was attempted (Table 14, entry 2). Unfortunately, this reaction only led to unidentified decomposition products. The same result was found when the reaction was attempted by using $\text{Mn}(\text{OAc})_3$ (entry 3).¹⁷⁵

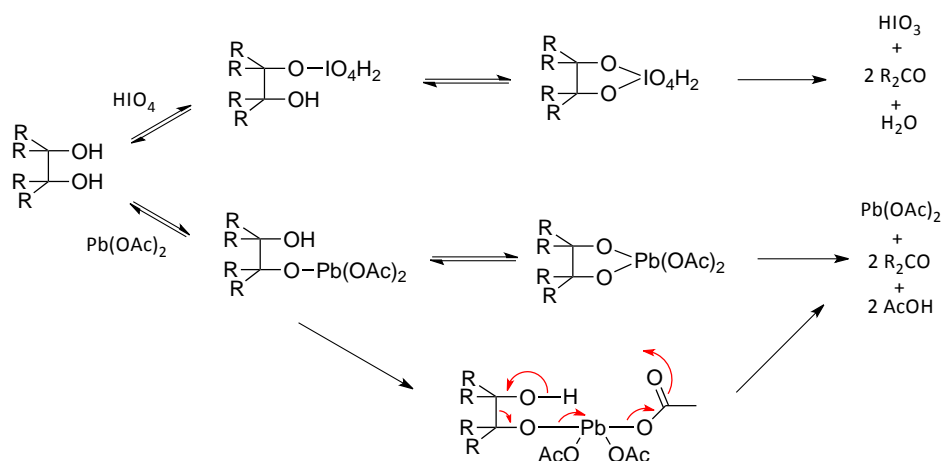
Entry	Conditions	Product
1	NaIO_4	329
2	$\text{Pb}(\text{OAc})_4$	decomposition
3	$\text{Mn}(\text{OAc})_3$	decomposition
4	$\text{KIO}_4/\text{KHCO}_3$, pH 7	329

Table 14. Attempted oxidative cleavage methodologies.

As it is shown in Scheme 78, the use of these standard reagents results in the acidification of the reaction medium thus favouring the retro-aldol process. For this reason, a combination of KIO_4 and KHCO_3 was finally tested. The lower solubility of KIO_4 (compared to NaIO_4) together with the addition of the potassium hydrogen carbonate, have been described to buffer the solution at pH 7-7.5.¹⁷⁶ However, when nucleoside **95** was submitted to these conditions, the acyclic compound **329** was obtained again (entry 4).

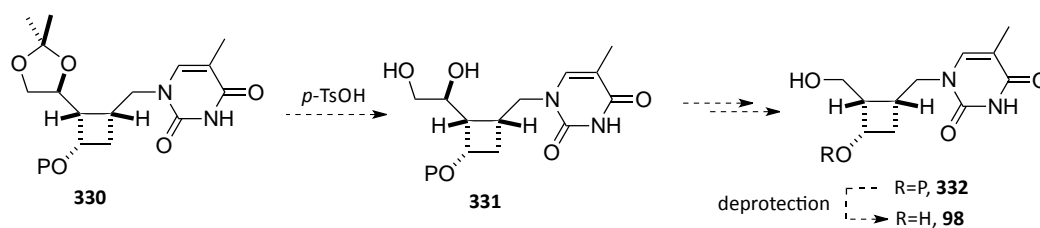
¹⁷⁵ Candela Lena, J. I.; Rico Ferreira, M. del R.; Martín Hernando, J. I.; Altinel, E.; Arseniyadis, S. *Tetrahedron Lett.* **2001**, *42*, 3179-3182.

¹⁷⁶ Schmid, C. R.; Bradley, D. A. *Synthesis*, **1992**, 587-590.



Scheme 78. Mechanism of glycol cleavage.¹⁷⁷

Because of the impossibility to get the desired cyclobutane nucleoside, we envisaged that a viable alternative would be to protect the 3'-hydroxyl with an acid resistant group. This protection should avoid cyclobutane opening (Scheme 79).



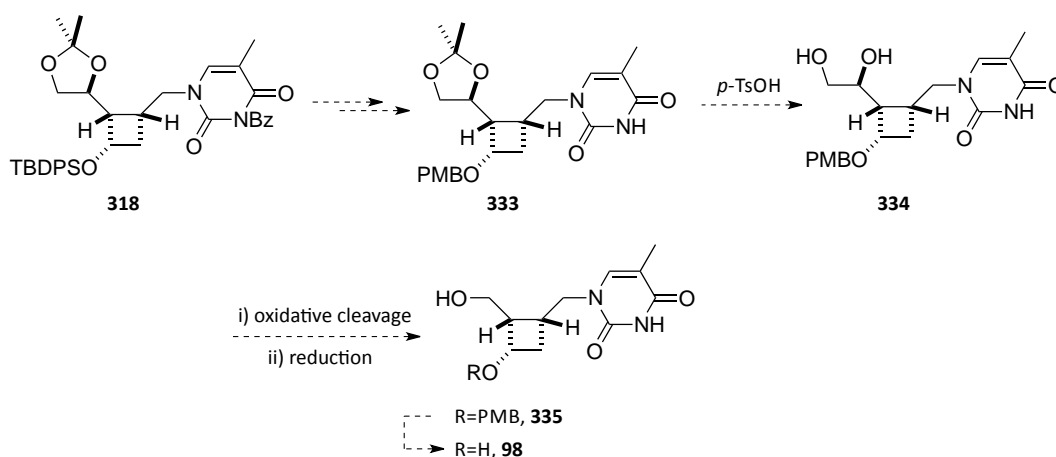
Scheme 79. Alternative pathway to **98**.

The *p*-methoxybenzyl group (PMB), which is acid resistant and can be easily cleaved by oxidation with e.g. DDQ, was considered an appropriate candidate.

2.3.2 Approximation A. *p*-Methoxybenzyl as the 3' protecting group

To achieve the synthesis of the PMB derivative we planned to change the TBDPS for the PMB group on intermediate **318** (Scheme 80).

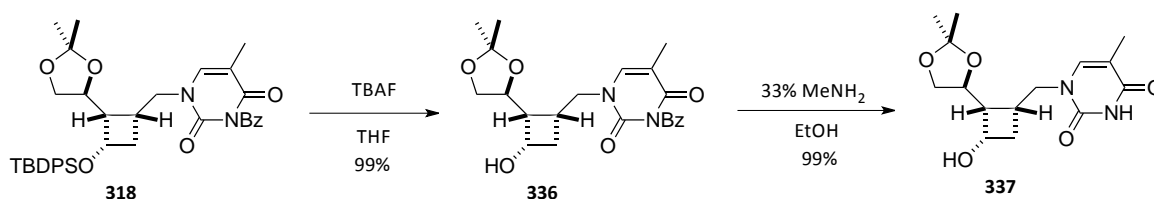
¹⁷⁷ Perlin, A. S. *Adv. Carbohydr. Chem. Bi.* **2006**, *60*, 183-250.



Scheme 80. Synthetic strategy towards **98** using the PMB protecting group from intermediate **318**.

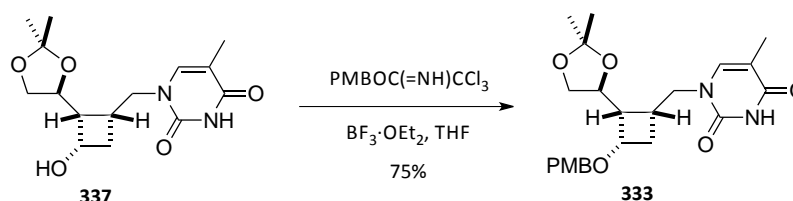
2.3.2.1 Synthesis of the *p*-methoxybenzyl intermediate **333**

Cleavage of the silyl ether of **318** with TBAF in THF provided alcohol **336** in almost quantitative yield (Scheme 81). Then, the nucleobase was deprotected by treatment of **336** with a 33% solution of methylamine in ethanol affording compound **337** in 99% yield.



Scheme 81. Synthesis of alcohol **337**.

Protection of the 3'-hydroxyl group of **337** as the PMB ether was accomplished by treatment with PMB trichloroacetimidate under BF_3 catalysis delivering **333** in 75% yield (Scheme 82).



Scheme 82. Protection of **337** as the PMB ether.

The presence of the PMB group was confirmed by the appearance of the aryl, benzyl and methoxy signals in the ^1H - and ^{13}C -NMR spectra (Figures 67 and 68).

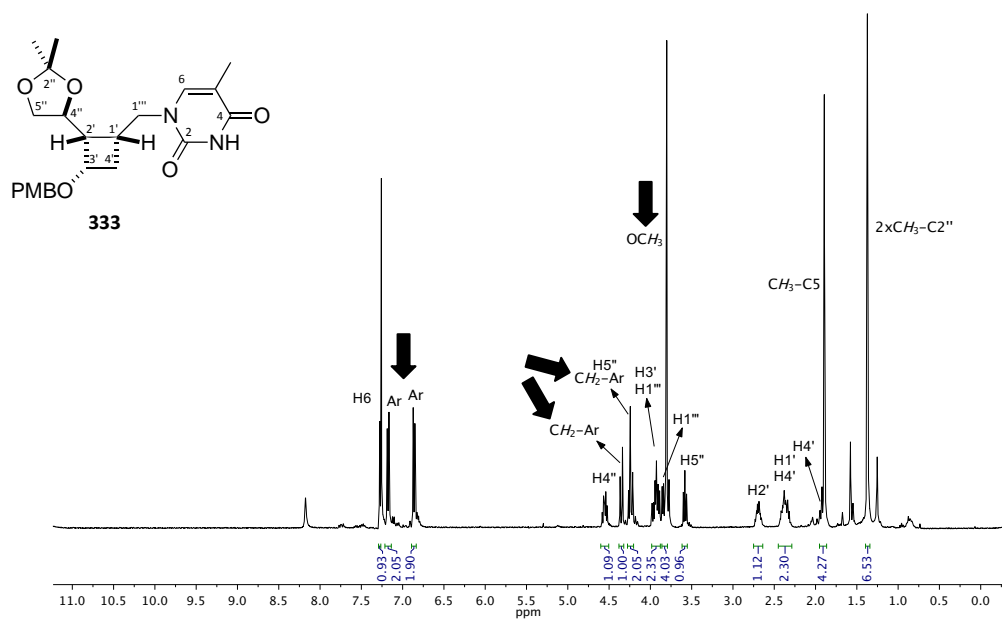


Figure 67. $^1\text{H-NMR}$ spectrum (400 MHz, CDCl_3) of **333**.

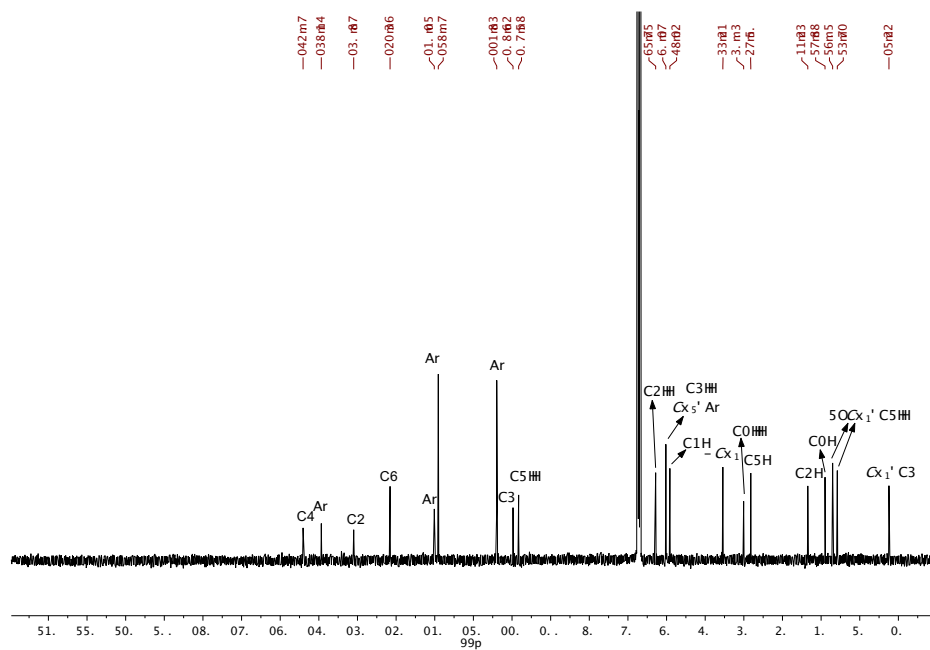
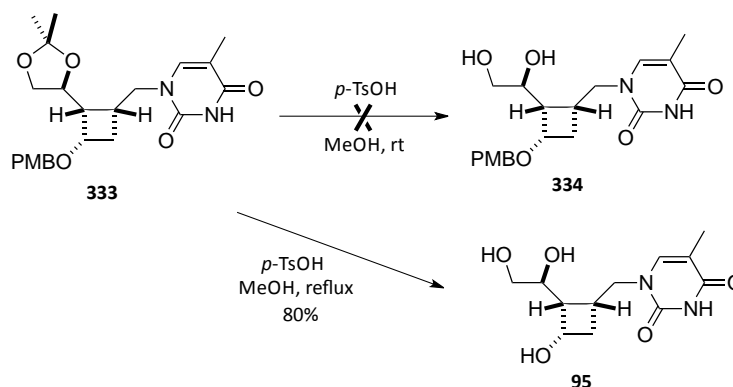


Figure 68. $^{13}\text{C-NMR}$ spectrum (100 MHz, CDCl_3) of **333**.

2.3.2.2 Attempt of diol deprotection

Finally, diol deprotection was undertaken. Unfortunately, when **333** was treated with *p*-TsOH in MeOH at reflux temperature, cleavage of the PMB ether was also observed, giving rise to nucleoside **95** instead of compound **334** (Scheme 83).



Scheme 83. Attempt of diol deprotection on **333**.

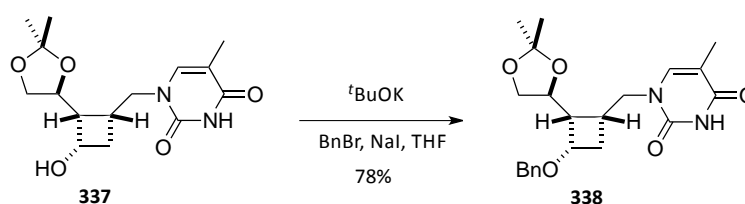
Performing the reaction at room temperature resulted in the recovery of the unaltered starting material, while when gentle heating was applied, formation of the triol **95** was observed.

Consequently, we decided to change the PMB protecting group for a benzyl group, which should be also easy to install and remove but should resist the acidic conditions needed for diol deprotection.

2.3.3 Approximation B. Benzyl as the 3' protecting group

2.3.3.1 Synthesis of the benzyl intermediate **338**

Since the use of a trichloroacetimidate derivative had proven useful to install the 3'-PMB group, we decided to apply the same methodology to introduce the benzyl group. However, when compound **337** was treated with BnOC(=NH)Cl_3 and a catalytic amount of triflic acid or $\text{BF}_3 \cdot \text{OEt}_2$, the reaction did not evolve. A second attempt consisted in the use of benzyl bromide, sodium iodide and potassium *tert*-butoxide in THF (Scheme 84). These conditions produced **338** in 78% yield.



Scheme 84. Protection of **337** as the benzyl ether.

Analogously to the case of compound **333**, the success of the reaction was confirmed by the presence of aromatic and benzylic signals in the proton and carbon spectra (Figure 69).

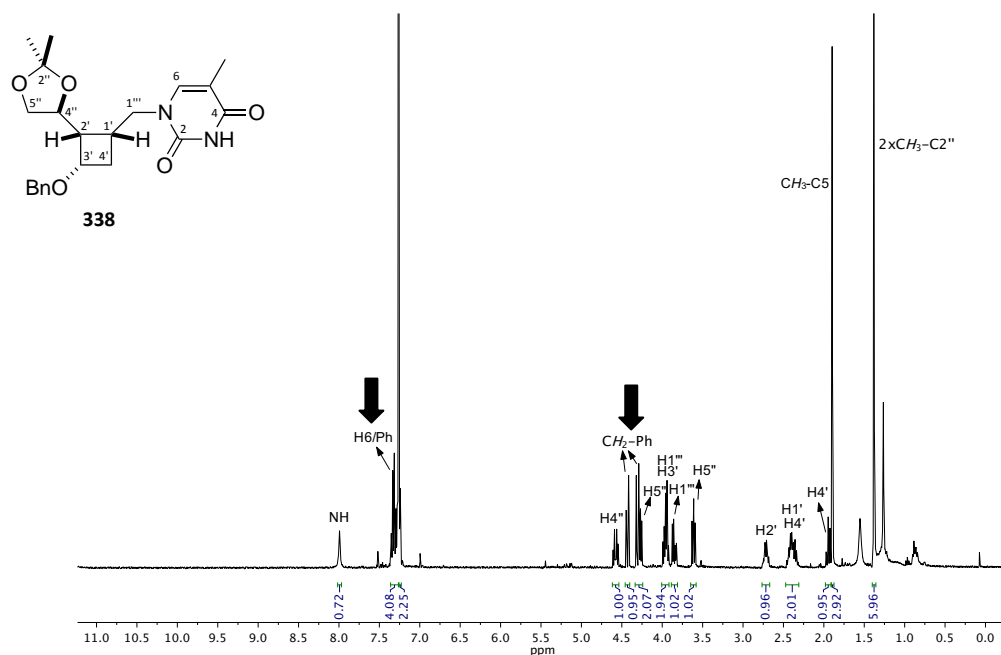
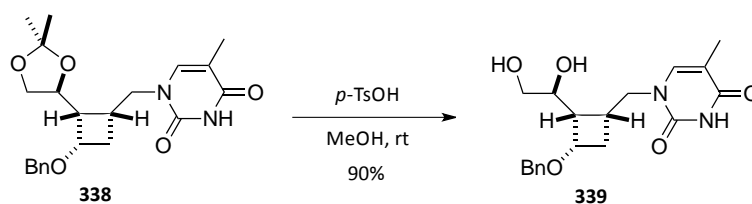


Figure 69. $^1\text{H-NMR}$ spectrum (400 MHz, CDCl_3) of **338**.

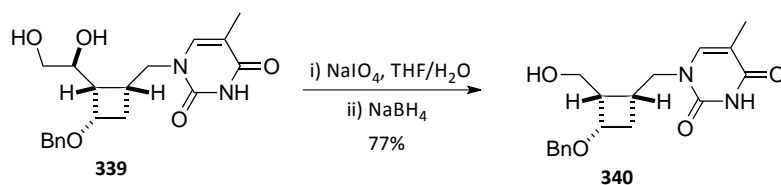
2.3.3.2 Synthesis of nucleoside **98**

Next the deprotection of the diol was faced. In this case, cleavage of the acetonide of **338** with *p*-TsOH proceeded smoothly at room temperature, providing diol **339** in excellent yield (Scheme 85).



Scheme 85. Cleavage of the acetonide of **338**.

With the presence of the free diol and the 3'-hydroxyl group protected, the oxidative cleavage and subsequent reduction were assayed. Gladly, the 3'-benzyl protecting group avoided the opening of the cyclobutane, rendering compound **340** in 77% yield (Scheme 86).



Scheme 86. Oxidative cleavage and subsequent reduction of **339**.

Proton spectrum of the obtained product showed the disappearance of one hydrogen atom in the zone comprised between δ 3.40-4.20, evidencing diol cleavage and formation of **340** (Figure 70).

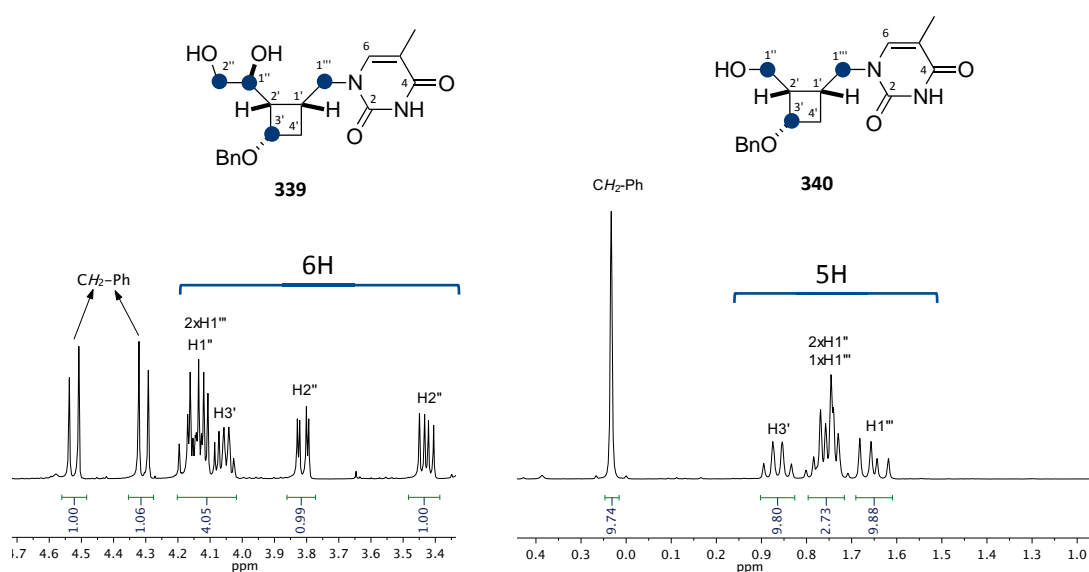


Figure 70. Comparison between the ^1H -NMR spectra (400 MHz, MeOD) of **339** and **340**.

The distinctive behaviour of the benzylic protons evidences that free rotation around the benzylic bond is impeded for **339**. This may be caused by the existence of stabilizing hydrogen bond interactions between the 2'' OH group, the 1'' OH group and the 3' oxygen atom. Formation of a hydrogen bond between the 1'' OH group and the 3' oxygen atom would establish a 6-member ring interaction HO...O (Figure 71, left).

In the case of compound **340**, collapse of the benzylic signals is observed indicating free rotation of this group. This conduct can be attributed to the fact that although hydrogen bond between the 1'' OH group and the 3' oxygen is possible, it is not stabilizing enough to fix the rotation around the benzylic bond (Figure 71, right).

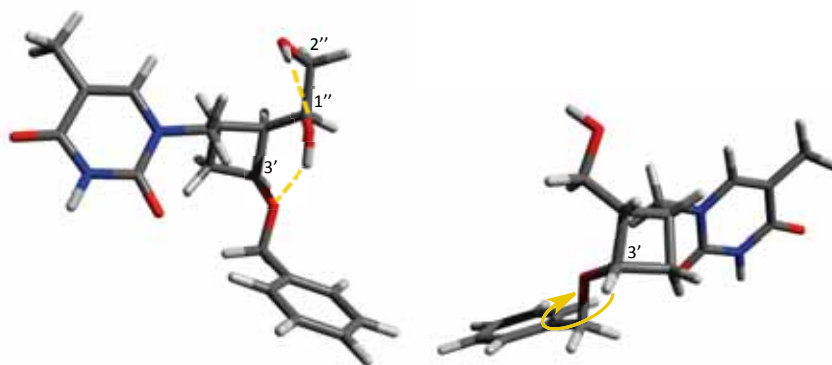
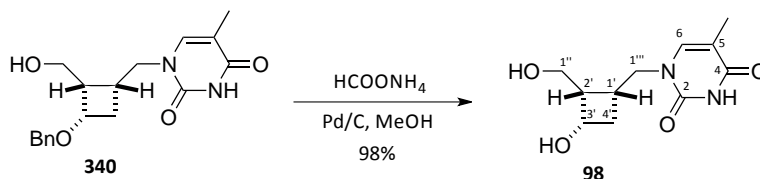


Figure 71. 3D models of **339** and **340**.

Additional evidence of the formation of **340** was given by the ^{13}C -NMR spectrum, where the chemical shift of C1'' was notably lower (δ 59.0) than that of **339** (δ 69.9).

Finally, the last step remaining to achieve **98** was the cleavage of the benzyl group. Hydrogenation of the benzyl derivative with ammonium formate and Pd/C in MeOH afforded nucleoside **98** in almost quantitative yield (Scheme 87).



Scheme 87. Synthesis of nucleoside **98** by hydrogenation of **340**.

To our delight, nucleoside **98** provided adequate crystals for X-ray analysis. The crystal structure showed a slightly puckered cyclobutane ring, with the nucleobase proton H6 pointing towards H1' and H1''' (Figure 72). The hydroxymethyl group adopts a practically *trans* disposition with the C1'-C2' bond (the dihedral angle C1'-C2'-C1''-O1'' is 170.5°) and the value of the dihedral angle C3'-C2'-C1''-O5'' is 72.4° .

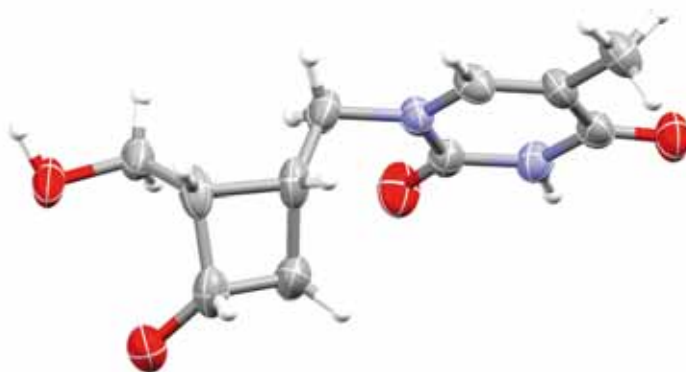
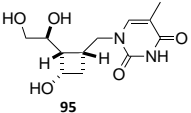
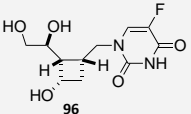
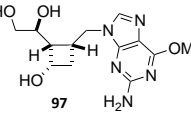
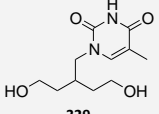


Figure 72. Crystal structure of **98** (thermal ellipsoids at 50% probability level).

3. EVALUATION OF THE ANTIVIRAL ACTIVITY

The cyclobutane L-nucleoside analogues **95-97** and the acyclic compound **329** prepared in this chapter have been evaluated against several viruses by the research group led by Prof. Jan Balzarini at the *Katholieke Universiteit Leuven*. The results are summarized in Tables 15-19. Unfortunately, the four tested nucleosides did not exhibit antiviral activity at concentrations up to 100 $\mu\text{g/mL}$ except for the thymine analogue **95**, which showed weak activity and considerable cytotoxicity against influenza viruses (Table 19). Nevertheless, a computational study to rationalize these results and improve future synthetic designs is currently underway.

Compound	Min. cytotoxic concentration ^a ($\mu\text{g/mL}$)	EC ₅₀ ^b ($\mu\text{g/mL}$)				
		HSV-1 (KOS)	HSV-2 (G)	Vaccinia Virus	Vesicular Stomatitis Virus	HSV-1 TK ⁻ KOS ACV
Brivudin (μM)	>250	0.01	96	1.8	>250	250
Cidofovir (μM)	>250	1.2	0.4	10	>250	2
Acyclovir (μM)	>250	0.4	0.08	>250	>250	126
Ganciclovir (μM)	>100	0.03	0.03	>100	>100	4
 95	>100	>100	>100	>100	>100	>100
 96	>100	>100	>100	>100	>100	>100
 97	>100	>100	>100	>100	>100	>100
 329	>100	>100	>100	>100	>100	>100

^a Required to cause a microscopically detectable alteration of normal cell morphology. ^b EC₅₀: Effective concentration 50 or needed concentration to inhibit 50% HIV-induced cell death, evaluated with the MTS assay.

Table 15. Cytotoxicity and antiviral activity of nucleosides **95-97** and **329** in HEL cell cultures.

Compound	Min. cytotoxic concentration ^a ($\mu\text{g/mL}$)	EC ₅₀ ^b ($\mu\text{g/mL}$)		
		Vesicular Stomatitis Virus	Coxsackie Virus B4	Respiratory Syncytial Virus
DS-5000	>100	100	100	1.8
(S)-DHPA (μM)	>250	>250	>250	>250
Ribavirin (μM)	>250	22	25	4.5
95	>100	>100	>100	>100
96	>100	>100	>100	>100
97	>100	>100	>100	>100
329	>100	>100	>100	>100

^a Required to cause a microscopically detectable alteration of normal cell morphology. ^b EC₅₀: Effective concentration 50 or needed concentration to inhibit 50% HIV-induced cell death, evaluated with the MTS assay.

Table 16. Cytotoxicity and antiviral activity of nucleosides **95-97** and **329** in HeLa cell cultures.

Compound	Minimum cytotoxic concentration ^a ($\mu\text{g/mL}$)	EC ₅₀ ^b ($\mu\text{g/mL}$)				
		Para-influenza-3 Virus	Reovirus-1	Sindbis Virus	Coxsackie Virus B4	Punta Toro Virus
DS-5000	>100	>100	>100	100	38	20
(S)-DHPA (μM)	>250	>250	>250	>250	>250	>250
Ribavirin (μM)	>250	29	112	>250	>250	29
95	>100	>100	>100	>100	>100	>100
96	>100	>100	>100	>100	>100	>100
97	>100	>100	>100	>100	>100	>100
329	>100	>100	>100	>100	>100	>100

^a Required to cause a microscopically detectable alteration of normal cell morphology. ^b EC₅₀: Effective concentration 50 or needed concentration to inhibit 50% HIV-induced cell death, evaluated with the MTS assay.

Table 17. Cytotoxicity and antiviral activity of nucleosides **95-97** and **329** in Vero cell cultures.

Compound	CC ₅₀ ^a (µg/mL)	EC ₅₀ ^b (µg/mL)	
		Feline Corona Virus (FIPV)	Feline Herpes virus
HHA	>100	12.2	18.8
UDA	52.4	0.9	1.6
Ganciclovir (µM)	>100	>100	0.7
95	>100	>100	>100
96	>100	>100	>100
97	>100	>100	>100
329	>100	>100	>100

^a CC₅₀: Cytotoxic concentration 50 or needed concentration to induce 50% death of non-infected cells, evaluated with the MTS assay. ^b EC₅₀: Effective concentration 50 or needed concentration to inhibit 50% HIV-induced cell death, evaluated with the MTS assay.

Table 18. Cytotoxicity and antiviral activity of nucleosides **95-97** and **329** in CRFK cell cultures.

Compound	Cytotoxicity		EC ₅₀ ^c (µg/mL)					
			Influenza A H1N1 subtype		Influenza A H3N2 subtype		Influenza B	
	CC ₅₀ ^a	Min. Cytotoxic Conc. ^b	Visual CPE Score	MTS	Visual CPE Score	MTS	Visual CPE Score	MTS
Oseltamivir carboxylate (µM)	>100	>100	9	12.6	0.8	2.0	20	32.1
Ribavirin (µM)	>100	>100	9	9.6	7	2.6	7	1.9
Amantadine (µM)	>200	>200	>200	>200	0.7	0.4	>200	>200
Rimantadine (µM)	>200	>200	40	48.1	0.7	0.1	>200	>200
95	50.2	100	>20	>20	>20	>20	>20	>20
96	>100	>100	>100	>100	>100	>100	>100	>100
97	>100	>100	>100	>100	>100	>100	>100	>100
329	>100	>100	>100	>100	>100	>100	>100	>100

^a CC₅₀: Cytotoxic concentration 50 or needed concentration to induce 50% death of non-infected cells, evaluated with the MTS assay. ^b Required to cause a microscopically detectable alteration of normal cell morphology. ^c EC₅₀: Effective concentration 50 or needed concentration to inhibit 50% HIV-induced cell death, evaluated with the MTS assay.

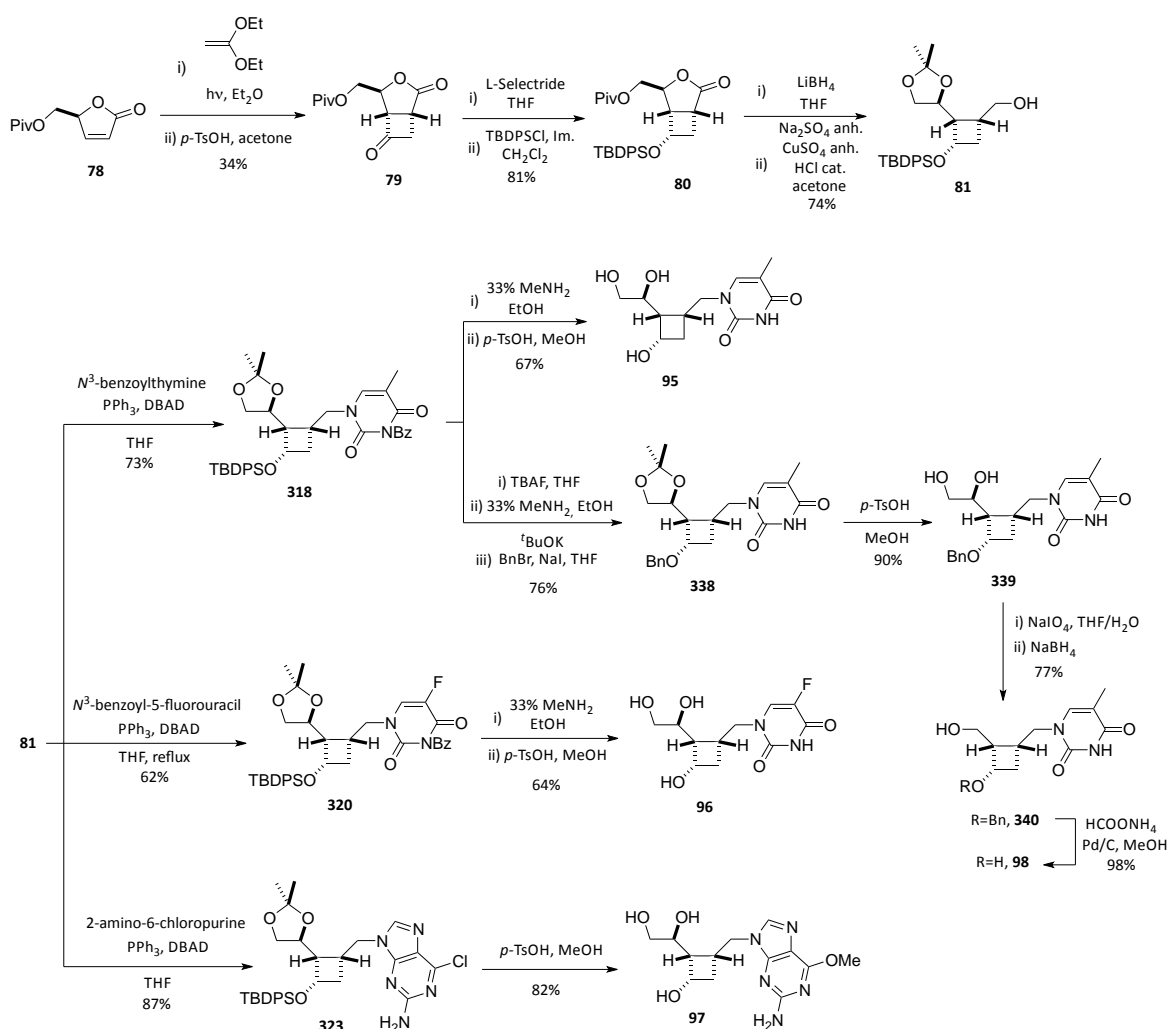
Table 19. Cytotoxicity and antiviral activity of nucleosides **95-97** and **329** in MDCK cell cultures.

4. CHAPTER IV OUTLINE

A synthetic strategy for the preparation of four cyclobutane L-nucleosides starting from the 2(5*H*)-furanone **78** has been developed (Scheme 88). Thymine nucleosides **95** and **98** have been obtained in 9 and 14 steps and 10% and 8% yield, respectively. The fluorouracil derivative **96** has been synthesized in 9 steps and 8% global yield. Finally, the purine nucleoside **97** has been achieved in 8 steps and 15% yield.

Remarkably, nucleoside **98** could be crystallized and its structure has been analyzed by X-ray diffraction.

Finally, the three cyclobutane nucleosides **95-97** and the acyclic compound **329** have been evaluated against several viruses. Unfortunately, none of them showed significant activity.



Scheme 88. Chapter IV summary.

V. Synthesis of Double-Headed Nucleosides

and Their Incorporation Into Oligonucleotides

